SWISS
CONSERVATION-RESTORATION
CAMPUS

haute école
neuchâtel berne jura

conservation
restauration
neuchâtel

Conservation of charred archaeological textiles. Consolidation treatments and long-term preservation strategies

Mémoire présenté par :

Andrea Ramírez Calderón

Pour l'obtention du

Master of Arts HES-SO in Conservation-restauration

Orientation objets archéologiques et ethnographiques

Année académique 2017-2018

Remise du travail : *16.07.2018*

Jury : *29.08.2018*

Nombre de pages *: 167*

Hes·so
Haute Ecole Spécialisée
de Suisse occidentale

« *J'atteste que ce travail est le résultat de ma propre création et qu'il n'a été présenté à aucun autre jury que ce soit en partie ou entièrement. J'atteste également que dans ce texte toute affirmation qui n'est pas le fruit de ma réflexion personnelle est attribuée à sa source et que tout passage recopié d'une autre source est en outre placé entre guillemets.* »

Date et signature :

Neuchâtel, 16.07.2018

Acknowledgements:

I want to express my gratitude to the **Swiss National Museum**, and especially to Dr. **Katharina Schmidt-Ott**, Head of conservation of the Archaeological Objects of the museum, and Mr. **Markus Leuthard**, Head of the Collection Centre, for giving me the chance to work on this exciting topic. My deepest thanks to the **Kantonsarchäologie Zurich**, especially to **Chantal Hartmann** and **Kathrin Trüllinger**, for providing me with the archaeological samples.

I would like to thank particularly Mrs. **Janet Schramm**, conservator-restorer of archaeological objects, for her inexhaustible enthusiasm in supervising my work. This project could not have been completed without the advice and support of the all conservators-restorers from the archaeological team, including Mr. **Alexander Dittus,** Mrs. **Stefanie Bruhin**, Mr. **Martin Bader**, Mr. **Cédric André** and Mrs. **Gaëlle Liengme**. A special thanks to them for their support and for answering all my questions without complaining.

I wish to sincerely thank the staff of the Swiss National Museum, particularly the conservation research team, Mr. **Erwin Hildbrand**, Dr. **Vera Hubert** and Dr. **Tiziana Lombardo**, for providing input and advice during the scientific experiments and analysis. I would like to thank Mrs. **Nikkabarla Calonder**, textile conservator, for sharing her knowledge about the conservation of archaeological textiles. Thanks also to Mrs. **Veronique Mathieu** and Mrs. **Anna Jurt Portmann**, paper conservators, as well as to Mr. **Peter Wyer**, sculpture conservator, for their advice about the all the materials used in this project.

Sincere thanks to professor **Pierre-Alain Montandon**, and Dr **Pierre-Antoine Gay**, for their help with the carbonisation of the samples.

Thank you to the reviewers Mrs. **Marianna Grynchuk** and Mrs. **Tessa Plakida**, for their patience and corrections.

Among the teaching staff of the Haute Ecole Arc, I would like to sincerely thank the supervising professors and the members of the jury: Dr. **Régis Bertholon** (Professor and Head of the sector), Mr. **Valentin Boissonnas**, Mrs. **Hortense de Corneillan**, Dr. **Christian Degrigny** and Mr. **Tobias Schenkel**. I would also like to warmly thank Mr. **Thierry Jacot**, professor of preventive conservation at the HE-ARC, for his help and loan of equipment for the mould tests.

I would also thank my dear friends, who were always there for me and distracted me when I needed it. All my infinite gratitude to **Irene Sanz Centeno** and **Oana Geanina Vasilache**, for their unconditional love and support. Thanks also to **Naïma Gutknecht**, for her patience and her friendship.

Finally, I wish to thank my family, for their unwavering encouragement and love, without them I would never be where I am.

Contents

Abstract

Archaeological textiles that were carbonised prior to their burial often survived to the present days. They are particularly friable and in recent years research has focused on the combination of consolidants and lubricants for their freeze-drying treatment.

For this master thesis, consolidation tests were carried out on wet charred archaeological samples from the late medieval archaeological site of Elgg. The aim was to find a conservation method which will allow their long-term preservation, and the conservation of a larger number of textile fragments from the same site.

The textiles were stabilized through freeze drying under vacuum and consolidation treatments. Before drying, half of the samples were treated with polyethylene glycol (PEG) 400, to compare the reaction of the textiles when dried with or without a plasticiser. The results indicated that applying a polyethylene glycol solution before drying is beneficial to the textile, as the cohesion of the fibres is increased, whilst they remain flexible. Then, both groups were consolidated with Klucel® G, Klucel® E, Aquazol® 500 and Paraloid® B72, except for one set of samples per group that was left untreated.

Modern charred samples were created and treated to increase the collection of data. The modern textile samples were carbonised, soaked in water, and then freeze-dried and consolidated, following the same methodology as for the archaeological samples.

Afterwards, the flexural rigidity, the tensile strength and the variation of lightness were calculated to compare the influence of the consolidation methods on the physical properties of the charred samples. Among the consolidants tested, Aquazol®500 seems to achieve the best results, either for the samples treated or untreated with PEG 400. The textiles remained flexible, and the loss of fibres was reduced due to the consolidant's adhesive properties.

However, due to the small number of archaeological sample tested, the results are still not fully significant and further research should be carried out.

Résumé

Les textiles archéologiques carbonisés font référence aux textiles qui ont survécu jusqu'à nos jours après avoir été carbonisés puis enterrés dans cet état. Ils sont particulièrement friables et, de ce fait, très difficile à préserver et à manipuler. Ces dernières années, les recherches se sont concentrées sur la combinaison de consolidants et de lubrifiants combinés à un traitement de lyophilisation.

Pour cette thèse de master, des tests de consolidation ont été réalisés en collaboration avec le Centre des Collections du Musée National Suisse. Les tests ont été menés sur des échantillons archéologiques carbonisés et en état humide, provenant du site archéologique d'Elgg, datant de la fin du Moyen Age. L'objectif était de trouver une méthode de conservation pour ces échantillons qui permette la conservation à long terme d'un plus grand nombre de fragments textiles provenant du même site.

Les textiles ont été stabilisés par lyophilisation sous vide et par des traitements de consolidation. Avant séchage, la moitié des échantillons ont été traités avec du polyéthylène glycol (PEG) 400, pour comparer la réaction des textiles lorsqu'ils sont séchés avec ou sans plastifiant. Les résultats indiquent que l'application d'une solution de polyéthylène glycol avant séchage est bénéfique pour le textile, car la cohésion des fibres est accrue, tout en restant flexible. Ensuite, les deux groupes ont été consolidés avec Klucel® G, Klucel® E, Aquazol® 500 ou Paraloid® B72, sauf pour un ensemble d'échantillons par groupe qui n'a pas été traité.

Des échantillons modernes carbonisés ont été créés et traités en parallèle aux échantillons archéologiques pour augmenter la quantité de données collectées. Les échantillons de textiles modernes ont été carbonisés et trempés dans l'eau, puis lyophilisés et consolidés.

Ensuite, la rigidité à la flexion, la résistance à la traction et la variation de la clarté ont été calculées pour comparer l'influence des méthodes de consolidation sur les propriétés physiques des échantillons. Parmi les consolidants testés, l'Aquazol®500 semble offrir les propriétés les plus performantes, que ce soit pour les échantillons traités ou non traités au PEG 400. Les textiles restent flexibles, et la perte de fibres est réduite grâce aux propriétés adhésives de l'Aquazol® 500.

Cependant, en raison du petit nombre d'échantillons archéologiques testés, d'autres recherches devraient être menés afin d'avoir une meilleure compréhension de la consolidation des textiles archéologiques carbonisées.

Zusammenfassung

Archäologische Textilien, die verkohlten, bevor sie in die Erde kamen, haben die Bodenlagerung oftmals bis zum heutigen Tage überstanden. Sie sind äusserst fragil, daher hat sich die Konservierungsforschung in den letzten Jahren eingehend mit der Kombination von Konsolidierungs- und Flexibilisierungsmitteln für deren Gefriertrocknungsbehandlung beschäftigt.

Für diese Masterarbeit wurden Versuchsreihen zur Konservierung von nassen, verkohlten archäologischen Proben aus der spätmittelalterlichen Ausgrabungsstätte Elgg durchgeführt. Ziel war es, eine Konservierungsmethode zu finden, welche die langfristige Konservierung einer größeren Anzahl von Textilfragmenten des selben Fundortes ermöglicht.

Die Textilien wurden durch Vakuumgefriertrocknung und Tränkung mit Festigungsmitteln stabilisiert. Vor der Trocknung wurde die Hälfte der Proben mit Polyethylenglycol (PEG) 400 behandelt, um das Verhalten der Textilien beim Trocknen mit und ohne Flexibilisierungsmittel zu vergleichen. Die Ergebnisse zeigten, dass das Auftragen einer Polyethylenglykollösung vor dem Trocknen für das Textil vorteilhaft ist, da der Zusammenhalt der Fasern erhöht wird, während sie flexibel bleiben. Dann wurden beide Gruppen mit Klucel® G, Klucel® E, Aquazol® 500 und Paraloid® B72 konsolidiert. Zudem gab es pro Gruppe einen Blindprobensatz ohne Konsolidierungsmittel.

Moderne verkohlte Proben wurden erstellt und behandelt, um eine statistisch auswertbare Datenmenge zu erhalten. Die modernen Textilproben wurden nach dem Verkohlen in Wasser eingeweicht. Anschliessend erfolgte eine Gefriertrocknung und Festigung, welche der Vorgehensweise bei den archäologischen Proben entsprach.

Danach wurden die Biegesteifigkeit, die Zugfestigkeit und die Veränderung der Helligkeit gemessen, um den Einfluss der Konsolidierungsmethoden auf die physikalischen Eigenschaften der verkohlten Proben zu vergleichen. Unter den getesteten Konsolidierungsmitteln zeigte Aquazol®500 die besten Resultate, sowohl für die mit PEG 400 behandelten Proben wie auch für jene ohne Vorbehandlung. Die Textilien blieben flexibel und der Verlust von Fasern wurde aufgrund der Bindeeigenschaften des Festigungsmittels reduziert.

Aufgrund der geringen Anzahl der getesteten archäologischen Proben sind die Ergebnisse jedoch nur eine Tendenz und weitere Forschungen in diesem Bereich wären wünschenswert.

Introduction

Archaeological textile conservation has received much attention in recent years for the value of the information that these objects provide. Their organic nature makes them particularly vulnerable materials, and thus constitutes rare finds. Among the different states in which archaeological textiles can be found, charred archaeological textiles are particularly friable. Their condition necessarily leads to the search of conservation-restoration treatments that will ensure their long-term preservation.

One way to stabilize wet archaeological textile is to freeze-dry them while consolidating their structure before and/or after drying them. The extensive research regarding freeze-drying treatments has been, however, focused on organic materials such as wood or leather, and little attention has been paid to the treatment of archaeological textiles. Publications related to this matter have focused on the combination of consolidants and lubricants before the freeze-drying treatment. Their results indicate that consolidation is required anyhow after drying the textiles in most cases, and hence further research is needed.

Particularly in the Canton of Zurich (Switzerland), charred archaeological textiles have been found in recent excavations. The Swiss National Museum collaborates closely with the Archaeological Service of the Canton of Zurich to preserve the many objects excavated, allowing their study and long-term conservation. Nowadays, conservators-restorers from the Swiss National Museum have to face the challenge of treating these textiles.

Consequently, the Archaeological Service of the Canton of Zurich donated to the museum several samples of late medieval charred textiles from the archaeological site of Elgg. Their aim was to allow the investigation and find a conservation method for a large number of textile fragments from the same site.

The present paper presents a study of products tested for the consolidation of those charred archaeological textiles. The samples were divided in two groups for the freeze-drying treatment. One group was previously treated with a polyethylene glycol treatment, and the other was not. In order to collect more data during this research, the consolidants were tried on archaeological samples as well as modern textiles (which have been carbonised).

Chapter 1 Literature review

1.1 Degradation process of textiles

1.1.1 Chemical degradation of textiles

Degradation of textiles can be physical, chemical or biological[1] [2] [3]. Table 1 shows a summary of the principal causes of deterioration of textile fibres. The presence of water and oxygen in the burial environment leads to hydrolysis and oxidation, which can deteriorate the textile fibres causing the weakening and embrittlement of the polymeric structure [4] [5] [6] [7]. While heat and light can accelerate the oxidation process, [8] the combination of temperature, pressure and pH can accelerate the rate of hydrolysis and, in consequence, the degradation of the textile [9]. Although, it has been demonstrated that in buried or submerged environments, the limited oxygen supplies make the oxidation process less harmful in comparison with open-air environments, such as museums [10].

Therefore, it has been demonstrated that in buried or submerged environments the limited oxygen supply makes the oxidation process less harmful in comparison with open-air environments such as museums[11]. Figure 1 shows a diagram of degradation and preservation factors for plant fibres.

Real-life usage in textiles	Environmental factors	Effects of treatments and/or conditions
Tensile forces	Visible light	Aqueous cleaning
Torsion or shear forces	Ultraviolet radiation	Non-aqueous cleaning
Bending and flexion	Water	Humidification
Twisting	Oxygen	Rotation
Elongation	Temperature	Display orientation
Abrasion	Biological	Light source
Fatigue	Soiling	Relative humidity
Compression	Particulate matter	Extreme temperature
Expansion	Organic	
Friction	Autoxidation processes	

Table 1 Causes of textile fibre deterioration[12]

[1] Huisman, 2009, p. 83
[2] Fedorak, 2005. p. 1
[3] Neilson & Allard, 2008, p. 3
[4] Brown & Brown, 2011, p. 237
[5] Von Holstein, 2012
[6] Von Holstein *et al.*, 2014, p. 2121-2133
[7] Solazzo *et al.*, 2013, p. 48-59
[8] Goffer, 2007, p. 76-77
[9] Serchisu, 2014, p. 55-56
[10] Serchisu, 2014, pp. 55-56
[11] Serchisu, 2014, p. 54-55
[12] France, 2005, p. 4

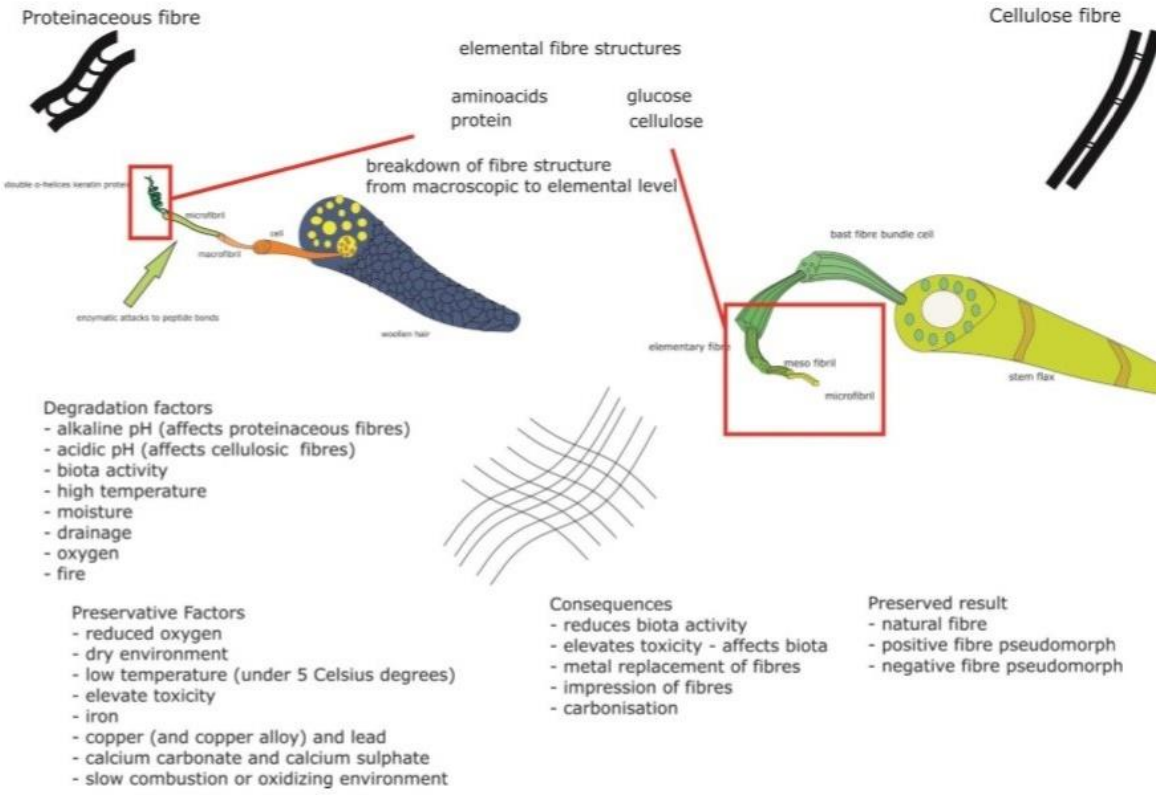

Figure 1 Diagram of animal and plant fibers degradation and preservation ©Serchisu

Physical damage for textiles can happen before, during or after burial. Specifically, linen textiles tend to crease and fold and those areas become brittle with time. In wet burial environments, from damp to waterlogged, the principal causes of physical deterioration of textiles are overburden[13], chemical hydrolysis and biologic attack, and the combination of these parameters leaves physically weakened structures. Overburden is the main reason why fabrics are frequently creased and non-recoverable.
Microorganisms (essentially fungi and bacteria), can break down the textile fibers and create physical damage when attacking the organic compounds still present in the charred textile, or in the soil[14] [15].
When textiles are charred, the degradation mechanisms mentioned before are slowed down by the carbonisation of the structure. Once the textiles are removed from the burial environments, they are exposed to changes in temperature, relative humidity, light, and oxygen-rich air.

[13] Pressure exerted on objects and structures located within the lower layers
[14] Von Holstein, 2012
[15] Peacock, 2003

These parameters can accelerate the rate of degradation of textiles, which is also dependent on the structure of the fibers in combination with their histories of fabrication, use, and initial burial[16].The charred archaeological textiles were recovered wet and in a relaxed state. The water in the cells and hollows of the fibres supports their arrangement, but in the case of flooding, disruption of the structure balance can occur (hence, the fibres break). When the water is removed, the textile becomes compact due to the surface area of the air-water interface being minimised by surface tension forces[17].

This degraded state of the charred textiles can be subject to further disintegration, leading to complete destruction, due to their fragility and brittleness. If untreated, the textiles will dry in an uncontrolled manner, leading to the shrinkage of the fibres, new broken threads and the disintegration of the ensemble. Nevertheless, one of the most usual causes of degradation of charred textiles after discovery is the way they are handled, as each manipulation provokes the loss of fibres.

1.1.2 The influence of the excavation environment

Textiles can be recovered from a diversity of site environments. Archaeological records demonstrate that the survival of organic finds (such as fabrics, basketry and cordage) is dependent upon the nature of the material and the nature of the surrounding environment. On one hand, the textile's resistance to biochemical breakdown depends on the combination of its structure, the polymer chemistry, and histology of the raw materials[18]. On the other hand, the environments must present exceptional conditions where the extent and rate of microbial degradation is reduced or inhibited. Otherwise, natural textile fibres cannot survive due to the natural biological disintegration.

In dry burial environments, textiles must be surrounded by extreme dryness, low temperature, or anoxia (lack of oxygen) for them to be preserved. Tombs and desert sites in Egypt, Peru and China are an example of dry environments where textile material has been recovered in excellent state. Freshwater lakes in southern Europe and marine sediments have also been excellent environments for wet textiles as they possess reduced oxygen levels. Other more recent finds include the artic zones were frozen mummies have been found, such as Otzi the Iceman in the Alps or finds from the Franklin Expedition in the Canadian Arctic). In frozen environments, moisture is locked up as ice, which enables the biological attack and perfectly preserves the structure[19] .

[16] Solazzo *et al.*, 2013, p. 48-59
[17] Peacock, 1992
[18] Peacock, 2003, p. 3
[19] Peacock, 2003

Anoxic conditions can yield the whole range of preservation state of archaeological textiles, from complete integrity to near total dissolution. More degradation-resistant fragments such as carbonised or mineralized complement the corpus of textiles finds replaced by the transition of some metal or other salts. Unfortunately, there is a lack of publication focused on carbonised textiles[20].

1.1.3 The carbonisation process

Carbonisation is defined as the transformation and reduction of organic substances into carbon through pyrolysis. It implies the thermochemical decomposition and breakdown of complex substances into simpler ones at elevated temperatures in the absence of oxygen [21] [22] [23] . The slow combustion of material that involves a limited supply of oxygen is generally called "charring". When this process is related to textiles, the cellulose oxidizes without the total disruption of the fibre structure, preserving the macro-structure of the original textile[24]. Charred archaeological textiles refers to textiles that survived to the present days because they were carbonised and then buried in that state. This process is observed when the combustion of an organic material is suddenly interrupted, when buried or immersed in water, because the lack of oxygen prevents its full conversion into ash[25].

To be able to understand the carbonisation stages, the publications relating to the formation of charcoal, under laboratory conditions and using wood, were considered (Table 2).

Temperature range	Stages in the conversion process
At 20°C to 110°C	The wood dries absorbing the heat and giving off its water vapour
At 110 to 270°C	The wood starts to decompose, emitting carbon monoxide, carbon dioxide, acetic acid and methanol
At 270 to 290°C	The exothermic decomposition starts. Mixed gases and tar are released
At 290 to 400°C	Breakdown of the wood structure
At 400 to 500°C	At 400°C the transformation of the wood to charcoal is practically complete. As tar is still present in the structure (around 30%), further heating raises the carbon content and produce a better-quality charcoal.
More than 500°C	Carbonisation is completed

Table 2 Carbonisation process of wood[26]

[20] Peacock, 2003
[21] Sease, 1987, p. 63-64
[22] Jones *et al.*, 2007, p. 15
[23] Miksicek, 1987, p. 219-221
[24] Cooke, 1988, p. 9
[25] Bjerregaard, 2016
[26] Domac and Trossero, 2008

In the case of textiles, the fibres lose the water present in their structure and shrink during carbonisation. Consequently, the density of the textiles decreases while the intercellular spaces close. During the process, the organic substances, normally attacked by microorganisms, disappear and thus there is an increase of their biochemical resistance[27]. After the carbonisation process, the textiles become insoluble and inert to chemical reactions in normal acidic or alkaline conditions[28].
Charred textiles of woven fabrics can present different characteristics depending on the burial environment and the carbonisation state, but generally, they are black, hard and brittle. The aesthetical appearance can be glassy or matt depending on the dry or wet condition of the fabric. When found, they are often small fragments, and the state of conservation will determine the study of the binding system, spinning, thread count etc.[29].

1.2 Conservation of archaeological textiles

1.2.1 Conservation of archaeological textiles: Past attempts

Archaeological textiles are usually found in a weakened and fragile state, and those recovered from damp, wet, or frozen burial environments are also wet. One alternative for these finds is not to dry them. The down side of this option, however, is that it requires specialized and well-monitored storage. Unfortunately, conservators had to face difficulties related to mould growth even with cold storage when the charred textiles are contaminated with organic compounds[30]. Frozen storage seems the best option for long-term maintenance when the textile is in a wet state. The accessibility of the objects for analysis, research and exhibition is, however, very limited if they are in frozen storage[31].

Drying the textiles seems then a critical first step for the stabilisation of the artefacts, which will allow the study and storage of these unstable wet materials[32]. Due to the stresses that natural drying procedures create on the materials, which can lead to loss of coherency, collapse, or shrinkage, several studies have focused on the effect of freeze-drying treatments. This procedure seems to reduce the effects of natural drying, but still can be distressing to the fabric[33]. Nowadays, it is the most common treatment but we must acknowledge that others do exist.

[27] Lopez Luján ,2016 p. 142
[28] Lopez Luján ,2016 p. 143
[29] Malmius, 2002, p. 63
[30] Logan and Young, 1987
[31] Peacock, 2003
[32] Peacock, 1992
[33] Peacock, 2003

On previous publications, researchers have tested the combination of different drying techniques with consolidants and lubricants. For example, Vazquez del Mercado (2000), and Garcia Lascurain (2012), treated their textiles with a mixture of glycerine and alcohol, and consolidated them after drying with a mixture of Methocel® and propylene glycol. Pearson (1987) tested a mixture of Ethulose, PEG 400 and glycerol in distilled water, which he believed strengthened and consolidated the textile without the swelling of the PEG 400 alone.

Currently, there is no consensus on the effectiveness of the freeze-drying treatment. Tarleton and Ordoñez (1995) compared the effect of air-drying and freeze-drying of soil-buried modern wool fabric subjected to tensile tests, and found the results inconclusive. Elizabeth E. Peacock[34] dried burial-degraded cotton, linen, silk and wool fabrics with a freeze-drying system and, after testing the yarn-breaking tenacity, also found the tests inconclusive when compared with air-drying treatments. Jakes and Mitchell[35] tested water-degraded linen with vacuum freeze-drying and, based upon the visual inspection of approximately 0-5cm² samples, concluded that this treatment can be disruptive to the fabric[36].

Studies carried out about consolidation of archaeological textiles have been focused on the application of the products before drying. Thereby, numerous problems have been recorded because the agents employed were not miscible with water (e.g. polyvinyl resins PVA and PVB), or are not recommended because it could increase the stresses during the drying procedure (e.g. polyvinyl alcohol PVOH, soluble nylon, mixtures of PEG and ethyl hydroxyethyl cellulose called Modocol[37], or hydroxypropyl cellulose[38]).

In recent times, publications on charred textiles focus mainly on the archaeological and chemical point of view, as well as the identification of fibers. Textiles have been consolidated with substances with a similar structure to that of cellulose. The investigations undertaken for the conservation of plant fibres studied materials and methods that have been proved to be suitable for wet and degraded woods, because of its high cellulose content. Few publications can be found about consolidation methods used or archaeological objects excluding wood (mainly ropes and basketry). Carrlee and Senge (2013) suggest the use of Butvar B-98® as a consolidant after applying a polyethylene glycol treatment, while Morton and Bernaciak (2013) propose the use of Paraloid® B-72 in acetone. For Marie Jordan-treated cordage (Jordan, 2013), the objects were treated with 10-15% of Paraloid® B-72 in acetone, after their impregnation in a solution of 2% v/v glycerol and 5% polyethylene glycol (PEG) 400 in water. However, there is still insufficient knowledge about the response of the archaeological textiles to certain treatments.

[34] Peacock, 1993
[35] Jakes and Mitchell, 1992
[36] Peacock, 1999, p. 16
[37] Thorvildsen, 1975, p. 70-86
[38] Morrison, 1989, p. 3

1.2.2 Literature review on the drying methods

Drying methods for archaeological textiles were studied during the nineties to understand the reaction of textiles to the different procedures (Tarleton and Ordeñez 1994, Peacock 1993, Peacock 1990), including air drying (AD), air drying using a vacuum table (VD), air drying following solvent exchange with ethanol (SD), vacuum freeze-drying (FD), and vacuum freeze-drying from a block of ice (FDB). The results of these studies indicated that freeze-drying methods produced more flexible fabrics than the other methods.

In addition, the studies show a correlation between the morphological breakdown present already on the textiles and the collapse of fibre due to stresses arising during the drying process[39]. Traditional drying methods (AD, VC and SD), brought about collapse of the degraded fabrics. The effects, generally irreversible, are shrinkage, movement of dyes, fibre fracture, shredding, brittleness and stiffness. Contrarily, freeze-drying methods avoided the breakdown by freezing the wet fabric structure before drying[40]. The sublimation normally occurs around -20°C to -30°C and, even if the process can take place at atmospheric pressure, in practice a partial vacuum speeds up the treatment[41].

1.2.3 The consolidation of textiles: Theoretical concepts

Consolidants should be able to fully penetrate the deteriorated substrate without altering its appearance, create bonds with the fibres[42], remain in the substrate[43], allow following treatments to be carried out, and have a stable long and functional life[44].

To achieve all these goals, conservators must consider the substrate being consolidated (porosity, permeability and surface properties), the adhesive properties (molecular weight and solubility parameters) and the solvent employed (vapour pressure), and the application technique[45] [46].To penetrate the substrate, low viscosity consolidants are preferred. The viscosity of a specific adhesive can be modified by the choice of solvent and the concentration[47]. The wettability of the surface is reliant on the surface properties of the substrate and depends on the adhesive forces overcoming the cohesive forces. It can be also altered by the selection of consolidant and solvent[48].

[39] Peacock, 2003
[40] Peacock, 2003
[41] Peacock, 1992, p. 365
[42] Down, 2015, p. 31
[43] Newey *et al.*, 1992
[44] Koob, 1981, pp. 86-94
[45] Kucerová and Drncová, 2009
[46] Down, 2015
[47] Koob 1981, p. 86
[48] Horie 2010

Removability is, sadly, much more problematic. The complete safe removal is near impossible, especially as consolidation is usually performed on objects of questionable stability to begin with. Conservators usually acknowledge that consolidation treatments are never completely reversible, because removing an adhesive from a porous, fibrous and weakened material can jeopardize the conservation of the ensemble. Although, re-treatability could be achievable is future consolidation treatments are not prevented by the actual treatment[49] [50].

1.3 Physical properties of fibres affecting their conservation

1.3.1 Absorption and desorption:

Fibres are constantly seeking an equilibrium moisture content (EMC) with the humidity of the environment[51]. Fibres tend to absorb moisture if relative humidity in the room is higher than the quantity of moisture in the fibres; or desorb it, if it is lower. When absorption and desorption occurs, the response of the fibre can be evaluated with the change in length, diameter, cross-sectional area or volume. Usually, dry fibres are 20% less strong than fibres saturated with water[52].

Fibres, which are composed by crystalline and amorphous regions, can absorb water and moisture. The absorption rate is high in amorphous areas, and negligible in the crystalline regions, especially when doing short-duration treatments at low temperature. This happens because the water molecules are attracted to the polar groups of the fibre polymer of the amorphous regions by hydrogen and dipole bonds. Then, the already absorbed molecules of water attach themselves to new molecules[53].

When looking at the chemical composition of natural plant fibres, cellulose and hemicellulose are hygroscopic, especially hemicellulose which, because of its low polymerisation degree, is an amorphous polysaccharide. Lignin, on the contrary, is hydrophobic, it is assumed that the quantity of hemicellulose and lignin present in a fibre will determine the absorption properties[54].

In practice, conservators constantly try to avoid the over-drying of the fibres by desorption when conditioning the textiles in controlled relative humidity storage rooms. To retain the flexibility of the fibres, the EMC must be at least at 55%RH, and any quick drying must be avoided.

[49] Down 2015
[50] Down 2015
[51] It is important to consider the hysteresis because at any given RH, the moisture content of a textile is dependent on whether it has previously been in equilibrium with a higher or lower RH than present. Physical properties of textiles are not affected the same way when winning or losing moisture, so it is important that samples start in the same conditions.
[52] Howell, 1996
[53] Timar-balazsy, 1999
[54]Timar-balazsy, 1999

This is crucial for archaeological textiles because the cells may collapse after losing the water in their structure, and consequently shrink severely[55]. Rapid drying increases also the rigidity and brittleness of the fibre because of the creation of crystalline structures when secondary bonds formed between new adjacent polymer chains[56].

In this particular case of the charred archaeological textiles, they were recovered wet and in a relaxed state. The water in the cells and hollows of the fibres supports their arrangement, but if it is flooded, disruption of the structure balance can occur (fibres break). When the water is removed, the textile becomes compact because the surface area of the air-water interface is minimised by the surface tension forces[57].

1.3.2 Stress relaxation:

Natural textile fibres act as viscoelastic materials, because when subjected to quick short forces, they can stretch and recover almost completely after the force has been removed. When the force is maintained, the fibre starts to deform in a viscous manner (bending, compressing, stretching or twisting). Once the force is removed after a long time, the fibre starts to recuperate slowly, but the recovery is often incomplete. The recoverable viscous deformation is called primary creep, and the non-recoverable deformation secondary creep[58].

Stress relaxation occurs when, after applying gradually increasing forces to a textile, the forces are progressively reduced while the deformation is maintained. If the forces continue, the textile eventually breaks. The relation between the amount of deformation (strain) and the tensile loading (stress) is normally represented with a stress-strain curve (Figure 2).
The curve normally represents the work of rupture (energy required to break the textile), the yield point (elastic limit after which the deformation is non-recoverable) and the elongation at break[59].

If a textile is under stress and the yield point is reached, the crease becomes permanent and it is non-recoverable at room temperature under dry conditions.

[55] Florian, 1988, p. 23
[56] McClintock, 1986, p. 146
[57] Peacock, 1992
[58] Morton and Hearle, 2008
[59] Dolez *et al.*, 2018, p. 26-39

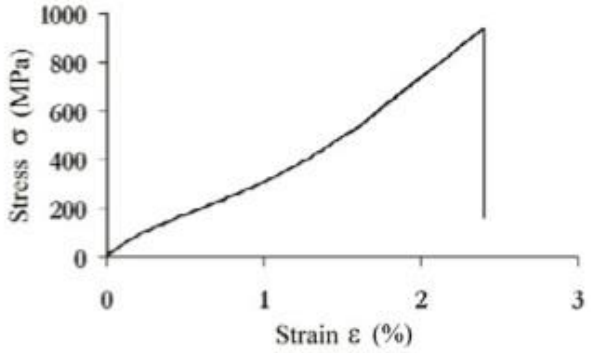

Figure 2 Example of a stress-strain curve of an elementary vegetable fibre[60]

1.3.3 Glass transition temperature and creasing:

Natural fibres have a glass transition temperature (Tg) very high at room temperature (around 230ºC for cellulose). Consequently, the secondary creep deformation is permanent when the textile is at room temperature, and will tend to recover when being above the Tg, bending more easily.
This fact is important when evaluating conservation treatments because the penetration of water in most natural fibres reduces its Tg to around room temperature[61].

1.3.4 The twist of the yarn:

The twist of the thread holds the fibres together, contributing to the strength of the ensemble. As the twist increases, the overall strength of the yarn increases as well, because of the lateral forces holding the fibres together. The moisture absorption is also limited depending on the twist, as the access of water to the interior of the thread can be restricted by it. Finally, aesthetical characteristics can be modified furthermore, depending on the twist, because it modifies the reflexion of the light[62].

[60] Charlet *et al.*, 2009, p. 234
[61] Cooke, 1988, p. 27-30
[62] Dolez *et al.*, 2018, p. 85-90

Chapter 2 Methodology: An overview

In this master thesis, the effect of different consolidation products applied to charred archaeological samples after freeze-drying them, as well as charred modern samples, is compared. After this evaluation, a discussion takes place, which analyses if the application of polyethylene glycol before freeze-drying has any effect on the results.

The first step is the study and analysis of the charred archaeological samples. The samples were found in the archaeological site of Elgg (Zurich). After the first investigation, carried out by the archaeological department, they were transported to the Collection Centre of the Swiss National Museum in Affoltern am Albis. Photographic documentation of the selected archaeological samples was created using a polyester film as support (to allow manipulation). The morphological characteristics of both surface and cross-section have been determined with microscopic techniques (such as polarised microscopy), and elementary analysis (Fourier-transform infrared spectroscopy or FTIR). For the identification of the white crystals on the surface of some samples, the Lumitester® PD-20 and LuciPac Pen® were used for the identification of mould, and RAMAN spectroscopy for the identification of salts.

The second step was the creation of charred samples with modern textile. Most of modern textiles receive finishing treatment during the fabrication process. A mixture separation test by solvent extraction was carried out, using a drop of Hexane, Ethyl Acetate, Toluene and Dimethyl Chloride, to identify the presence of finishing products before and after carbonisation. The modern textile was then washed in a washing machine V-Zug Adora S®, with surfactant Held® by Ecover®. For the carbonisation process, a ceramist oven Nabertherm® L3/11/C6 was used, and a thermocouple was added inside to control the temperature of the chamber as well as the temperature of the samples. FTIR was then used to identify the degree of carbonisation of the modern samples (depending on the temperature and the time), and to compare the results with the archaeological samples.

Because the archaeological samples were wet after the excavation, the modern samples were submerged in deionized water for 5 days (120h) to create comparable conditions of preservation. Ethanol (0.5mL per litre of water) was added to the solution to lower the surface tension of the textiles. During that time, the archaeological samples were cleaned with deionized water using an airbrush and a pressure from 0.1 to 14 psi. Both the archaeological samples and the modern samples were separated in two groups. One of them was treated with 8%v/v of polyethylene glycol (PEG) 400 in deionized water for one week. Because the charred textiles are very fragile, they could not be treated in a bath solution. Instead, they were drizzled 3 times a day with a PEG-solution. The other group of samples was kept moist with deionized water.

For the preparation of the freeze-drying treatment, a non-acidic blotting cardboard (wet with deionized water) was used on top of the metal plate as a support for the textiles. Then, the textiles were wrapped with one layer of Hollytex® (Article number: 3257) from Deffner & Johann® and attached to the metal plate with magnets. Everything was then wrapped with plastic film and conditioned in the fridge (at 4°C for 3 days) and then in the freezer (at -10°C for 24h). The freeze-drying treatment lasted 4 days and was carried out in a freeze-drier modified with a cooling system by Lyotec®. The freeze-dryer was pre-cooled at -50ºC, and then the textiles were treated setting the machine firstly at -43ºC, and then at -30ºC to speed up the sublimation process. During the process, iced cubes of deionized water and 8%v/v PEG 400 with thermocouples were added to the freeze-dryer, to control the temperature and the sublimation process. Apart from this, thermocouples were added to the textiles and the metal plates. After this treatment, some archaeological samples were cleaned again with a small vacuum.

The third step was the consolidation of the samples. The consolidants were selected for their physico-chemical characteristics, their ageing properties and their possible interaction with the textile. The chosen consolidants were Klucel® G, Klucel® E, Aquazol® 500 (all three from Kremer®), and Paraloid® B72 from Lascaux®. All four were applied with a pipette and diluted in ethanol. The treated samples were air-dried during 72 hours before testing the results. Three physical tests were carried out after drying. A Spectrophotometer CM-2600d by Konica Minolta® was used to compare the surface gloss before and after consolidation. For the bending strength test, to compare the flexibility and stiffness of the samples, the Cantilever test was applied, which was carried out on a Shirley Stiffness tester[63]. Finally, the tensile strength (hardness) of the fabric was also tested under a 90° angle[64]. All details about the equipment and conservation materials used during this project are described in Appendix 1.

[63] The test was based on the ISO Standard NF EN ISO 9073-7 (1998): *Test methods for nonwovens. Part 7: Determination of the bending length*.
[64] The test was based on the ISO Standard NF EN ISO 13934-1 (2013) *Textiles – Tensile properties of fabrics – part 1: Determination of the maximum force and elongation at maximum force using the strip method*

Chapter 3 Charred archaeological textiles from Elgg

3.1 Archaeological context of the textiles

The textiles studied in this Master thesis were found in the excavation of Elgg Kirchgasse 1 (Zurich, Switzerland) in 2017[65]. The site dates from the Late Medieval Period, and textiles were found buried and piled up inside the weaving cellar, which probably burned and collapsed (Figure 3)[66]. Thanks to the fire that destroyed the site, the textiles charred and were able to survive till our days. The blaze caused the textiles to carbonise, instead of burn and turn to ashes. No more information about the site is accessible nowadays, as the archaeological service of the Canton of Zurich is preparing a publication.

Figure 3 Block rescued with charred textiles from Elgg, Kirchgasse 1 ©Canton of Zurich

Studying the production of textiles during medieval times will allow us to understand the morphological characteristics of our samples. Late medieval textiles were made of plant fibres (flax, hemp and nettle), or animal fibres (wool and more rarely silk). During the long elaboration process, fibres were produced, harvested, spun into yarns and woven into fabrics. In the case of flax and hemp, the stems were gathered in bundles and combed (rippled) to eliminate the pods from the upper stems. Afterwards, the stems were left to rot for weeks until the stems break down. Then, once the stem is broken up, the fragments were swiped with a wooden blade to have clean fibres. As the fibres are still in their natural bundles, they are splatted into single fibres (heckling)[67].

For the spinning process of yarns, a spindle is generally used. Depending on the direction of rotation, the threads are twisted either clockwise or anticlockwise (z- or s- spun thread) (Figure 4). A horizontal treadles loom was then use for the weaving process (Figure 5), which can determine the appearance of a fabric depending on the way the horizontal weft threads are woven into the vertical warp threads.

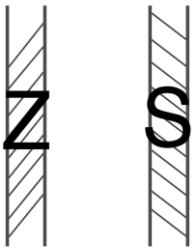

Figure 4 Directions of the twist of a yarn, indicated as Z or S

[65]Gisler and Moser, 2018, p.46
[66] Hartmann, 2018
[67] Brandenburgh, 2016, p. 19-24

One of the most common types of weaves used during the early Middle Ages is the tabby weave (also called plain weave), where weft threads regularly pass over and under each warp thread. In the case of linen fabrics, they were often washed and bleached after weaving to achieve a white colour[68] [69].

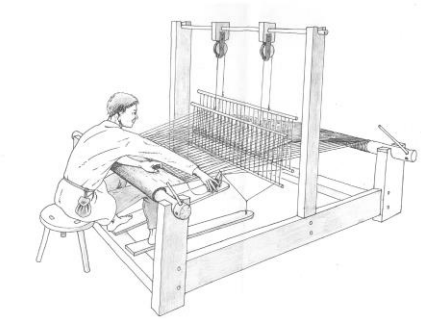

Figure 5 Reconstruction of a horizontal treadle loom. ©C. van Hees

3.2 Characterisation of the textiles

Seventy-five samples founded in Elgg, Kirchgasse 1 were separated of the ensemble of textiles for research purposes. Of those 75 samples, 72 are flat textiles and 3 remain attached to some layers of soil. They were delivered to the Swiss national Museum in three boxes (Figure 6, 7 and 8).

Figure 6 Charred archaeological textiles from Elgg, Kirchgasse 1. Test material from the box 2/3 ©HE-Arc

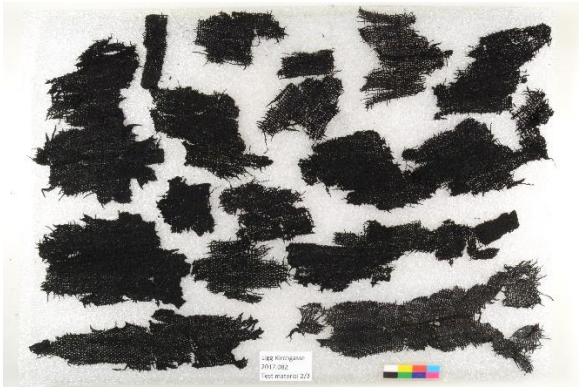

Figure 7 Charred archaeological textiles from Elgg, Kirchgasse 1. Test material from the box 2/3 ©HE-Arc

Figure 8 Charred archaeological textiles from Elgg, Kirchgasse 1. Test material from the box 3/3 ©HE-Arc

[68] Brandenburgh, 2016, p. 19-24
[69] Rast-Eicher, 2016

3.2.1 Identification of the fibres

Fibres from the archaeological textiles have been identified with microscopic techniques. The identification of the fibre is useful to predict the behaviour of a textile, to understand its degradation state, and to plan an appropriate conservation treatment and storage method. To facilitate the characterisation of the samples, an identification number was given to each one[70].

For the identification of the fibres, the surface appearance and cross-section characteristics were observed. Unfortunately, fibres in poor condition, very dark and degraded, make the identification with a microscope harder because not all distinctive features are preserved. In addition, when plant materials are charred, the rays shrink with carbonisation, so the diameter of fibres can change[71].

The cross-section features

A copper metal plate was selected for the cross-section observation, with a thickness of 0.45mm. Holes with 0,7mm were created to trap the fibres inside. Two fragments of threads were chosen from the samples 3.4 and 3.8, one from each direction of the fabric (Appendix 2). The threads location is visible in the Appendix 2. Polyester threads are pulled through a small perforation in the metal plate, with the charred fibre placed in the middle of the synthetic fibres. The fibre will be trapped inside once the polyester is pulled through the cavity (Figure 9). The remains are cut with a razor blade[72]. Using light coloured polyester threads will help lo differentiate the black charred fibre.

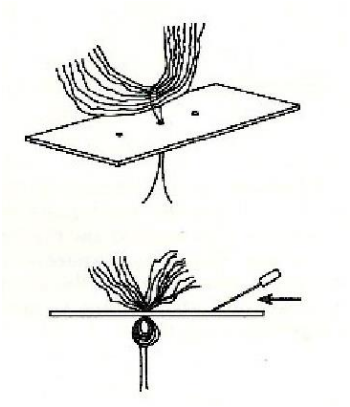

Figure 9 Plate Cross-section method procedure ©Goodman M

The cross section of the fibre was observed under the optical microscope [73] (2,5x, 5x, 10x, 20x, and 50x objectives). The interior central lumen is very small, less than half of the full width of the fibre, and is like a dotted form (Figure 10). The shape of the cross-section varies from five to seven sides, with sharp peaks (Figure 11).

[70] Two numbers separated with a dot compose the identification number. The first digit belongs to the number of the storage box, and the second digit to the sample inside the box (e.g. 2.14 alludes to the samples number 14 from the box number 2). Only three samples have an identification number with a letter (A and B), which indicates that the textile fragment is still attached to layers of soil. The sample B.1 is a broken fragment that belongs to the sample B.
[71] Rast-Eicher, 2016, p. 21
[72] Rast-Eicher, 2016, p. 67
[73] Information about the microscope: Zeiss® (Carl Zeiss, Germany), Axioplan, EL-Einsatz, 451898, 115-230V, 50…60Hz, 200VA

Diameter of the fibres is around 23µm (Measurements were done through the AxioVision® Rel.4.6 software). OX and YX fibres from both samples presented the same features, so probably they are made of the same material.

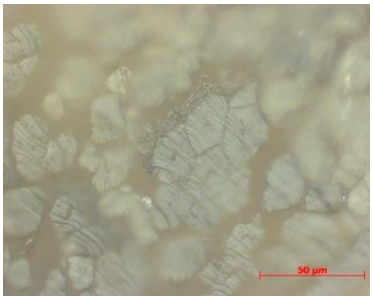

Figure 10 Cross section of the fibre from sample 3.4, under the microscope x50 ©HE-Arc

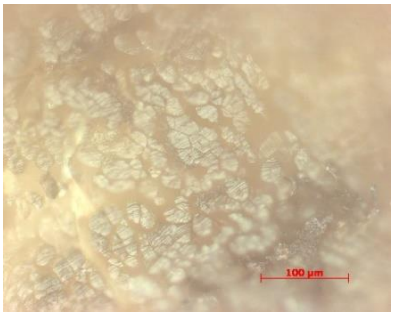

Figure 11 Cross section of the fibre from sample 3.8, under the microscope x20 ©HE-Arc

The transversal features

Fibres were observed under the polarised microscope, and prepared on a glass microscope slide. Meltmount® was used as mounting medium, and the glass slide was pre-heated to reduce its viscosity. One thread from the archaeological samples 2.4, 2.19 and 3.3, were selected (Location described on Appendix 3). To allow the identification, the fibres were separated from one another but, because of their charred state, it was not always possible without breaking the fibres. In those cases, the ensemble was observed together (Figure 12). After placing the fibres on the glass slide, a drop of hot Meltmount® was added. The fibres were then covered with a small glass and let them dry.

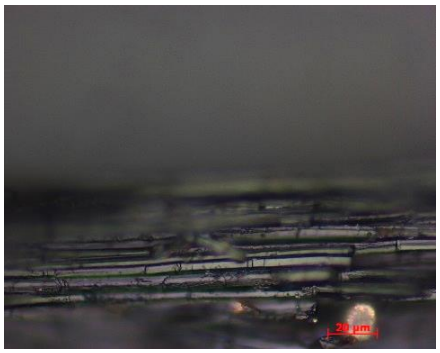

Figure 12 Group of fibres from sample 3.3 under the polarised microscope x50, bright field ©HE-Arc

Figure 13 Single fibre from sample 2.19 under the polarised microscope x50, bright field ©HE-Arc

Under the microscope, the fibres are smooth lengthwise, long and tubular. The nodes are visible at intervals along the length of the fibres. Cross markings are present and shaped in I, V and X (Figure 13). The interior of some broken fibres was observed and their canal is well-defined and regular in width. No crystals were visible.

Results and comparison

The features observed on the cross-section and the transversal-section are similar to flax (linen) or hemp fibres. The main morphological characteristics are similar, like the cross-section bundles and the longitudinal view[74], so the differentiation is scarce in the fibre form. Anyhow, hemp fibres are longer and, in cross-section, hemp is flat, circular, and has an internal lumen bigger than flax[75].Flax is polygonal when observed with the cross-section[76] and the lumen is smaller (Figure 14). However, because of the shrinkage of the fibres during carbonisation, the observed features could also be identified as hemp.

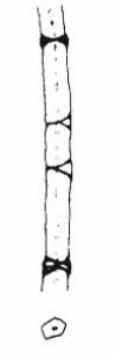

Figure 14 Longitudinal representation of flax in good condition ©CCI

Finally, **the fibres were identified as flax (linen) or hemp.**

The comparison between the characteristics of modern fibres and archaeological fibres can be used to reinsure the identification. The modern linen fibre[77] was also mounted with Meltmount® and, when compared, both modern and archaeological fibres presented similarities in terms of nodes and cross-markings, as well as the lumen (Figure 15). The difference between carbonised and un-carbonised linen was more apparent when observed under the polarized microscope with the analyser plate. Both fibres were observed with polarized light at maximum brightness and at extinction (Figure 16 and 17). No coloration was visible on the charred fibre at maximum brightness.

Figure 15 Modern flax fibre under polarised microscope x20, transmitted light ©HE-Arc

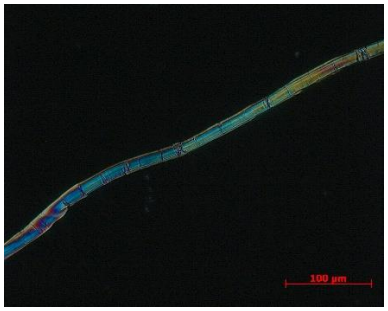

Figure 16 Modern flax fibre under polarised microscope x20, analyser plate, fibre at maximum brightness ©HE-Arc

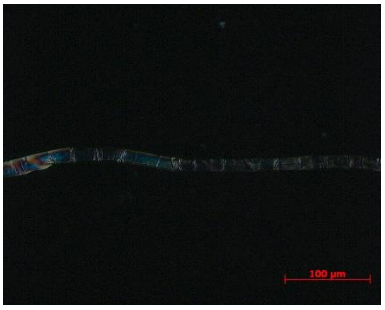

Figure 17 Modern flax fibre under polarised microscope x20, analyser plate, fibre at extinction ©HE-Arc

For the complete photographic documentation of the fibres, go to Appendix 4.

[74] Horrocks and Anand 2000, p. 380
[75] Thygesen 2006
[76] Sponner et al. 2005, 179
[77] Pure linen L40® from Lascaux®

3.2.2 Characteristics of the fabric and the threads

For the characterisation of the fabric, each sample has been observed under the microscope. All samples present a plain weave or tabby weave, which means that the weft threads pass over each warp thread in a regular way. The proportion is one thread of weft and one thread of warp (1:1) (Figure 18). Because of the lack of selvedge on the samples, it is difficult to establish which threads are the warp threads, and which ones are the weft threads. Henceforth, references to them will be made as the vertical (OY) and horizontal (OX) threads. The vertical threads belong to the direction with the highest number of threads per centimetre square[78].

All fibres have been twisted in the Z- direction to create both vertical and horizontal threads (Figure 19). The angle of torsion, which determines the tightness of the twist[79], is between 5 and 30 degrees depending on the sample. It is a primary torsion because there is no combination of threads to create a bigger ensemble.

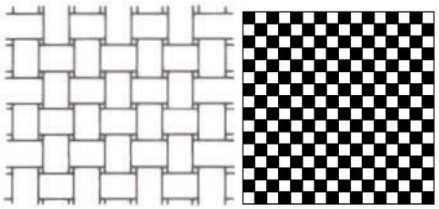

Figure 18 Example of plain weave (left) and its geometrical representation (right) ©The J. Paul Getty Trust

The dimensions of the samples have been measured with an electronic calibre. The measured dimensions belong to the maximum dimensions of both X- and Y-axes. All samples have different dimension. The biggest sample (2.01) measures 14.19 x 6.2cm, while the smallest sample (1.10) measures 1.98 x 1.8 cm. In the Appendix 5, you will find a table where all morphological characteristics per sample are described.

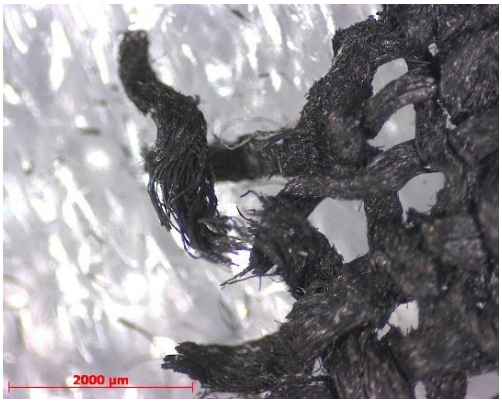

Figure 19 Detail of the sample 2.14 under the microscope x1.6, Z-twist visible ©HE-Arc

Depending on the sample, the following characteristics may be different: the number of threads per centimetre square, the diameter of the thread, the distance between the threads, and the angle that a vertical thread creates when crossing a horizontal thread.

To calculate the number of threads per centimetre square, three areas of the sample have been counted to assure that the number of threads is homogeneous in all parts. A microscopic picture of each sample has been taken with an AxioCam® MRc from Zeiss®, and the image has been treated with the software AxioVision® Rel.4.6 to add and scale, and allow the count (Figure 20, 21 and 22).

[78] Moulhérat, 2011

[79] The angle between the vertical axis of the thread and the slant of the twist. Tight fibres have angles higher than 25 degrees, angles of 10 to 25 are considered medium, and up to 10 degrees are loose (Florian *et. al.,* 1990)

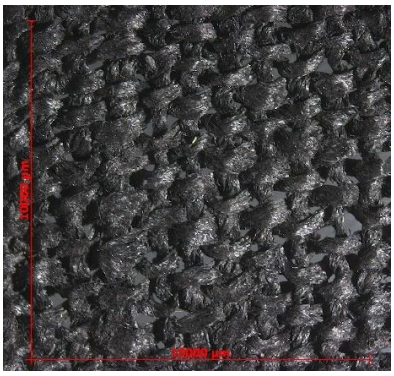

Figure 20 Detail of sample 2.2 under the microscope x0.65 ©HE-Arc

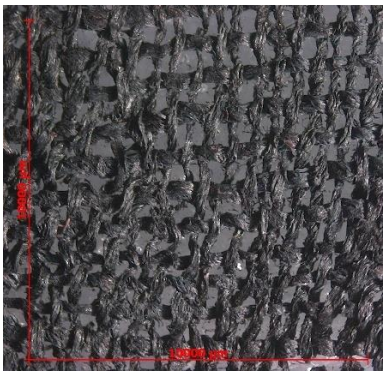

Figure 21 Detail of sample 3.11 under the microscope x0.65 ©HE-Arc

Figure 22 Detail of sample 3.6 under the microscope x0.65 ©HE-Arc

All samples have been classified in six main groups depending on the number of threads per centimetre square[80]: 37 samples with 17x10(±1) threads/cm², 13 samples with around 20x10(±1) threads/cm², 10 samples with 15x9(±1) threads/cm², 5 samples with 12x17(±1) threads/cm², 3 samples with 21x14(±1) threads/cm², and a last group with random count. This last group is composed of five samples impossible to classify, and two samples so degraded that it is not possible to count their threads.

The diameter of the thread is variable in its length[81] (Figure 23). Yarns in the archaeological samples have diameters that range between 0.25mm to 0.79mm for the OY direction, and between 0.26mm to 0.74mm for the OX direction. The mean value is around 0.50mm for the OY direction and 0.52mm for the OX direction. In most cases, the vertical threads have the same mean diameter as the horizontal threads. Only in specific cases, there is a difference and the vertical threads are thinner than the horizontal threads.

Figure 23 Detail of the sample 1.21 under the microscope x0.65. Vertical threads are thinner than horizontal threads ©HE-Arc

[80] Based on the ISO Standard NF EN ISO 4602 (2011): *Reinforcements – Woven fabrics – Determination of number of yarns per unit length or warp and weft*

[81] Microphotographs of the samples treated with the software AxioVision© have been used to calculate the diameter of the threads.

No fibre length or linear density can be calculated from the archaeological samples, because the crimp from the yarn must be removed in advance, and this is not possible when textiles are charred (Figure 24).

Figure 24 Example of crimped yarn that after carbonisation keep the form weaved. Detail from the sample 2.17 under the microscope x1 ©HE-Arc

Three categories were stablished for the distance between threads. An open fabric refers to samples where the distance is higher than 0.3mm and the support below the fabric is perfectly visible. If the distance is between 0.05mm and 0.3mm, the sample will belong to the semi-open fabric type. If there is no space between the threads or the distance is smaller than 0.05mm, it is a closed fabric (Figure 25, 26 and 27).

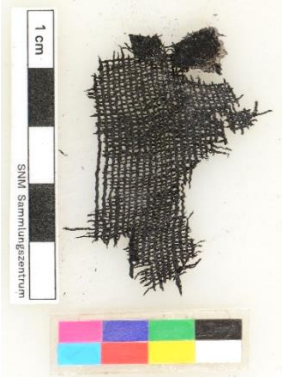

Figure 25 Sample 3.11. Open fabric ©HE-Arc

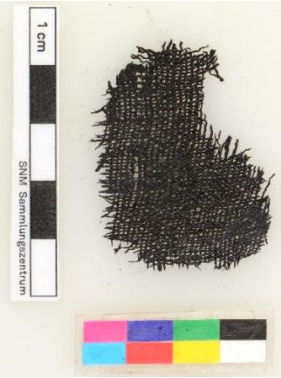

Figure 26 Sample 3.18. Semi-open fabric ©HE-Arc

Figure 27 Sample 2.18. Closed fabric ©HE-Arc

Finally, the samples have been classified depending on the angle created when a vertical thread crosses a horizontal one. Perpendicular will denote 90° between OY and OX threads, diagonal will correspond to 45°, and partially diagonal - to an angle between 90° and 45° (Figure 28, 29 and 30).

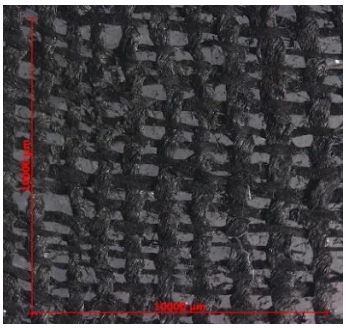

Figure 28 Detail of sample 3.5 under the microscope x0.65. Perpendicular weave ©HE-Arc

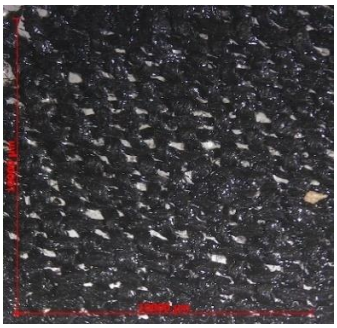

Figure 29 Detail of sample 1.11 under the microscope x0.65. Partially diagonal weave ©HE-Arc

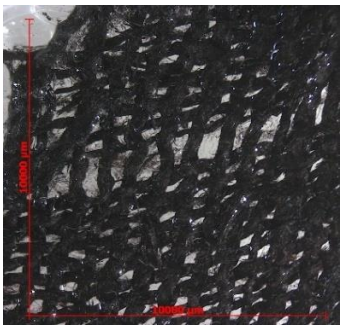

Figure 30 Detail of sample 1.38 under the microscope x0.65. Diagonal weave ©HE-Arc

3.2.3 Peculiarities of some samples

Specific characteristics have been discernible in some samples. The sample 2.19 presents a seam perfectly preserved with an extra thread used as link (Figure 31), and sample 2.01 has a little fragment of edge still attached to the sample (Figure 32).

Figure 31 Detail of the seam from sample 2.19 under the microscope x0.65 ©HE-Arc

Figure 32 Fragment of selvedge from the sample 2.01 under the microscope x0.65 ©HE-Arc

Samples 1.29, 1.17, 1.22, 1.24, 1.14 are composed of two or more layers of textiles, or present some threads which do not belong to the samples, indicating that the fragment was recovered from a pile of fragments (Figure 33 and 34). Lastly, a few samples are charred fragments with a big layer of soil and charcoal underneath (Figure 35). In two of them, A and B, the layer of soil is thicker than 0.5cm. Sample B.1 is a fragment detached from the sample B.

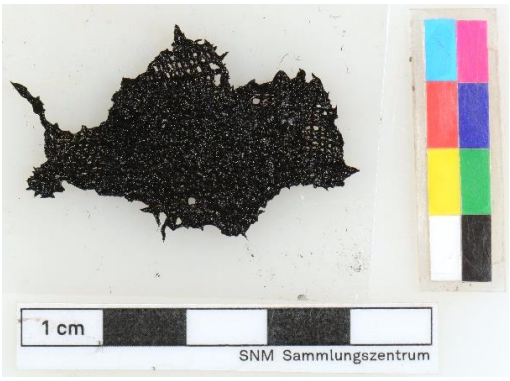

Figure 33 Sample 1.17 with two layers of textile ©HE-Arc

Figure 34 Sample 1.24 with two layers of textile ©HE-Arc

Figure 35 Detail of sample 1.14 with a layer of soil attached to the textile ©HE-Arc

3.3 Determination of the state of preservation

The samples were already pre-cleaned by the archaeological department of Zurich. All selected samples were received in a wet state; some of them were moist, while others were soaked in a mixture of alcohol and water. They have been preserved in their received condition, waiting for the conservation treatment, in a fridge at 4°C to protect them from both moisture loss and bio-deterioration[82]. Detailed information about the characteristics and degradation state per sample is available in Appendix 5.

3.3.1 Surface degradation:

Soil and dust are present on the surface of all archaeological samples. The soil is visible to the naked eye, and comes from the burial environment (Figure 36 and 37). Other non-adherent materials, which are only visible under the binocular or microscope, also create the dirt on the surface. White, green and red synthetic fibres, which are most probably coming from the archaeologist clothes and materials used during the excavation, are visible under the microscope (Figure 38 and 39).

Figure 36 Detail of sample 3.7 under the microscope x1.25. Soil and dust trapped between the fibres ©HE-Arc

Figure 37 Detail of sample 3.14 under the microscope x0.8. Soil and dust trapped between the fibres ©HE-Arc

Figure 38 Detail of sample 2.02 under the microscope x2. Green fibres ©HE-Arc

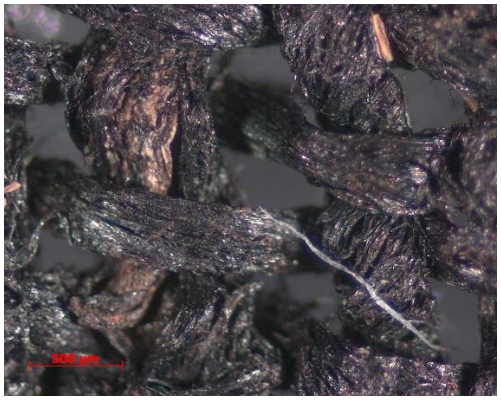

Figure 39 Detail of sample 3.01 under the microscope x3.2. White fibre ©HE-Arc

[82] Rothenhäusler and Travis, 2003

Another common material present in most samples is charcoal shards, which have no homogeneous shape or surface characteristics, and do not belong to the textile (Figure 40 and 41). In addition, two samples (3.1 and 2.2) present a green compact non-adherent powder (Figure 42 and 43). Both charcoal and corrosion materials are probably contamination products coming from the surrounding burial environment.

Figure 40 Detail of sample 1.06 under the microscope x2. Fragment of charcoal ©HE-Arc

Figure 41 Detail of sample 3.07 under the microscope x2.5. Fragment of charcoal ©HE-Arc

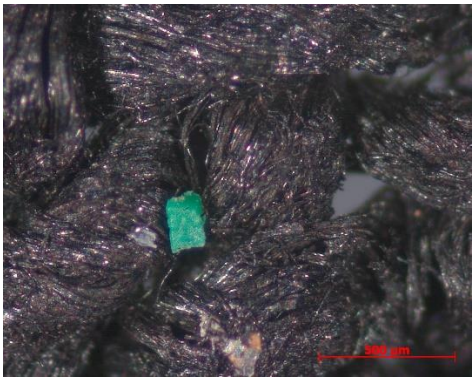

Figure 42 Detail of sample 2.02 under the microscope x5. Green deposit ©HE-Arc

Figure 43 Detail of sample 3.01 under the microscope x5. Green deposit ©HE-Arc

Finding two or more layers of fibres, threads or even textile fragments on the same sample is also common (Figure 44), due to the conditions of the recovery of the textiles, which were found as a pile of textile material.

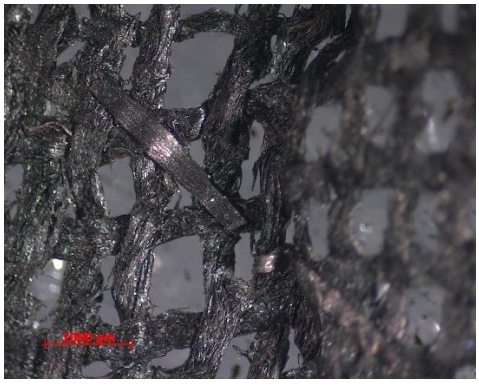

Figure 44 Detail of sample 3.03 under the microscope x1.6. Fragment of thread belonging to another layer of textiles ©HE-Arc

Several samples had a whitish appearance, because of the transparent crystal-like materials attached to the surface (Figure 45, 46, 47 and 48). A first attempt to identify the materials was made with RAMAN spectroscopy, to see if they were mineral-based materials, but no identification was possible.

Then, FTIR analysis classified the material as organic[83]. The presence of mould was tested with the Lumitester® PD-20 and LuciPac Pen®, but the results were inconclusive, maybe because there was not enough material on the area tested. For the details about the tests, go to Appendix 6 and Appendix 7.

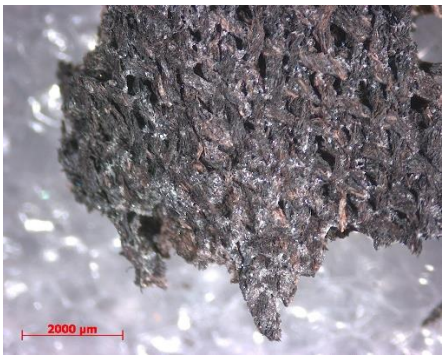

Figure 45 Detail of sample 3.11 under the microscope x1. White crystal-like deposits ©HE-Arc

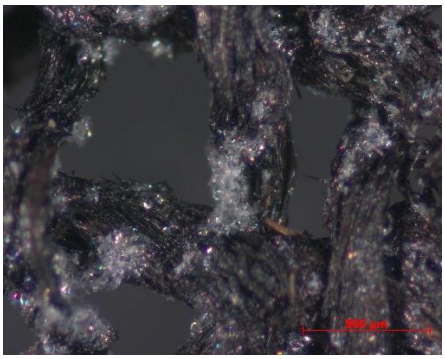

Figure 46 Detail of sample 3.11 under the microscope x5. White crystal-like deposits ©HE-Arc

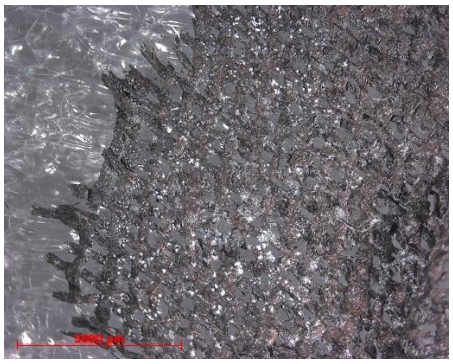

Figure 47 Detail of sample 3.19 under the microscope x0.65. White crystal-like deposits ©HE-Arc

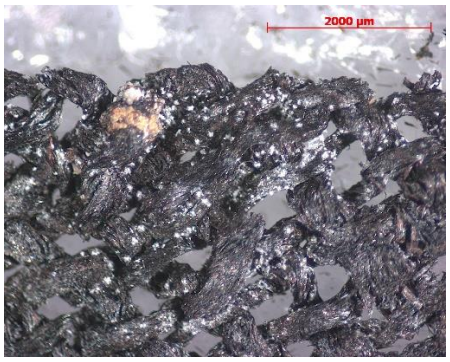

Figure 48 Detail of sample 3.22 under the microscope x1.6. White crystal-like deposits ©HE-Arc

3.3.2 Degree of carbonisation:

FTIR spectroscopy analysis helped us understand the degree of carbonisation of the charred archaeological textiles. The analyses were carried out in an FTIR spectrometer[84] (Excalibur Series FTS 3500GX with UMA-500 Microscope Biorad Co.) with a diamond press cell.

Two fibres were selected for the analysis, one vertical thread from sample 2.3 (Figure 49) and one vertical thread from the sample 2.6 (Figure 50). Neither sample showed evidence of organic substances or oxidation. The carbonisation seemed to be complete on the archaeological textiles.

[83] Is a long-chained organic compound with a C=O group (ester) and a hydroxide part
[84] The FTIR analysis were carried out by Erwin Hildbrand.

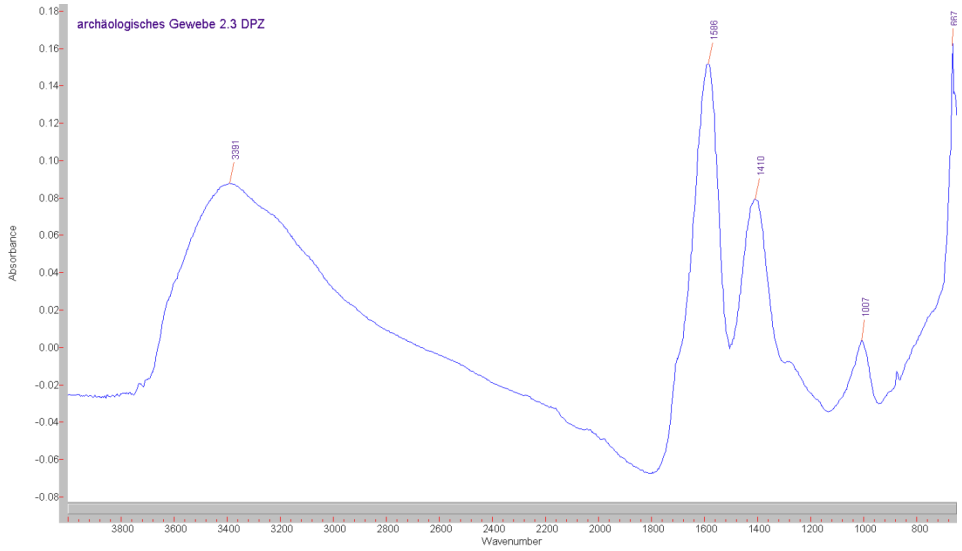

Figure 49 FTIR spectrum of the sample 2.3. The peaks at 3391, 1410 and 1007 cm^{-1} are signs for –OH groups, and the peak at 1586 cm^{-1} might be the -C-C- of carbon.

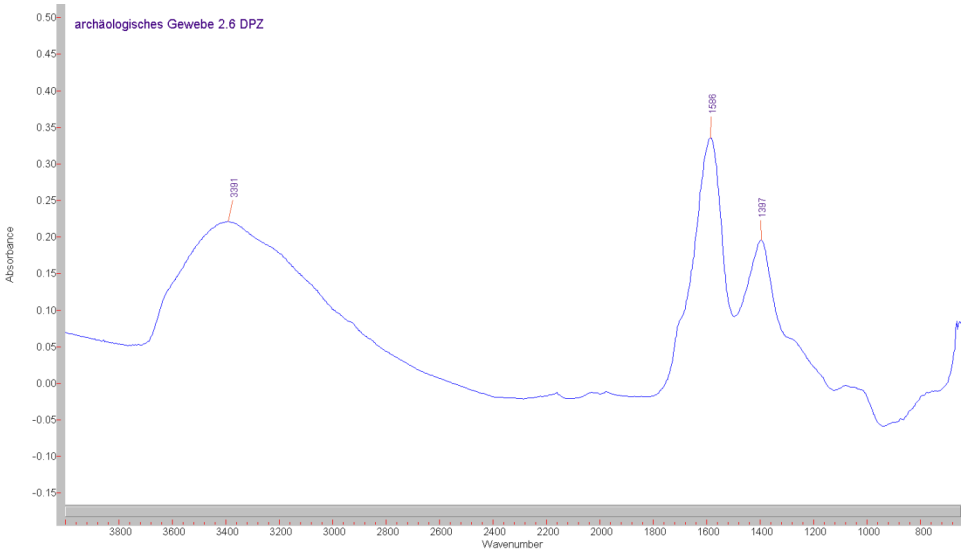

Figure 50 FTIR Spectrum of the sample 2.6. The peaks at 3391 and 1397 cm^{-1} are signs for –OH groups, and the peak at 1586 cm^{-1} might be the -C-C- of carbon

3.3.3 Structural stability:

All samples have fibres and threads that are broken or missing (Figure 51, 52, 53 and 54). Quite frequently, the deterioration is not uniform throughout a textile, because fibres on the surface of the textile are more exposed to the atmosphere and abrasive action[85]. None of the samples are complete, so individual fragments compose the ensemble of charred textiles. The lack of documentation does not allow us to relate one sample to another, aside from relating their morphological characteristics and the site where they were found.

[85] Peacock, 1992, p. 199

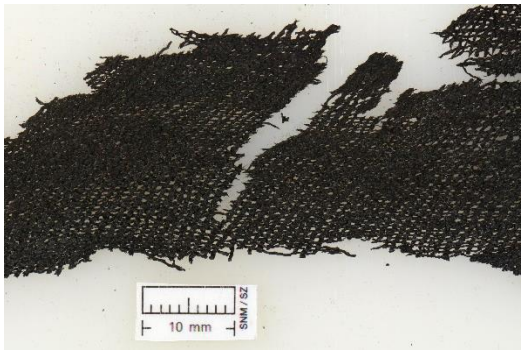

Figure 51 Detail of the sample 3.16. Broken threads ©HE-Arc

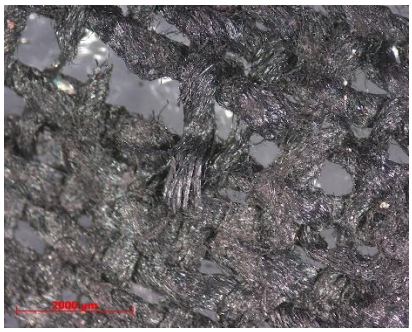

Figure 52 Detail of the sample 2.7 under the microscope x1.25. Broken fibres ©HE-Arc

Figure 53 Detail of the sample 2.9 under the microscope x2.5. Broken fibres ©HE-Arc

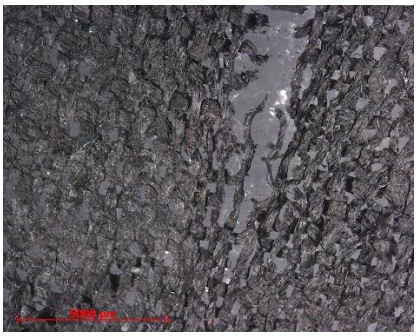

Figure 54 Detail of the sample 3.13 under the microscope x0.65. Broken threads ©HE-Arc

Because of the charred state, rigid and brittle fibres compose the structure. Brittleness is the main characteristic that defines the state of degradation of the fabric, indicating the loss of the original flexibility of the threads (Figure 55 and 56). Although, due to the presence of water in-between the fibres, which acts like a lubricant and keeps the fibres together thanks to the surface tension, the threads can move easily. Consequently, any movement of the textiles can lead to new broken threads and fibres.

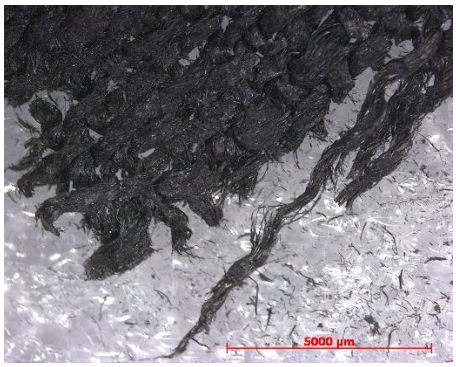

Figure 55 Detail of the sample 2.8 under the microscope x0.8. Brittle and broken fibres ©HE-Arc

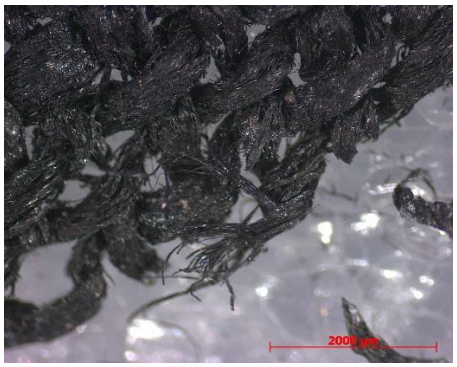

Figure 56 Detail of the sample 1.4 under the microscope x1.25. Brittle and broken fibres ©HE-Arc

Folded edges are visible in most samples (Figure 57), as well as threads that are displaced or mixed (so they are no longer in their original emplacement) (Figure 58 and 59). Observed under the microscope, crushed fibres are visible, as if something heavier was on top of the textiles and compressed the threads (Figure 60).

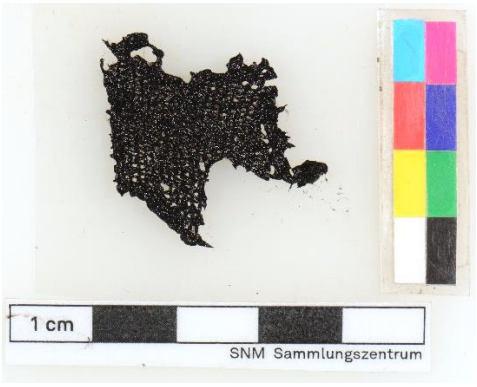

Figure 57 Sample 1.05. Folded edges ©HE-Arc

Figure 58 Detail of the sample 3.2 under the microscope x1. Displaced thread ©HE-Arc

Figure 59 Detail of the sample 2.01 under the microscope x0.65. Displaced thread ©HE-Arc

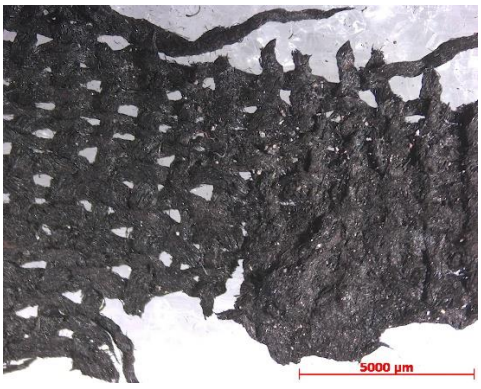

Figure 60 Detail of the sample 2.15 under the microscope x0.65. Crushed and uncrushed threads ©HE-Arc

Most of the samples are also deformed, torn, and warped. Samples like 2.01, 2.16 and 2.07 present the same symmetric crease (Figure 61), which could mean that they were one on top of each other when found in the soil.

Finally, broken pieces are also a problem for samples like 3.12 among others (Figure 62). The fragment remains in its original location but is disaggregated of the sample. Damage like this one, are most likely related to the physical manipulation of the object.

Figure 61 Sample 2.16. Detail of the horizontal creep ©HE-Arc

Figure 62 Sample 3.12. Disaggregated fragment ©HE-Arc

3.4 Conclusion and Classification

Because of the consolidation experiments developed in this master thesis, a homogenous group of charred archaeological textiles to test was needed. Consequently, all archaeological samples were categorized depending on the physical characteristics (type of fabric, number of threads per cm², diameter of fibres, etc…). The aim of the classification is to select a group of samples with the same characteristics in order to have comparable results.

Samples were sorted in five groups, indicated with the colours blue, pink, yellow, brown and green (See Appendix 5). The feature used for the classification was the number of threads per cm². Table 3 shows the specific number of threads per cm² for each group. **The blue set was selected** because of the number of samples available. Detailed photographic documentation can be found in Appendix 8.

Number of samples on the group	Number of threads per cm²	Colour
37	17x10 ±1	
13	20x10/21x11 ±1	
10	15x9 ±1	
5	17x12 ±1	
3	21x14 ±1	
7	Various	None

Table 3 Assigned colour for each group of samples

Chapter 4 Production of test samples

4.1 Aim

To allow a wider investigation on the effect that different consolidants can have upon carbonised textile, modern charred samples had to be created. The idea is to have several samples with the same dimensions, material and physical characteristics so that their comparison is possible before and after being carbonised and consolidated. The modern samples will allow us to test their physical properties in a standard and homogeneous way, as they are all created in identical conditions and following the same methodology.

4.2 Preparation of the samples

4.2.1 Selection of the modern textile

After studying the morphological characteristics of the archaeological samples, a modern textile with the equivalent characteristics was bought. The final choice was made with focus on the type of material, the type of fabric, the number of threads per cm² and the diameter of the threads most similar.

The linen for lining and painting 300 from Lascaux® (Article number 4452) was chosen. It is a 100% pure Belgian linen, untreated, unbleached, and not calendered textile. This linen fabric has a 1:1 plain weave with approx. 16 warp threads per cm and approx. 12.5 weft threads per cm. The weight of the textile is 305g/m² (The technical information provided by the supplier is available in the Digital Appendices). Because of the secret of manufacture, no specification about finishing products were found in the technical sheet offered by Lascaux®[86].
Therefore, a mixture separation test by solvent extraction was performed on a sample of the same article from their catalogue before buying it, to know if the linen was untreated by the supplier company.

Mixture separation test by solvent extraction

For this procedure, a sequence of solvents was applied to a sample, to selectively remove one or more components from a mixture. Figure 63 shows the scheme of solubility for many natural and synthetic materials, which was followed for this test.

[86] In Lascaux's web page, they recommend that "Raw linen, cotton and other natural textiles should be thoroughly washed in warm water prior to stretching onto stretchers to remove most of the finishing agent", but no finishing agent was mentioned in the technical sheet of the textile.
A textile as pure as possible was wanted, Lascaux's office was contacted and they told us that, even if they do not treat the textiles, the company to whom they buy the textiles could add some finishing products. No more information was available because of the secret of manufacture.

The Lascaux® sample from the catalogue was divided in three squares. The first square was tested as it was. The second square was washed for 2h in hot deionized water with a surfactant[87]. The third one was also washed, and then carbonised at 500°C wrapped in aluminium foil.

Some fibres of the first square (unwashed) were selected for the solvent extraction and left on a glass plate. The test started with a drop of hexane, but no extraction was visible. Then, a drop of ethyl acetate was added and a sticky and transparent material was dissolved. The residues of the extraction were visible under the microscope after the evaporation of the solvent. Toluene and Dimethyl Chloride were also tested following the same methodology but, as the extraction was produced when adding ethyl acetate, no new information was acquired when testing those two solvents.

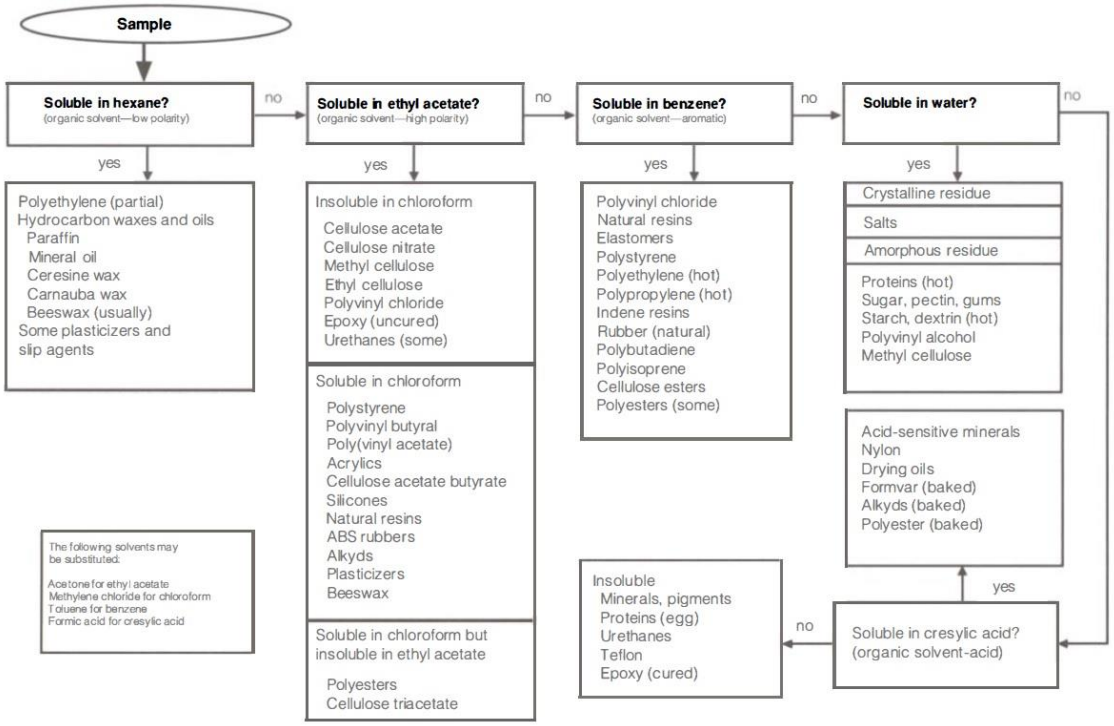

Figure 63 A solubility schematic for many natural and synthetic materials ©Getty Conservation Institute

The same procedure was repeated on fibres from the other two squares. Fibres from the washed sample also emitted the same product when tested with a drop of Ethyl acetate, but in this case, less residues of product dissolved on the glass plate were observed. The test performed on the carbonised sample showed negligible residues, almost invisible under the microscope. It was no possible to tell if those residues came from the sample or from the drop itself.

[87] Held® by Ecover® was used as surfactant following the recommendation of the textiles conservators from the Swiss National Museum. It is used by them when textiles are washed in the washing machine.

It was determined that, even if there is an unknown material recovering the fibres of the Lascaux® textile, washing it helps reducing the amount of finishing product present on the threads. Also, it was assumed that during carbonisation the finishing product burns and no residues are left, leaving an almost pure linen fabric. In conclusion, **Lascaux's Linen 300® is a suitable textile to create the samples** for this Master thesis.

4.2.2 Washing procedure before sampling

According to the textile conservators in the Swiss National Museum, any textile bought nowadays must be washed before use, to avoid chemical products applied during the fabrication process[88]. This advice, in addition to the results of the mixture separation test by solvent extraction, prompted me to follow this necessary step of washing the textile.

The textile was washed three times at 60°C during 1.30h, in a V-Zug Adora S® washing machine. The first time I added to the process the surfactant Held® by Ecover® to facilitate the removal of the finishing products[89]. The second and third time the textile was washed only with water, to remove the residues from the surfactant.

The textile was left dry for 48 hours. After drying, the textile was deformed and creased. Such deformations do not allow sampling the textile in a homogeneous manner, so I ironed it with a PFAFF® steam ironer 580, using the linen mode and deionized water.

4.2.3 Sampling process

The sampling process was inspired on standards created by the International Organization for Standardization (ISO[90]), corresponding to the physical tests applied in this research project[91].
I wanted to test bending length (flexibility), the tensile strength (hardness), and the changes in colour and gloss, all before and after consolidation. In consequence, the following recommendations for the sampling process were considered:

[88] Calonder, 2018
[89] The extraction of finishing products was visible when the surfactant foam inside the washing machine turned yellow.
[90] ISO is a non-governmental international organization that brings together experts to share knowledge and develop voluntary, consensus-based, market relevant International Standards that support innovation and provide solutions to global challenges.
[91] Sampling process based on the following ISO Standards:

- NF EN 12751 (1999): *Textiles - Sampling of fibres, yarns and fabrics for testing*
- NF EN 13934-1 (2013): *Textiles - Tensile properties of fabrics – Part 1: Determination of maximum force and elongation at maximum force using the strip method*
- NF EN ISO 9073-7 (1998): *Textiles - Test methods for nonwovens – Part 7: Determination of bending length.*

- The dimensions of the samples taken must be sufficient to carry out the physical test
- Samples must be cut in both warp and weft directions, as the properties in each direction can differ because of the different number of threads per cm² in each direction[92]. Woven fabrics are normally orthotropic, they present two orthogonal preferential directions (warp/weft). Therefore, their mechanical response can be very different depending on the direction of the force applied[93].
- Any sample should not be cut closer than fifteen centimetres from the edge of the textile, to avoid deformations and edges, which can react differently to the forces applied.
- To have statistical results, the minimal number of 5 samples per direction, dimension, freeze-drying procedure and consolidants must be established.
- For the dimensions, threads shall be removed from each side of the sample until having a full thread of the desired length.

	Minimum number of test	**Number of test per sample**	**Dimensions**	**Cutting process**	**Preparation**
Tensile strength	5 each direction	1 time each	250±1 x 50±0,5 mm	Let 150mm from the edge	Threads shall be remove from each side until you have a full thread of 50±1mm
Bending length	5 each direction	4 times each sample (both ends, and both above and under face)	250±1 x 25±1 mm	Let 150mm from the edge	Threads shall be remove from each side until you have a full thread of 50±1mm
Colour and gloss	No specification for the sampling procedure				

Table 4 Detailed information about the sampling procedure for each ISO standard

During the sampling process, long strips of textile with the same yarns were cut in both directions, as the Figure 64 shows. This method allowed to have the same longitudinal yarns in several samples, to reduce morphological differences in-between them. First, four types of samples were selected:

- Samples with 25 x 5cm with the longest dimension corresponding to warp threads
- Samples with 25 x 5cm with the longest dimension corresponding to weft threads
- Samples with 25 x 2.5cm with the longest dimension corresponding to warp threads
- Samples with 25 x 2.5cm with the longest dimension corresponding to weft threads

[92] Dolez *et al.*, 2018, 14
[93] Dolez *et al.*, 2018, p. 26

To reach these dimensions, two facts must be considered. On one hand, the dimensions of textile can be subjective (depending on the person who takes the measure), and may vary from one person to another because of the properties of this organic material. Hence, a specific number of threads per type of sample was established (based on the number of threads per cm²), which corresponded to the desired dimensions (Table 5). On the other hand, all samples were cut 0.5cm bigger than the dimensions established to be able to remove the threads from each edge, until I had full threads of the desired dimensions (Figure 65). They were all cut with sharp scissors.

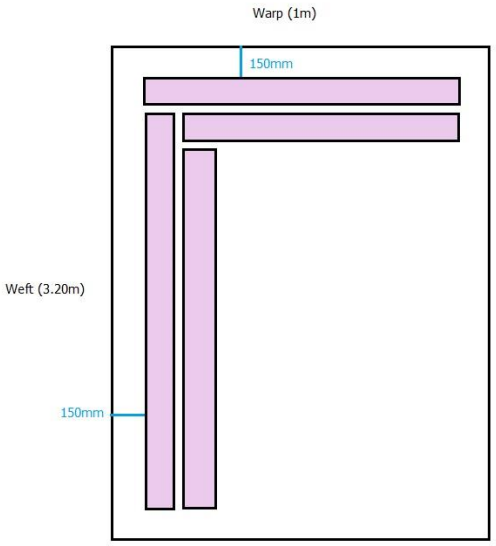

Figure 64 Location of test specimens cut from the Linen 300®

Figure 65 Schematic representation of the dimensions before (red) and after (orange) removing the smaller threads from the edges

Before removing threads from each edge		**After removing threads from each edge**	
Dimensions of the sample	Number of threads	Dimensions of the sample	Number of threads
25,5 x 5,5 cm	≥90 warp threads on the warp samples	25 x 5 cm	80 warp threads on the warp samples
	≥75 weft threads on the weft samples		65 weft threads on the weft samples
25,5 x 3 cm	≥50 warp threads on the warp samples	25 x 2,5 cm	40 warp threads on the warp samples
	≥40 weft threads on the weft samples		33 weft threads on the weft samples

Table 5 Number of threads per sample before and after the removal from the edges of the incomplete threads

Final modification of the dimensions

Because of technical problems with the oven[94], the longest dimension of each sample was cut in half, so that they could fit inside the oven that was eventually used. As the result of the sampling process, samples of 12.5x5cm and 12.5x2.5cm in both warp and weft dimensions were created (Table 6).

Direction of the sample	Dimensions	Number of samples	Extra samples	Future references in this paper
Warp direction	12,5 x 5 cm	50	1	Big warp sample
	12,5 x 2,5 cm	50	6	Big weft sample
Weft direction	12,5 x 5 cm	50	5	Small warp sample
	12,5 x 2,5 cm	50	3	Small weft sample

Table 6 Total number of samples per direction and dimension

4.2.4 Carbonisation of the samples

The carbonisation process depends on three parameters: temperature, time and quantity of oxygen. Having performed different test series with the modern linen varying those three parameters, I analysed the results with FTIR. The aim was to create samples with a carbonisation degradation state, like the ones the archaeological samples have. To do so, I compared the different spectrums of the modern samples after carbonisation with the spectrum of the archaeological samples. The carbonisation parameters which would create a sample with the most similar properties, would then be selected for the treatment of all modern samples.

To avoid a huge loss of modern material during these destructive tests, smaller samples were prepared for two of the three tests. Six samples (10x8cm) for the tests varying the temperature, and nine samples (8x5cm) for the tests varying temperature and time.

Selection of the method

Two tools were necessary to carbonise the samples. An oven to serve as the heat source, and a malleable but heat-resistant material to wrap the samples and create the reducing atmosphere.

[94] The first oven chosen for the carbonisation process broke, so another oven with smaller dimensions was finally used for the same purpose.

An oven that could reach high temperatures (more than 300°C) was needed. The most common oven with these conditions is the oven used by ceramists and glass makers. The oven available in the Swiss National Museum for the test was a Naber® L51/5 R (Figure 66). Because of technical problems, the oven Nabertherm® L3/11/C6 was ultimately used for the carbonisation process of all samples

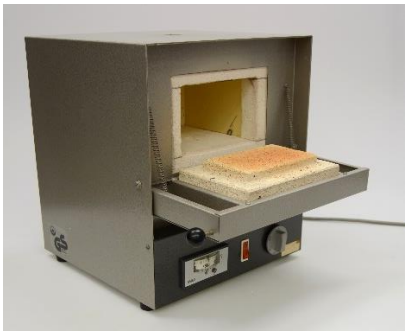

Figure 66 Oven Naber® L51/5 R. Swiss National Museum ©HE-Arc

For the malleable material, aluminium foil was selected. Aluminium is a thermal conductor and can resist high temperatures. It is also a malleable and soft metal (Vickers hardness 160-350 MPa) whose melting temperature is 660.32°C, and has a good resistance to corrosion. It has a thermal conductivity of 237 W/m.K.

Test varying temperature:

The aim of the test was to understand how the linen reacts depending on the temperature used for the carbonisation treatment. The oven was preheated at the desired temperature and, once the temperature was stable, the samples were introduced inside. Opening the door of the oven and the manipulation of the samples meant a decrease in temperature of 200°C inside the oven. After closing the door, only 5 seconds were needed to reach the desired temperature again.

Six samples were tested with dimensions 8x6cm. Each sample was wrapped with aluminium foil and carbonised separately (Figure 67). The standard time of treatment was setted at 30 min, and only varied the temperature with a difference of 100°C from one sample to another (100°C to 600°C). The highest temperature I wanted to test was 600°C as, with a temperature higher than that, there would be a risk of damaging the aluminium.

Figure 67 Modern samples. Starting from the left: Original, heated without oxygen at 100°C, at 200°C, at 300°C, at 400°C, at 500°C, and at 600°C ©HE-Arc

Sample	Temperature	Time	Wrapping system	Colour of the textile before treatment	Colour of the textile after treatment[95]	Shrinkage during treatment
1	100°C	30 min	Aluminium foil	Beige	Beige	No
2	200°C	30 min	Aluminium foil	Beige	Beige	No
3	300°C	30 min	Aluminium foil	Beige	Light Brown	Yes
4	400°C	30 min	Aluminium foil	Beige	Black	Yes
5	500°C	30 min	Aluminium foil	Beige	Black	Yes
6	600°C	30 min	Aluminium foil	Beige	Black	Yes

Table 7 Description of physical changes after the carbonisation tests varying the temperature

After carbonisation, the physical changes of the samples were observed (see Table 7), change iof colour was analysed with a spectrophotometer (Appendix 10), and each sample was analysed with FTIR (For detailed information about the analysis, go to Appendix 9). It was concluded that the spectrum of the specimen carbonised at 600°C was the most similar to the spectrums of the archaeological samples. Unfortunately, because of the variation of the temperature inside the oven during the process (±40°C), carbonising the samples at 600°C was risky. The temperature came close to the melting point of the aluminium. For this reason, the oven was set at 570°C, knowing that samples would reach 600°C (because of the variation of temperature).

Test varying time:

The objective of the test was to understand the evolution of the linen while carbonising when the time inside the oven is increased. By lowering the temperature but increasing the time, maybe it was possible to arrive at the same carbonisation state as that with higher temperatures and shorter times.

Nine samples (8x5cm) were prepared for this test. Each sample was wrapped with the aluminium foil following the same method as for the previous test. For this test, three samples were carbonised separately per temperature range (from 300°C to 500°C), but varied the duration for which each sample was left inside the oven (30min, 1h and 2h) (Figure 68).

[95] Detailed information about the colour spectrum can be seen in Appendix 16

Figure 68 Modern samples. Carbonisation results varying the time (30min, 1h and 2h ; left to right), and temperature (300°C, 400°C and 500°C ; up to down) ©HE-Arc

Sample	Temperature	Time	Wrapping system	Colour of the textile before treatment	Colour of the textile after treatment[96]	Shrinkage during treatment	Deformation after treatment
1	300°C	30 min	Aluminium foil	Beige	Light Brown	No	No
2	300°C	1h	Aluminium foil	Beige	Dark brown	No	No
3	300°C	2h	Aluminium foil	Beige	Dark Brown	No	Yes
4	400°C	30 min	Aluminium foil	Beige	Black	Yes	No
5	400°C	1h	Aluminium foil	Beige	Black	Yes	Yes
6	400°C	2h	Aluminium foil	Beige	Black	Yes	Yes
7	500°C	30 min	Aluminium foil	Beige	Black	Yes	Yes
8	500°C	1h	Aluminium foil	Beige	Black	Yes	Yes
9	500°C	2h	Aluminium foil	Beige	Black	Yes	Yes

Table 8 Description of physical changes after the carbonisation tests varying the time and the temperature

[96] Detailed information about the colour spectrum can be seen in Appendix 16

After the test, the physical changes of the samples were observed (see Table 8). The sample treated 2h at 500°C was then analysed with FTIR spectroscopy (Appendix 9) and compared to the spectrum of the sample treated 30min at 600°C. The results indicated that the time of the treatment did not vary the results as much as the temperature did, and the carbonisation state of the textiles was not very different if the sample was treated for 30 min or 2h. Because of the number of samples carbonised for the consolidation tests (a total of 200 samples), it was decided to treat them for 30 min, to be more efficient.

Test varying the quantity of oxygen:

The purpose of the test was to evaluate how the quantity of oxygen present during the treatment can vary the carbonisation process. Knowing that the oven available to carbonise the textiles did not allow creation of a reduced atmosphere inside, the only option to vary the quantity of oxygen was the wrapping system.

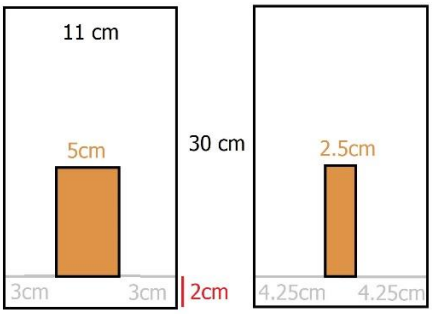

Figure 69 Dimensions of the aluminium foil and final position of the sample inside the wrapping system

Samples were tested with different wrapping methods using the aluminium foil, always employing the same dimensions and quantity of aluminium (Figure 69), and carbonised them at 550°C for 30min. The three methods tested used the same amount of aluminium foil, variations were made for the folding method. To see all the folding methods tested go to Appendix 11.

Method two of the methods allowed too much oxygen inside the aluminium. The textiles were partially burned instead of carbonised (Figure 70). Method 3 (Figure 71) carbonised the sample completely, except for the edges, which were slightly burned (the ashes were visible under the microscope). To reinforce the third method and reach complete carbonisation, a second layer of aluminium foil was added folded in the same way.

Figure 70 Results of the carbonisation varying the wrapping system. Two of the three samples burned (ashes visible with the naked eye) ©HE-Arc

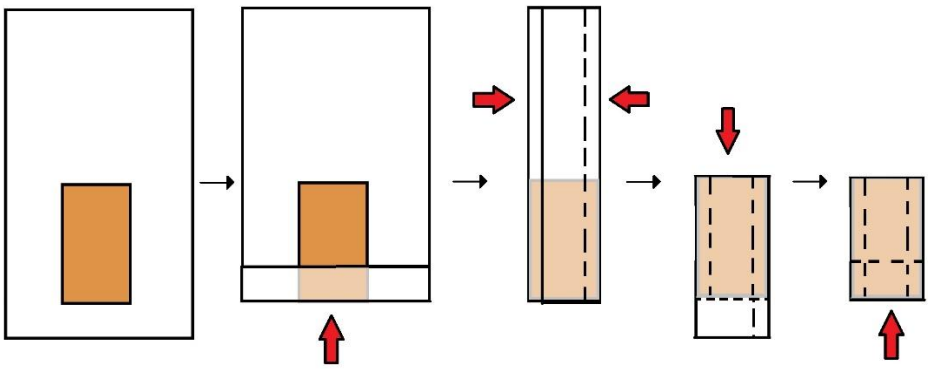

Figure 71 Schematic representation of the folding method selected for the carbonisation of the modern samples

Another problem which arose during the carbonisation test, was the deformation of the aluminium foil during the process. The foil swelled and consequently, the textile became deformed. Not every sample deformed in the same way, which became a problem when wanting to create homogeneous samples. To avoid the deformation, the swelling of the aluminium foil was blocked by adding a weight on top of the sample (Figure 72). Thus, the textile and the foil remain flat during the carbonisation and therefore there is no deformation.

Figure 72 Two layers of samples ready to be carbonised, with a weight in between ©HE-Arc

4.3 Results and discussion

Based on the carbonisation tests results, all samples were carbonised at 550°C for a duration of 30min, with the wrapping method type 4, also adding a weight to avoid deformations. The experiment was conducted outdoors for safety reasons and temperatures during the treatment were recorded (Appendix 12). When comparing yarn diameters of the un-carbonised linen fabric with the charred samples, as well as the number of threads per cm² (Table 9), it can be said that burning conditions affects the final yarn diameter and the shrinkage of the fabric (Figure 73 and 74). It is also visible that there is a big change on the dimensions of the fabric, especially for the warp threads, which seem to shrink more than the weft threads. These results lead to an assumption that the dimensions of the archaeological samples have drastically reduced in comparison with their dimensions before charring (Figure 75 and 76).

The differences are likely the result of both proximity of the temperature (intense fast carbonisation) and time of exposure. Photographic documentation of the samples carbonised is in Appendix 13.

Sample type	Number or threads per cm² before carbonisation	Number or threads per cm² after carbonisation
Warp	16	21
Weft	13	18

Table 9 Number of threads per cm² before and after carbonisation

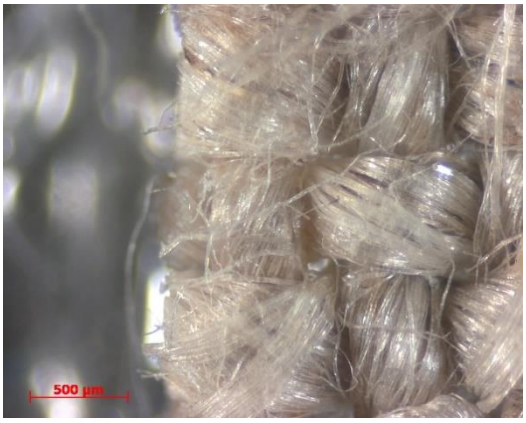

Figure 73 Details of the modern sample before carbonisation, microscope view x3.2 ©HE-Arc

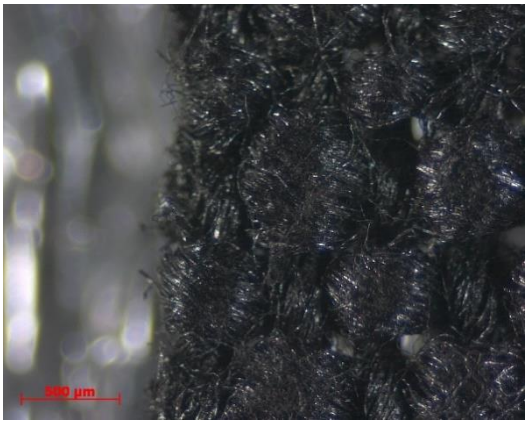

Figure 74 Details of the modern sample before carbonisation, microscope view x3.2 ©HE-Arc

Figure 75 Comparison of the dimensions before and after carbonisation of a weft sample (left) and a warp sample (right) with dimension 12.5x5cm ©HE-Arc

Figure 76 Comparison of the dimensions before and after carbonisation of a weft sample (left) and a warp sample (right) with dimension 12.5x2.5cm ©HE-Arc

As well, these tests suggest that several factors seem to play a role in the condition of archaeological samples. These include the intensity of the heat source, duration of exposure, protection from the heat source (including other layers of fabric), as well as other factors not considered in this research, like the proximity to the heat source. After the carbonisation process, **two hundred samples of carbonised linen were ready to proceed to the freeze-drying and consolidation tests**.

Chapter 5 Freeze drying the textiles

5.1 Pre-treatment: Soaking the modern samples

5.1.1 Aim

The modern charred textiles, after the carbonisation process, were in a dry state. The same procedures used for the archaeological samples was selected for their treatment, including the PEG 400 impregnation and the freeze-drying treatment, in order to apply the same stress factors. To do so, the modern samples had to be wet, but no publications were found on soaking charred modern textiles for freeze-drying treatments.

5.1.2 Methodology

A test was done with one big sample of warp and weft to evaluate the surface tension of the samples (Figure 77). When introduced to the solution, both samples were floating in the surface of the water. In consequence, some drops of ethanol were going to be added to the water to reduce the surface tension. For each litre of water, 0.5mL of ethanol was added.

Figure 77 Soaking test of one big sample of warp (left) and one sample of weft (right) to evaluate the surface tension ©HE-Arc

To wet them, the samples were immersed in deionized water[97] for 5 days. The warp and weft samples measuring 12.5x5cm were divided in groups of 10 (because of the shape of the containers) and immerged in 1L of deionized water. Samples with dimensions 12.5x2.5cm were also divided into groups of 10, but immersed in 300mL of deionized water, also due to the shape of the containers and their reduced dimensions. After adding the ethanol, all containers were then closed with their plastic covers, and samples remained in the solution for 5 days (Figure 78).

Figure 78 Big containers with the modern samples already wet inside ©HE-Arc

5.1.3 Results

After the treatment, all samples were completely soaked, and a number of them lost some fibres in the solution. The pH of the water was measured per container, as well as the amount (Table 10). No significant change was visible and the loss of water was assumed to be related to the evaporation of the solution during the treatment.

[97] In the museum, the pH of the deionized water is 5.5

Type of sample	Before the soaking process				After the soaking process			
	Number of samples	Litres of deionized water	Amount of ethanol	pH	Number of samples	Litres of deionized water	pH	Fibres remaining in the solution
Warp 12.5x5cm	10	1L	0.5mL	5.5	10	975mL	5.5	Yes
Weft 12.5x5cm	10	1L	0.5mL	5.5	10	980mL	5.5	Yes
Warp 12.5x2.5cm	10	300mL	0.15mL	5.5	10	288mL	5.5	Yes
Warp 12.5x2.5cm	10	300mL	0.15mL	5.5	10	292mL	5.5	Yes

Table 10 Values of the pH and millilitres of deionized water are given per container, before and after soaking the modern samples. The mean value of the containers per type of sample is represented in this table.

5.2 Pre-treatment: Cleaning and reshaping the archaeological samples

5.2.1 Aim

Different facts must be considered when cleaning degraded fragments, like the type of information that the soil is giving or the condition of the fibres among others[98]. Careful washing can improve the long-term stability, the aesthetical appearance, and will allow to have better and clearer results of the consolidation tests[99]. In certain samples, removing the dirt will also highlight information that was previously covered, improving the visibility; as such deposits frequently hide details, colours and patterns of the yarns and fabrics[100].

Also, cleaning before the drying treatment is strongly recommended because when drying textiles, the remaining soil dries as well and its adherence to the textile is incremented, which therefore demands the use of a harder and more aggressive cleaning treatment to remove the dirt after drying. In addition, when the fibres swell, they are flexible, which makes it possible to unfold the edges and remove deformations with less risk[101].

5.2.2 Methodology

Aqueous cleaning is frequently the method chosen since the archaeological fragments recovered from damp environments are already wet. Distilled or deionized water is the safest option to avoid future concretions[102].

[98] Peacock, 1992, p. 197
[99] Lundwall, 2003, p. 49
[100] Rice, 1964, p. 8-17
[101] Peacock, 1992, p. 198
[102] Geijer, 2011, p. 80

Although, great care must be taken to restrain the fibrous assembly while the supportive soil disperses, because when the textile is already degraded, the water in the cells and hollows of the fibres (which structurally supports the fibre) becomes flooded and the structural balance can be disrupted[103].

To clean the archaeological textiles, an airbrush was used with deionized water[104]. The pressure applied went from zero to one bars depending on the adhesion of the soil and the fragility of the textile. A new support for the cleaning procedure was created, which allows turning the samples without stressing the textile (See Appendix 14). A polyester mesh[105] (100µm) from GMW® was used as support, which allowed the passage of water but not the passage of fibres. Used at 45°, the dirt slips through the net, while the fibres stay put (Figure 79). The samples that were too fragile to manipulate and set down in the mesh, were directly cleaned of the polyester support (Figure 70).

Figure 79 Cleaning tools ©HE-Arc

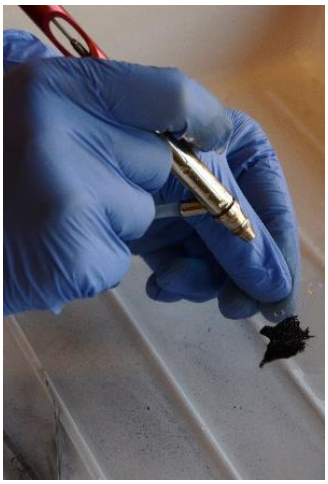

Figure 80 Cleaning sample 1.5 on its polyester support ©HE-Arc

5.2.3 Results

The soil and dirt was removed from the surface of the textiles. Soil present inside the threads was not eliminated because to do so, un-twist the fibres or apply too much pressure to the threads was necessary, and thus it could be risky for their structural stability.
Unfortunately, some fibres that were already broken disaggregated from the sample during the passage of water.

[103] Stelton, 1975, p. 15-20
[104] Rice, 1966, p. 15-38
[105] Polyester, mesh-size 100 µm, 65 gsm

5.3 Pre-treatment: Adding polyethylene glycol (PEG) 400

5.3.1 Aim

Adding protective agents to an organic material before drying can reduce stresses during the drying procedure and increase the flexibility and structural stability of the textiles. Unfortunately, the reaction in between polyethylene glycols (PEG) applied before drying and consolidants applied after drying has not been extensively studied. In consequence, comparison will be done after drying as well as after consolidation between a group of samples treated with PEG and another with no protective agent. The comparison will hopefully clarify if a treatment with PEG 400 is necessary or not before drying textiles, knowing that a consolidation post-drying is needed anyhow, and the interaction between the consolidants tested and the PEG 400 is unknown.

5.3.2 Selection of the protective agent

As the standard procedure for the freeze-drying of organic materials in the museum, a polyethylene glycol treatment is normally carried out before the drying treatment. Janet Schramm, conservator-restorer of the archaeological department, performed a series of experiments in 2017 with charred archaeological samples treated with different lubricants and protective agents[106]. The results indicated that textiles pre-treated with 8% polyethylene glycol (PEG) 400 in deionized water were more flexible, less glossy in the surface, and stable (less fibres lost) than other mixtures. Colleagues from the Bavarian State Office for Historic Monuments also carried out a series of tests with protective agents for the treatment of charred textiles, and they choose 8% PEG 400 as well as the best solution[107].

Low molecular polyethylene glycols (PEG), like PEG 400, act like lubricants (or softening agents, they increase the moisture for lubrication), bulking agents (strengthens the weak cells) and impregnants (replace the water in the hollows of the fibres with a chemically inert material) [108]. PEG 400 is a hygroscopic substance that increases the flexibility and redistributes the stresses of the textile enabling the fibres and yarn to slide past one another (reducing the damage during the drying treatment). Because of its low molecular weight, it can diffuse into the degraded cell walls and reinforce them, which reduce shrinkage during drying. In extremely degraded textiles, the PEG 400 remains in the fibres during the treatment, avoiding the fibre collapse induced by the capillary action of the sublimating water.

[106] Schramm, 2017
[107] Heitmann, 2010
[108] Peacock, 1992, p. 203-204

In addition, Peg 400 keeps the flexibility of the fibres, something that higher molecular weight compounds like PEG 4000 cannot assure[109]. They are normally used in concentrations lower than 10%, and its application must be carried out while the textile is wet.

For the reasons mentioned before, an **8% PEG 400 solution was chosen** for the pre-freeze-drying treatment.

5.3.3 Methodology

The archaeological and modern samples were divided into two groups, A and B. Group A was composed of 18 archaeological samples[110], and 100 modern charred samples (25 big warp samples, 25 big weft samples, 25 small warp samples and 24 small weft samples). Group B was composed of 19 archaeological samples[111], and the other 100 modern charred samples (25 big warp samples, 25 big weft samples, 25 small warp samples and 24 small weft samples).

Group A was treated with 8% PEG 400 in deionized water for one week. Before applying the solution, the water on the surface of all samples was slightly absorbed with a cotton tissue (Figure 81 and 82), so that the penetration of the solution is more efficient when re-moisturised with the protective agent. Care was taken to avoid completely drying the sample and to not touch the surface of the textiles. Then, a pipette with 8% PEG 400 was used to soak the samples (Figure 83 and 84). The quantity of solution varied from 0.5mL to 1.5mL for the archaeological samples (depending on the dimensions) and from 1mL to 2mL for the modern samples (depending as well on the dimensions). This procedure was repeated every day at the same hour for one week. To minimize the evaporation of the solution, the containers were sealed with plastic film.

[109] Hiron, 2003, p. 34
[110] The following samples were selected for group A: 1.1, 1.2, 1.16, 1.17, 1.29, 1.31, 3.1, 3.3, 3.4, 3.7, 3.8, 3.11, 3.12, 3.13, 3.14, 3.16, 3.18, and 3.19. Samples were selected with different dimensions to observe if big fragments shrink differently than the smaller ones.
[111] The following samples were selected for group B: 1.5, 1.6, 1.10, 1.18, 1.21, 1.23, 1.30, 2.2, 2.3, 2.4, 2.5, 2.6, 2.8, 2.10, 2.11, 2.15, 2.16, 2.18, and 2.19. Same selection criteria were applied than for group A.

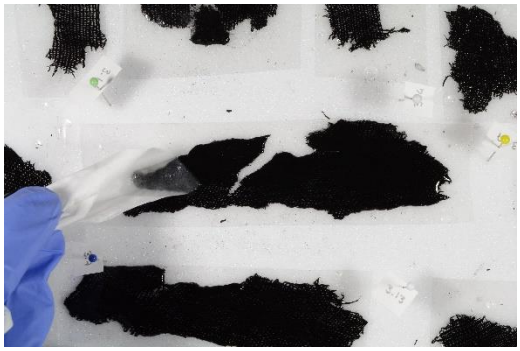

Figure 81 Absorption of the water on the surface of the sample 3.16 with a cotton tissue ©HE-Arc

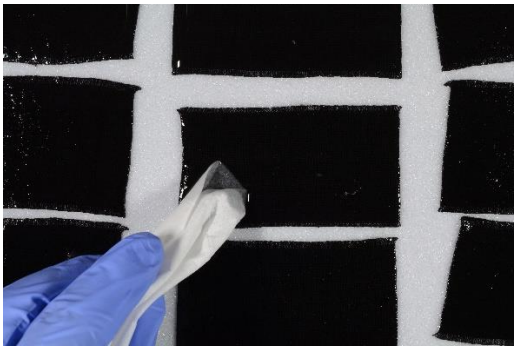

Figure 82 Absorption of the water on the surface of a big warp sample with a cotton tissue ©HE-Arc

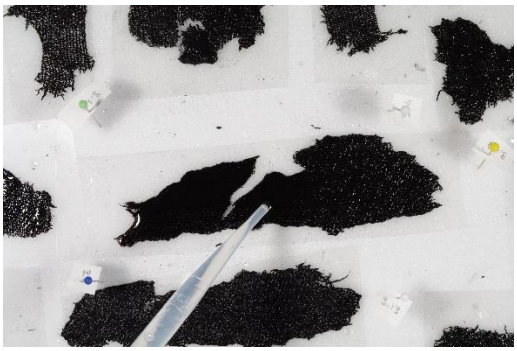

Figure 83 Application of the PEG solution with a pipette to the sample 3.16 ©HE-Arc

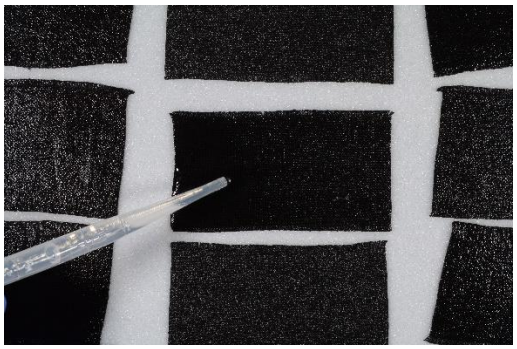

Figure 84 Application of the PEG solution with a pipette to a big warp sample ©HE-Arc

Group B was kept moist only with deionized water waiting for the freeze-drying treatment. The samples were placed in storage boxes with a layer of deionised water-soaked paper in each box, underneath the foam support. As in Group A, to minimize the evaporation of the solution, the containers were sealed with plastic film.

5.3.4 Results

After one week of treatment, the Group A presented a shinier appearance than Group B due to the addition of the PEG 400. Because of the risk of slow air-drying of the samples, deionised water was added to the storage boxes of Group B after three days.

5.4 The freeze-drying treatment

5.4.1 Aim

Freeze-drying under vacuum was necessary to dry the samples under controlled conditions without creating stresses on them. This is possible thanks to the process of sublimation, which is the transformation of water from its solid form (ice) directly to vapour without passing through the liquid

state[112]. Doing so prevents the physical and chemical interactions are prevented as the iced matrix blocks the histological structure during sublimation. As a consequence, the textile can retain its shape, state and appearance. However, the freeze-dried textile will not present a better state than the initial wet textile[113].

5.4.2 Methodology

Freeze-drying under vacuum was selected as the method for drying the charred textiles. The Swiss National Museum has a vacuum freeze-dryer modified with a cooling system, which allows treatments at lower and more stable temperatures.

The preparation for the freeze-drying treatment of textiles involves three critical aspects: the packing, the temperature, and the rate of cooling.

Group A and Group B were prepared and packed in two different metal plates, but following the same procedure. First, the metal plate was covered with one layer of Buvar® (1.1mm thick) from Lascaux®, which acted like a protective cushion layer between the textiles and the metal plate. The Buvar® was pre-soaked with deionized water to prevent it from absorbing water from textiles. Then, a layer of Hollytex from Deffner & Johann® was put on top of the Buvar® to reduce the sublimation rate during the freeze-drying treatment, as well as to fix the textiles to the metal plate. The dimensions of the Hollytex® sheet were twice the width of the metal plate, so once the textile samples laid on the Buvar®, it could be folded and fixed with magnets to the metal plate (Figure 85). No magnets were placed near the samples.

Figure 85 Archaeological and modern samples, only moist with water, on the metal plate already prepared to be introduced in the fridge ©HE-Arc

Figure 86 Attaching the thermocouple to a big warp sample pre-treated with 8% PEG 400 in deionised water ©HE-Arc

Before wrapping all the layers together with a polyethylene film (to reduce the evaporation rate during the cooling procedure inside the fridge and freezer), one thermocouple (K-Type) was fixed to one modern sample per group (Figure 86).

[112] The water is transform from ice directly to vapour without passing through the liquid state.
[113] Peacock, 1992, p. 200

The thermocouples connected to the samples will give an idea of the temperature on the surface of the sample during the freeze-drying treatment. Recording measurements of both samples will allow the comparison between the temperatures during the freeze-drying treatment when the textiles are pre-treated, or not, with PEG 400. (Data available in the Digital Appendices).

Figure 87 Both metal plates inside the freezer ©HE-Arc

Both metal plates, already wrapped with the plastic foil, were introduced inside the fridge for three days and conditioned at 4ºC. After that period, they were inserted inside the freezer and conditioned at around -22ºC for 24h (Figure 87). The pre-freezing of the textiles was carried out by cooling the samples at atmospheric pressure. The samples must be slowly conditioned and frozen before freeze-drying to avoid a sudden solidification of the water present in the cells walls which could lead to destruction of the material due to the sudden increased dimensions of the ice crystals.

In addition to the metal plates, four iced cubes of deionized water (two with 2mL and two with 15mL) and four iced cubes of the same 8% PEG 400 solution used for the samples (two with 2mL and two with 15mL) were prepared as a system to control the sublimation rate during the treatment. Little disposable plastic cups with a millilitre scale were used as containers for the creation of the iced cubes. The iced cubes with two millilitres were created as a reference for the sublimation progress on the samples, as it was the maximum amount of solution added on one sample. The iced cubes with 15mL were created as a visible reference of the sublimation process, which normally should reduce the dimensions of the iced cube from the outside to the inside. In addition, one thermocouple was added to one iced cube of each type (four thermocouples in total) to record the temperature of the ice while sublimating.

The cubes were placed on a frozen glass plate, on which two strips of pH paper (cross-shaped) had previously been fixed. On the pH paper, some grains of citric acid had been added (Figure 88). In this way, if the water in the ice cubes melts instead of sublimating, the citric acid will dissolve, changing the colour of the pH paper to red. A mirror was placed under the glass plate to visualize the dimensional changes from bellow as well (Figure 89).

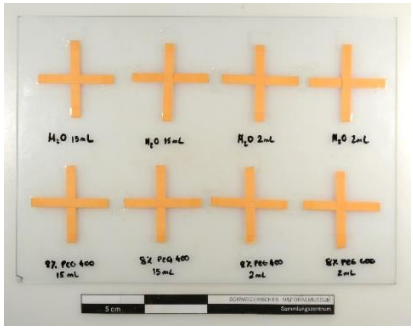

Figure 88 Glass plate with the strips of pH paper already attached. ©HE-Arc

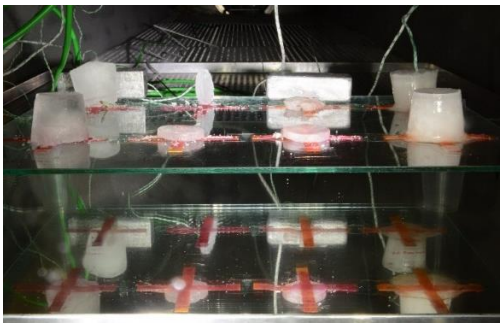

Figure 89 Iced cubes with the thermocouples already placed inside the freeze-dryer, with the mirror under the glass plate. ©HE-Arc

The freeze-dryer was pre-cooled at -50°C. Before inserting the textiles and the iced cubes, the chamber was conditioned first at -45°C and then at -43°C, which is the temperature selected for the treatment. Two thermocouples were inserted inside the chamber of the freeze-dryer, one in the front part (where the samples with no protection agent were placed), and another in the back part (where the samples treated with 8% PEG 400 were placed). After three days of treatment, the temperature of the freeze-dryer was slowly increased to -30°C for the removal of the samples from the chamber.

5.4.3 Results and discussion

The freeze-dryer treatment lasted 87h. Looking at the graph of the temperature settings (Figure 90), the conditioning of the chamber is visible on the three first hours, when the temperature was brought from -45°C to -43°C. Then, the temperature settings were kept for 56h at -43°C, and slowly increased to -30°C as explained in the previous chapter. During the following nine hours, a big peak is visible in the graph, which it is assumed to be a problem when changing the machine temperature settings. That peak goes from -30°C to 0°C and back to -30°C. That sudden change in temperature will be reflected in all following graphs. As a consequence, the sublimation rate was sped up.

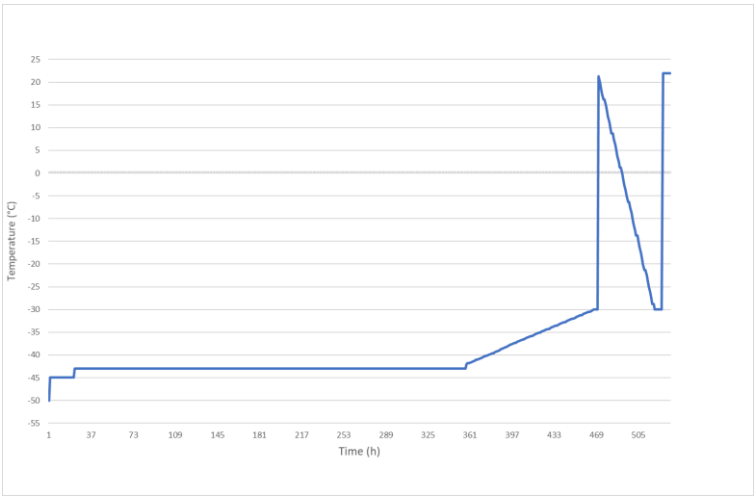

Figure 90 Temperature settings during the freeze-drying treatment

Attention must be paid to the difference between the temperature settings and the real temperature inside the chamber of the freeze-dryer, which is ten degrees warmer than the temperature settings. In addition, the thermocouples in the front part of the chamber recorded temperatures five to eight degrees higher than in the front part during the whole treatment. The difference between the front and the back will also influence the speed of the drying process, being quicker in the front part than in the back zone (Figure 91).

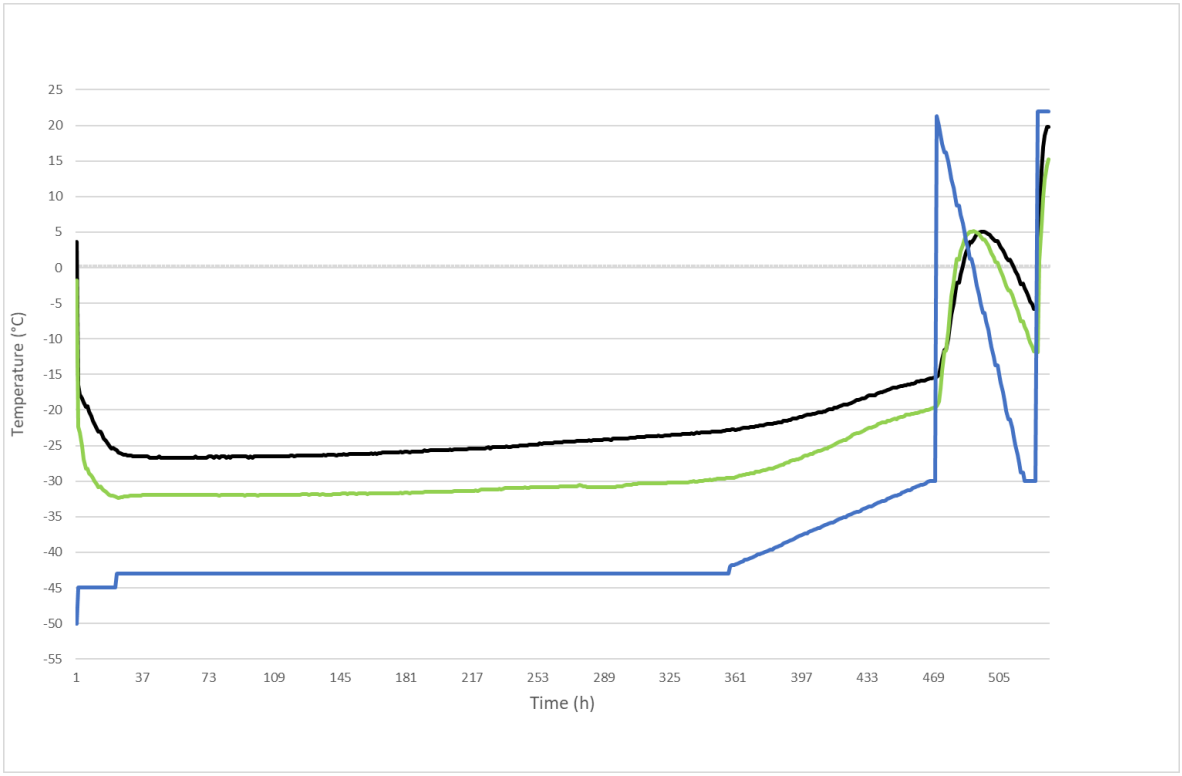

Figure 91 Juxtaposition of the temperatures belonging to the settings of the freeze-dryer (blue), the back of the chamber (green) and the front of the chamber (black), during the treatment

The textile samples were removed from the freeze-dryer after 87h of treatment when the temperature inside the chamber was between -5°C and -10°C, and they were completely dry. The sublimation process of the Group A (treated with 8% PEG 400), which took 87h, was slower than for group B, which only needed 18h (Figure 92). The end of the sublimation process of Group B is visible because of the sudden increase in temperature, indicating that there was no more iced water still present inside the fibres. The difference of the sublimation rate can be related to the varied temperature inside the chamber as well as the presence of PEG 400, which slows down the sublimation rate.

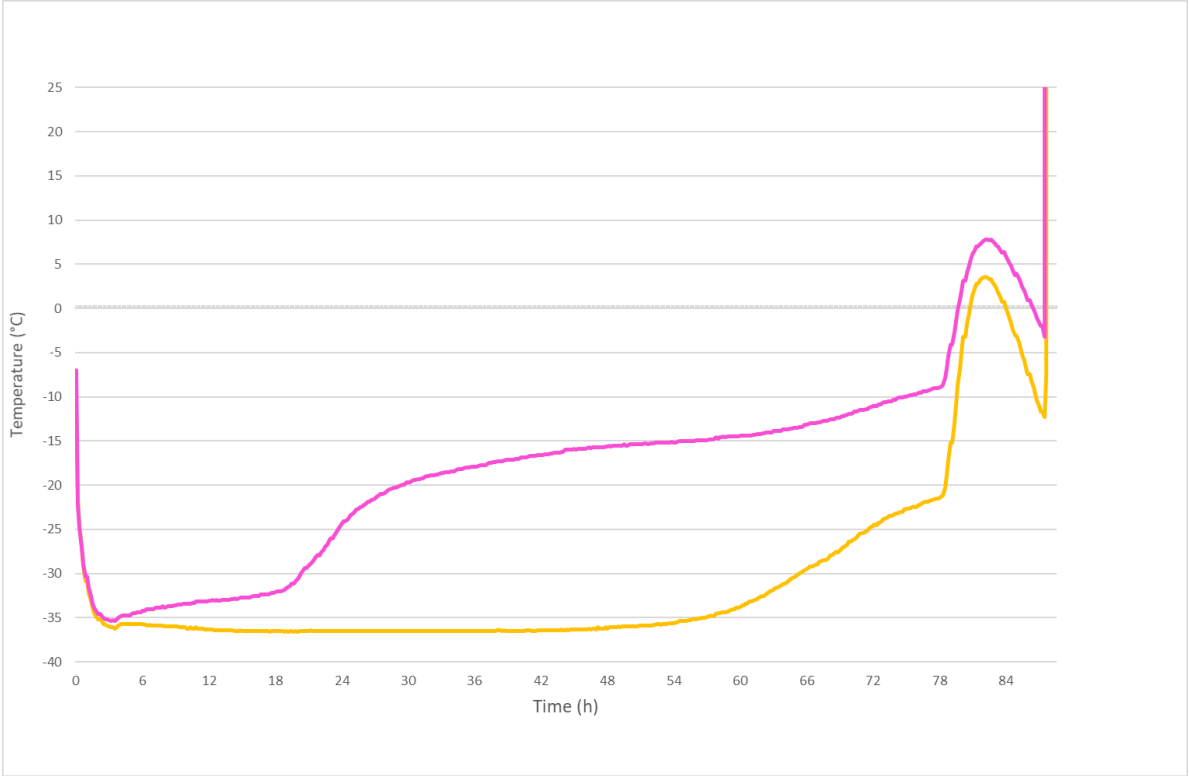

Figure 92 Juxtaposition of the temperatures belonging to the Group A (orange) and Group B (pink) during the treatment

The sublimation of the iced cubes was recorded, on one hand with the thermocouples which indicated the temperature, and on the other hand with a digital camera, which took a picture every 3min (Figure 93 and 94). Crossing the information of the data-logger and the properties of the pictures (which gave specific information of the date and hour when the picture was taken), it was possible to know exactly how they were melting, and if anything unexpected happens. Unfortunately, due to a technical problem with the computer, the camera stopped taking pictures 12h after starting the procedure, and re-started 12h after that.

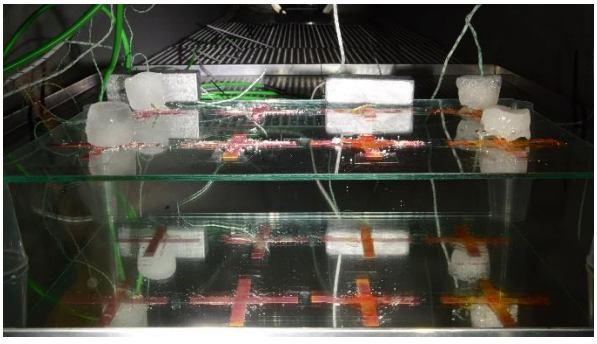

Figure 93 Iced cubes inside the freeze-dryer after 11h of treatment. The 2mL iced cubes sublimated completely ©HE-Arc

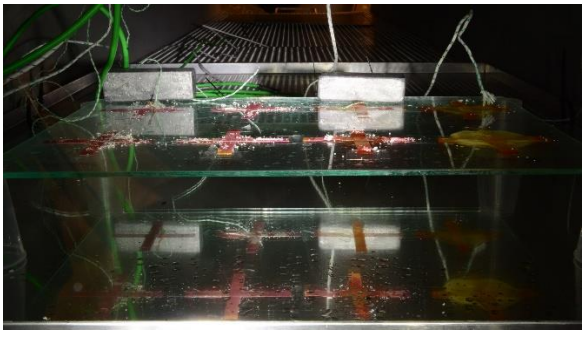

Figure 94 Iced cubes inside the freeze-dryer after 78h of treatment. All iced cubes sublimated completely ©HE-Arc

When the freeze-drying treatment started, a condensation effect was visible on the surface of the glass plate and the mirror, due to the difference in temperature between the surface of the plates and the chamber. The two iced cubes with 2mL of PEG 400 took 9h to completely sublimate, and they were the first to do so (Figure 95). One of the two iced cubes broke before starting the freeze-drying, because of the manipulation of the thermocouple inside it. The iced cube was too thin, not resistant to any stresses, and broke into several pieces, which implied larger surface exposed to the sublimation process and therefore the procedure was sped up.

After 11h of sublimation, the iced cubes made with 2mL of water sublimated entirely. The sudden change of temperature that the thermocouple attached to the 2mL water iced cube, after eleven hours, is not related to the sublimation of the water but to the fact that the thermocouple was no longer in touch with the iced cube. This fact is only visible when looking at the pictures of the iced cubes.

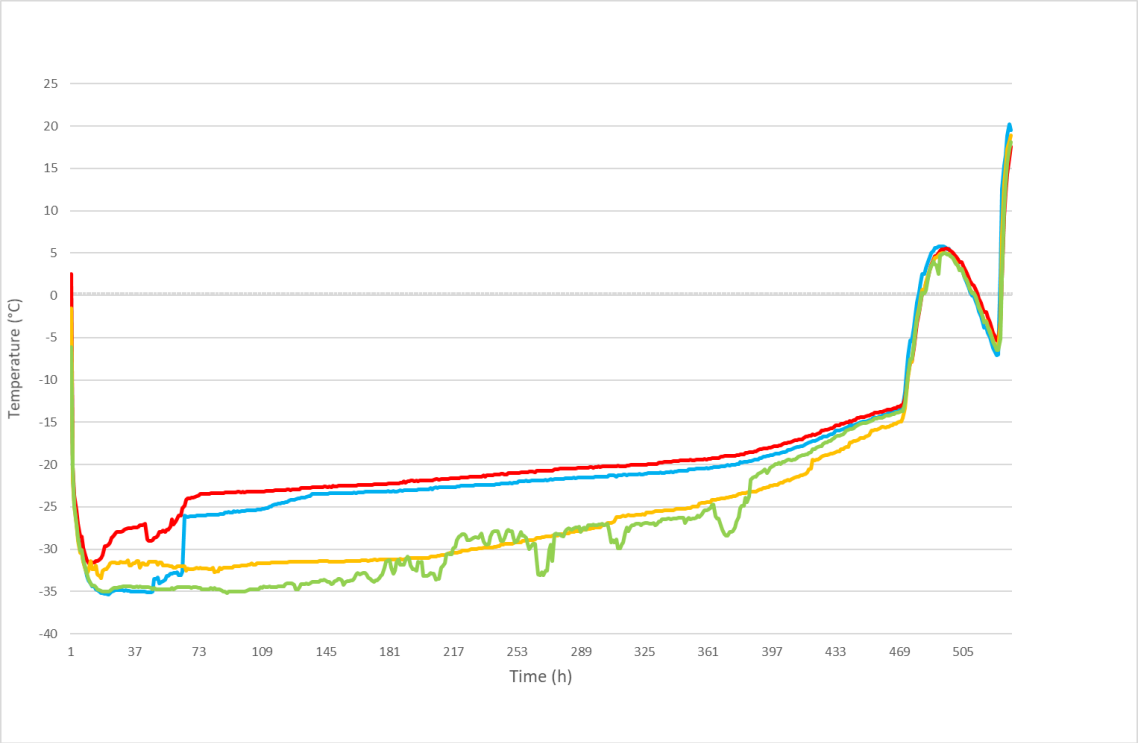

Figure 95 Juxtaposition of the temperatures belonging to the iced cubes during the treatment: 2mL 8% PEG 400 in red, 2mL deionized water in blue, 15mL 8% PEG 400 in green, 15mL deionized water in yellow

The bigger iced cubes took longer to sublimate, around 66h for the iced cube made of 15mL of 8% PEG 400, and around 78h for the iced cube made of 15mL of deionized water. The temperatures recorded during the sublimation of the first one is not stable. It could be possible that, during the sublimation process, while the PEG was melting, the water was sublimating, giving to the iced cube a porous structure. The difference between the frozen and the liquid state in touch with the thermocouple could have led to the continuous variations in temperature.

In the end, the pH paper experiment was finally not taken into account, because during the installation of the thermocouples and the glass plate inside the freeze-dryer, the iced cubes started to slightly melt. Consequently, the citric acid grains were solubilised and the paper turned red before the sublimation process started (Figure 96). When the drying treatment ended, a green viscous solution was visible on the pH papers where iced cubes, made of PEG, were laying. This solution is the PEG that did not sublimate during the freeze-drying treatment.

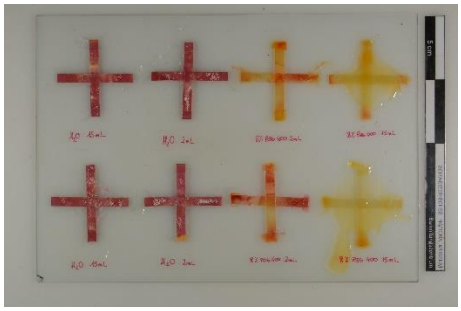

Figure 96 Glass plate with the strips of pH paper already attached. ©HE-Arc

Finally, in order to evaluate the effects of the freeze-drying treatment under vacuum, the dimensions and weight of the samples of both groups were compared before and after drying (See Appendix 15). The archaeological samples of Group A lost an average of 0.88±0.18g per sample, which indicates a loss of around 30% of its initial weight; and Group B recorded a loss of 0.274±0.2g in average (or around 40% of its initial weight). The difference between the initial weight and the weight after drying is due to the sublimation of the water that was previously present between the fibres of the textiles. There is a 10% difference between Group A and Group B because of the presence of PEG 400 between the fibres that does not sublimate like the water does.

When looking at the dimensions, before and after drying, there is a loss of surface area of about 3.966±2.835cm² for the Group A, and 2,339±2.372cm² in the case of Group B. These numbers have been calculated as an average based on a group of samples that presented different dimensions. Therefore, we can deduce that samples from Group A in theory shrank more than samples from Group B, but in practice it was not the case. More information was added to this discussion when comparing the difference of the thread count on several samples before and after consolidation (Table 11). When comparing the thread count of several samples from each group, the results contradict the ones mentioned before, as they indicate that samples from Group B shrank more than samples from Group A. After drying, Group B samples have more threads per cm² in the samples from Group B.

	Samples	Before freeze-drying	After freeze-drying
Group B	1.30	18x11	19x12
	2.06	16x10	18x11
	2.08	16x9	16x11
Group A	1.01	16x10	18x11
	3.1	18x10	18x10
	3.19	18x11	18x11

Table 11 Thread count before and after freeze-drying of three samples per group which present different dimensions

In addition, the shrinkage is visible through the photographic documentation. For the comparison, a support was prepared in which the initial shape of all samples was showed in red. Then, for the visual comparison, the support was overlapped with the samples (Figure 97 and 98).

A clear shrinkage occurred in all samples of both groups. Sometimes the dimensional change was more evident in samples that, due to manipulation with them, had lost several fibres. In general, archaeological samples from B seems to have shrank more than samples from Group A.

Figure 97 Sample 2.16 from Group B. Visual comparison of the dimensions before (red line) and after freeze-drying ©HE-Arc

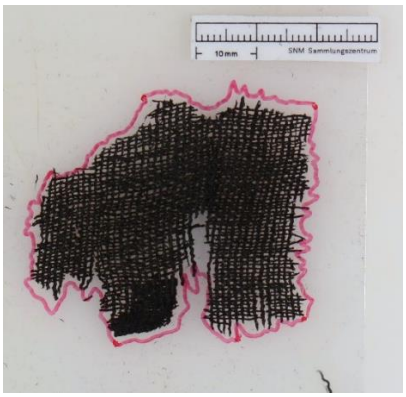

Figure 98 Sample 3.3 from Group A. Visual comparison of the dimensions before (red line) and after freeze-drying ©HE-Arc

When looking at the loss of fibres of the archaeological samples during the freeze-drying treatment (visible on the surface of the support, Figure 99 and 100), samples that were not previously treated with PEG 400 lost more fibres during the treatment than those which were pre-treated. It is assumed as well that using PEG 400 as pre-treatment was not strong enough to stabilise the samples and avoid any loss. Consequently, it can be affirmed that a consolidation post-drying is needed for the long-term stabilisation of the charred textiles.

Figure 99 View of the support used to freeze-dry Group B (water). Comparison between the loss of fibres from the archaeological samples (left) and the modern samples (right) ©HE-Arc

Figure 100 View of the support used to freeze-dry Group A (PEG 400). Comparison between the loss of fibres from the archaeological samples (up) and the modern samples (down) ©HE-Arc

When comparing the modern samples before and after consolidation, less differences are noticeable. There was almost no weight loss between the samples in their dry state (before soaking) and after freeze-drying. Changes in dimension are scarcely visible, only noticeable when comparing the photographic documentation, following the same procedure than described for the archaeological samples (Figure 101 and 102). A more remarkable aspect is that, when the sample presented a deformation before drying, the deformation further increased while drying.

Figure 101 Modern samples from Group A: Visual comparison of the dimensions before (red line) and after freeze-drying ©HE-Arc

Figure 102 Modern samples from Group B: Visual comparison of the dimensions before (red line) and after freeze-drying ©HE-Arc

Chapter 6. The consolidation of carbonised textiles

6.1 Aim

After the drying treatment, textiles can be very brittle. Consolidants are introduced into a deteriorated and crumbling material, to compensate the loss of their natural binding media[114]. In the case of textiles, they bond the fibres together and prevent their shedding and fracture[115]. An adhesive film is formed around the fibres, adhering one to each other and strengthening the threads[116].

[114] Down, 2015
[115] Geijer, 2011, p. 80
[116] Peacock 1992, p. 204

Research and practice (Karsten, 2003[117]) advocates that an effective stabilisation of a material through consolidation is more dependent on the combination of materials and methods to create an adhesive bond strong enough to accomplish treatment goals, rather than the choice of the adhesive alone[118]. Also, the characteristics of the textile (the fibres, conditions, etc.) will dictate the adhesives, solvents and procedure, which should not be applied to it to avoid further damage[119].

6.1.1 Selection of the criteria

In general terms, the ideal consolidant should be compatible with the substrate, be chemically and physically stable over time (no change in pH, colour, flexibility, strength, shrinkage etc., when aging), be strong enough to create the adhesive bond but stay weak enough to avoid damage on the substrate, be non-tacky as not to pick dust, be minimally invasive, be easy to apply, be non-toxic, remain removable, be inexpensive and allow future re-treatment[120].

All consolidant known nowadays cannot satisfy all these demands completely so, depending on the substrate, the one with the most significant properties must be chosen.

Charred textiles must be treated with a consolidant miscible in other solvents than water, because after freeze-drying them, it could be possible to re-moisturise and solubilize the PEG 400 inside the fibres. On one hand, a low viscosity solution will be preferable, to avoid the accumulation of the adhesive on the surface, which could change the aesthetical appearance of the textile. Thus, solvents with high evaporation rates (like acetone) must be avoided, to allow the deep penetration.

On the other hand, the bond between the consolidant and the fibres must be strong enough to stabilise the structure, having a high cohesive and adhesive strength. The adhesive has to overcome stresses exerted at the site during handling, display, transit and possible changes in relative humidity and temperature[121].

To allow a long-term stabilisation, the adhesive must not shrink with time and remain flexible. Otherwise, future fractures of threads and fibres will appear. The flexibility is controlled by the glass transition temperature (Tg). Consolidants with a lower Tg are more flexible, but if their Tg is around or below room temperature, they remain tacky and can attract dirt or stick to other materials. Flexibility also depends on adhesive thickness, solvent retention and adhesive penetration into the substrate[122]. Consolidants with low Tg, close to the atmospheric temperature, should be avoided. The pH has to be

[117] Karsten, 2003
[118] Down, 2015
[119] Down, 2015
[120] Down, 2015
[121] Down, 2015
[122] Down, 2015

considered as well. The selected products must also remain chemically stable, and pH should stay between 5.5 and 8.

6.1.2 Selection of the application method

The application technique can affect the viscosity of the solution, therefore the ability to penetrate the substrate[123], and the pros and cons of the wet application of non-aqueous solutions for textiles were evaluated (Table 12).

Advantages	Disadvantages
- Avoids water or heat - Fast to apply, minimal preparation required - Variety of adhesives and properties possible - Variety of solvents possible, providing control of properties such as evaporation rate, viscosity, etc	- Unwanted penetration, stiffening, staining possible - Limited working time depending on solvent evaporation rate - Fume extraction required – health concerns

Table 12 Advantages and disadvantages of the wet application of non-aqueous solutions

A search for a method which allowed a quick and easy application while maintaining a low viscosity was undertaken. As the samples were going to be fully consolidated, unwanted penetration or staining marks was not a problem. Priority was given to methods which avoided a direct contact between the tool and the surface of the fibres, because of the risk of breaking more fibres, so the application with brush and syringes was inevitably avoided. Sprayers can deliver large quantity of consolidant, but droplets can be created by the time the consolidant reaches the object (higher viscosity), not allowing an even consolidation of the textile.

Finally, the application method chosen was the pipette, which keeps the low viscosity during the application, avoids the direct contact with the surface, and is a very handy and low-cost tool.

6.1.3 Selection of the products

Adhesives, which did not match the specific criteria mentioned before for the consolidation of charred archaeological textiles, have been avoided.
To reduce differences, ethanol was chosen as solvent for all consolidants, so that, if there is a difference on the viscosity and penetration of the solution, it will be related to the adhesive. This decision implies that any consolidant not miscible with ethanol was also removed from the list.

[123] Down, 2015

The selection of the products was then based on the properties of the adhesive, the results that other researchers had when applying them to archaeological textiles, and their availability in the museum. The selection of the proportion between adhesive and solvent was also based on the publication's recommendations. The consolidants selected were Klucel® G, Klucel® E, Paraloid® B72 and Aquazol® 500 (Characteristics per adhesive are described in Appendix 16, and the technical data is in the Digital Appendices). In the case were no publications were found for its use as a consolidant for archaeological textiles, the choice was given to options highly recommended by the paper and painting conservators from the museum.

6.2 Consolidation of the archaeological and modern samples: Methodology

Group A and Group B samples were separated in five sets each. Each set was composed of twenty samples of modern textiles, and two to five samples of archaeological charred textiles depending on the dimensions and the degradation state of the fragments. The twenty modern samples consist of four big samples of warp, four small samples of warp, four big samples of weft, and four big small samples of weft (Figure 103).

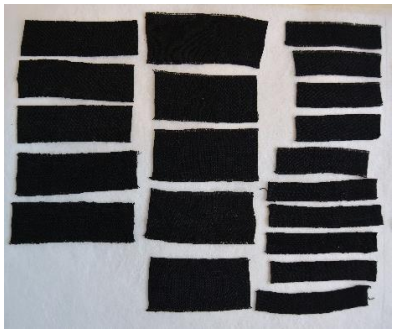

Figure 103 Example of modern charred samples selected for one set ©HE-Arc

A total of eight sets, four from Group A and four from Group B, were prepared for consolidation. One layer of Buvar® (Article number 4551) from Lascaux® covered with Hollytex® was used as support during the consolidation, which would avoid the accumulation of the solution on its surface (and thus, samples will not have one face glossier than the other). The fifth set per group was left unconsolidated to have a reference of modern and archaeological samples without consolidant. Detailed information about which samples have been treated with each solution can be found in Table 13.

The solutions were prepared mixing the adhesives with ethanol in the following concentrations: 1%w/w for Klucel® G, 5%w/w for Klucel® E, 5%w/w for Paraloid® B72, and 1%w/w for Aquazol® 500. When preparing the Paraloid B72, it was necessary to pre-dissolve it in 12% Butanone, otherwise the solution precipitated when adding the Ethanol.

Each consolidant was then applied with a pipette to all samples of the same set (Table 13). A total of two sets were treated with the same consolidant (one from Group A, which was previously treated with 8% PEG 400, and one from Group B). All consolidants air-dried for four days before testing.

Product	Solvent	Concentration	Group A samples		Group B samples	
			Archaeologic	Modern	Archaeologic	Modern
Klucel® G	Ethanol (with 2% Butanone)	1%w/w	1.01 1.29 3.1 3.14	5 big warp 5 big weft 5 small warp 5 small weft	1.10 1.23 2.11 2.15	5 big warp 5 big weft 5 small warp 5 small weft
Klucel® E	Ethanol (with 2% Butanone)	5%w/w	1.17 3.4 3.11 3.16	5 big warp 5 big weft 5 small warp 5 small weft	2.05 2.06 2.08 2.10	5 big warp 5 big weft 5 small warp 5 small weft
Paraloid® B72	Ethanol (with 2% Butanone)	5%w/w	1.02 3.12 3.13 3.19	5 big warp 5 big weft 5 small warp 5 small weft	1.18 1.19 2.2 2.19	5 big warp 5 big weft 5 small warp 5 small weft
Aquazol® 500	Ethanol (with 2% Butanone)	1%w/w	1.31 3.3 3.7 3.8	5 big warp 5 big weft 5 small warp 5 small weft	1.30 2.04 2.16 2.18	5 big warp 5 big weft 5 small warp 5 small weft
No consolidation			1.16 3.18	5 big warp 5 big weft 5 small warp 5 small weft	1.5 2.03	5 big warp 5 big weft 5 small warp 5 small weft

Table 13 Information about the samples treated with each consolidant

6.3 Results and interpretation

Once the solvent evaporated, no aesthetical differences were appreciable to the naked eye in any sample. None of them had a glossy appearance, and stains were not created by the consolidant during its application or drying, in neither faces of the sample. Dimensions of the samples were not altered either.

When calculating the weight gain of the archaeological samples after consolidation, some values appeared in negative. This means that the weight of the sample has decreased instead of increasing, and it can only be related to the loss of fibres. Those values were not taken into consideration when interpreting the results.

For every consolidants, samples treated with PEG 400 gained more weight, except for the Klucel® E, which remained almost the same. The weight gain goes from 0,001±0,001g of the samples from Group B treated with Aquazol® 500, to 0,014±0,009g of the samples from group B treated with Paraloid® B72. The two consolidants that provoked the higher weight gain were Paraloid® B72 and Klucel® E, and it is probably because of their higher concentration.

Unfortunately, for the samples treated with Paraloid® B72 and Klucel® G, some fibres of the modern and archaeological samples remained attached to the support, most of all the fibres were situated on the edges of the samples, which have weak mechanical bonds to the ensemble. For the same samples,

few non-adherent white fibres are also visible on the surface of the sample facing the support. Fibres forming the Hollytex® have less cohesive strength between them than the adhesion strength created between the consolidant, the sample and the surface of the Hollytex®.

Chapter 7 Physical testing of textiles

7.1 Physical properties of Flax: Literature review

After the identification of the fibres and the selection of the linen as the material for the modern samples, it is important to focus on the properties of flax fibres in order to have a better understanding of it response to the physical tests.

Flax is a fibre obtained from the stem of the *Linum usitatissimum*, which grows in many sub-tropical and temperate regions of the world. Following extraction, the fibres and processing it into threads and fabrics, linen is formed. Its quality depends on the growing conditions, the age of the plant and the fibre processing[124].

Flax contains cellulose as the principal component, and then lignin, pectin, ash, proteins, fat and wax as secondary components[125] (Table 14). The polymer structure contains a mixture of amorphous and well-organised crystalline regions. These last ones have a lower capacity to absorb moisture and, in consequence, they are more resistant to chemical attack[126]. Moreover, flax also has an ability to regain more moisture because of the presence of hemicellulose in the lumen of the fibres. In addition, fibres like hemp or flax increase their strength, extensibility and elongation when absorbing moisture[127].

[124] Cook 1988
[125] Serchisu, 2014, p. 48-50
[126] Peacock, 2003
[127] Tímar-balázsy, 1999

Property	Flax
Cellulose content	65-87% (blanched, up to 98%
Lignin content	Small
Hemicellulose content	7-9%
Pectin content	1.5-2.5
Fats and waxes content	5-2
Proteins content	2-0
Ash content	4-1
Length of elementary fibres	3 – 6 mm
Shape of cross-section by elementary fibre	5- to 7- sides, with sharp peaks
Moisture	12%
Fineness	0.25 – 0.33 tex
Breaking length	52 km
Elongation at break	1 – 2.5% dry 2 – 4% wet
Elasticity	Slight
Shape of lumen	Small, less apparent even at the dotted form
Texture of fibre	Hard or coarse
Ends of the elementary fibres	Sharp

Table 14 Chemical composition and properties of modern flax. The values refer to the dry weight and are reported in percentages [128] [129]

7.2 Aim of physical testing

The primary objective of textile testing was to evaluate the properties of the fibres and predict its future performance[130]. The mechanical properties can reflect the changes occurred before, during and after burial. Therefore, tensile properties provide an evaluation of handling characteristics. Tensile properties can reflect changes as well on the textile, due to forces or deformations spread along the fibre axis, because of their high ratio of length to thickness[131].

Testing the bending length, flexibility, hardness and other characteristics before and after carbonisation, will allow us to understand how the physical properties of textiles can change because of it. It will also make us comprehend better the state of conservation of archaeological textiles, and the way carbonisation influence their degradation.

[128] Serchisu, 2014
[129] Wiener et al., 2003, p. 58
[130] Dolez *et al.*, 2018, p. 4
[131] Dolez *et al.*, 2018

To be able to evaluate the results of the physical tests, it is necessary to first understand the physical properties of the fibres that can potentially affect them. For each test, the standard error of the arithmetic mean was calculated based on the coefficient of variation and the number of samples.

Changes in dimensions, count of threads, weight and colour/gloss are evaluated in both archaeological and modern samples to compare the consolidation results. To do so, several property-based test methods are normally used measuring the physical or chemical characteristic of the textile[132]. Unfortunately, it was not possible to test the bending strength and the tensile strength on the archaeological samples. For the bending strength test, some samples were too small to allow measuring anything, and the bigger samples had fragmented threads which could result in total breakage during the test. The tensile strength is a destructive test, and not an option for archaeological samples.

7.3 Physical Tests: Methodology

7.3.1 Atmospheric conditions

Tests must be reproducible, but differences can arise because of the sample size, temperature and humidity conditions, the equipment used, the conditions of the test, and the influence of the operator[133]. Regarding the temperature and humidity conditions, textile testing can be strongly affected by the hygroscopic behaviour of natural fibres, and their tendency to absorb or give up moisture depending on the relative humidity of the environment. Thus, it can affect the measurement of their physical properties[134]. To ensure comparable and meaningful results during the tests, standardized temperature and relative humidity conditions were used. The ISO standard 139/A1 (2011)[135] establishes 20.0±2ºC and 65.0±4 % RH for modern textiles, or 23.0±2ºC and 50.0±4 % RH as a standard alternative atmosphere if the parties involved agree on its use[136] [137].

The Collection Centre where the textiles were tested had stable conditions in the laboratories during the year (22±2°C and 48±4% Relative humidity). Knowing that the modern samples were completely dried during the carbonisation, they were let in the laboratory to regain moisture and be in equilibrium with the conditions on the laboratory. No further pre-conditioning of the samples was applied during the tests.

[132] Dolez *et al.*, 2018, p. 9
[133] Dolez *et al.*, 2018, pp. 3-4
[134] Dolez *et al.,* 2018
[135] NF EN ISO 139 (2005): *Textiles - Standard atmospheres for conditioning and testing*
[136] Dolez *et al.,* 2018, p. 12
[137] It is important to do the test at the same relative humidity because if not, the effect on the fibres will vary. (Morton and Hearle, 2008).

7.3.2 Bending length test

The stiffness and flexibility of the modern samples was analysed calculating their bending length. The stiffness (flexural rigidity) of a fabric is an indicator of its resistance to bend, and is directly affecting the flexibility of the textile. Resistance to bending arises when friction impedes the mobility of the yarns in the fabric and the fibres in the yarn [138].After drying the textiles, stiffness relates to less mobility within the system, brought about by the collapse of yarns and fibres.

The bending length was measured on a hand-made Shirley Stiffness tester created in 1969, applying the Cantilever test (Figure 104). Four measurements were taken per sample (corresponding to the two extremities and both faces), according to the ISO Standard NF EN ISO 9073-7[139]. The bending rigidity can be calculated with the equation provided by the standard.

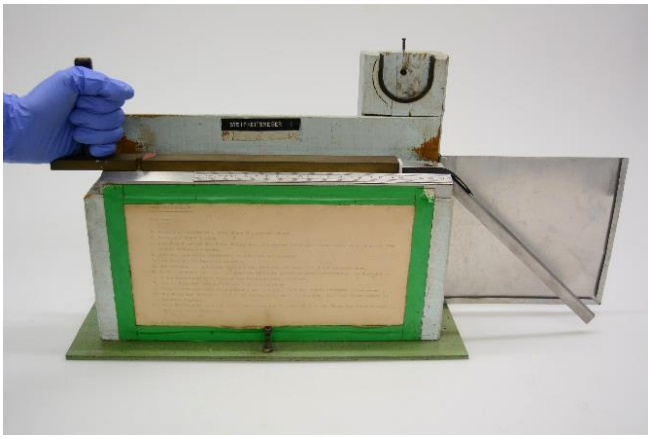

Figure 104 Hand-made Shirley Stiffness tester ©HE-Arc

The principle is to advance a rectangular sample at a constant speed in a horizontal platform, in the direction of its length, until one extremity overhangs and bends down under its own weight (Figure 105 and 106). Usually, the long weight is place over the sample, and then moved to one side, dragging the sample below (Figure 107 and 108). Because of the fragility of the textiles, we weight could not be place on the textile, so we place the weight behind the sample and push it at a constant speed, using a piece of foam as protection between the sample and the weight. For the smaller modern samples, a smaller and more weight was used in other to better control the speed. The overhanging length can be measured when the edge reaches the platform inclined at 41.5 degrees below the horizontal, after 8±2 seconds. The bending length (C) is equivalent to half of the overhanging length. The flexural rigidity (G) is calculated with the equation: $G = m \times C^3 \times 10^{-3}$[140], with m as the mass of the sample per unit area (g/m^2).

[138] Janaway and Wyeth, 2005, p.4-5
[139] NF EN ISO 9073-7 (1998): *Textiles - Test methods for nonwovens – Part 7: Determination of bending length.*
[140] This equation is obtained by approximating the acceleration due to gravity g by $10m/s^2$ instead of $9.81m/s^2$.

Figure 105 Modern sample on the starting point of the Shirley Stiffness tester ©HE-Arc

Figure 106 Modern sample touching the surface at 41.5 degrees, and ready to measure its bending length ©HE-Arc

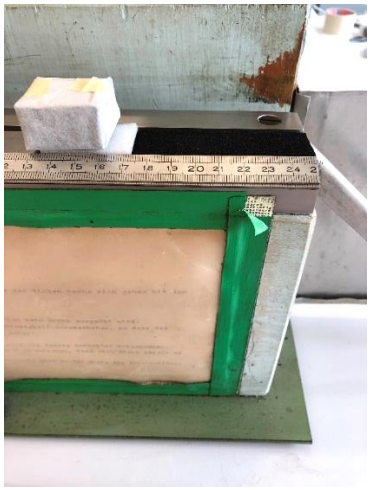

Figure 107 Modern sample on the starting point of the Shirley Stiffness tester with a smaller weight ©HE-Arc

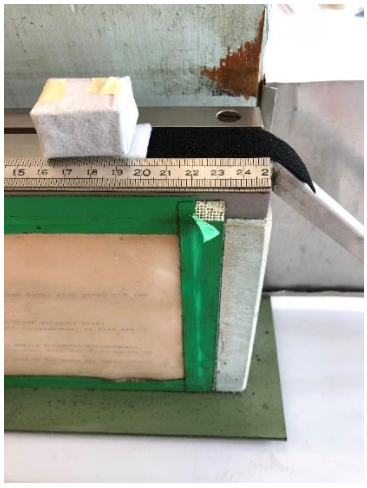

Figure 108 Modern sample touching the surface at 41.5 degrees, already moved by the smaller weight, and ready to measure its bending length ©HE-Arc

7.3.3 Tensile strength test

For this test, the dimension of the sample was extended at a constant rate until the rupture of the specimen. There are two main international standards for tensile tests of textiles: NF EN ISO 13934-1 (2013)[141] and NF EN ISO 13934-2 (2014)[142]. The test informs about the strength of a fabric, which can give a measure of the resistance to extension (the force at which a specimen breaks is directly proportional to its cross-section area)[143]. The work of rupture, which is the energy needed to break a fibre, informs about the ability of the material to resist a sudden input of a given amount of energy[144].

[141] NF EN 13934-1 (2013) : *Textiles – Tensile properties of fabrics – Part 1: Determination of maximum force and elongation at maximum force using the strip method*
[142] NF EN ISO 13934-2 (2014*): Textiles – Tensile properties of fabrics – Part 2: Determination of maximum force using the grab method*
[143] Dolez *et al.*, 2018, p. 116
[144] Janaway and Wyeth, 2005

After charring the samples, they were still flexible, but too friable to use a tensile strength machine, which meant that it was not possible to measure the forces applied in newton[145], and consequently no stress-stain curve was created. Taking inspiration from the tensile strength test on the standards mentioned before, some necessary modifications were carried out to measure the results.

For the test, the weight necessary to break a certain dimension of the sample (3cm) was measured, when the weight is pulling the fabric vertically (at 90° from the horizon). To do so, the sample was fixed to a horizontal, metallic and magnetic surface with soft magnets, and in a position perpendicular to its edge. Three centimetres from one extremity of the strip were left hanging under its own weight out of the surface. To those three centimetres, a paper clip was attached, to which a paper recipient was attached with a cotton thread. The recipient had an inverted-pyramidal shape to allow the pulling forces concentrate in the same direction. Non-acidic cardboard was used as a protection layer between the clamp and the textile as well as between the magnets and the metallic surface.

Once the sample was fixed and the recipient clamped, the weights were added. Small lead weights spheres were used for the test. The weight of each sphere was around 0,1g. To reach the extension at a constant rate, one sphere was added per second[146].
Using a scale[147], the total weight needed to break the strip (the leads plus the clamp, the cotton thread and the paper recipient) was calculated. The dimensions of the broken piece were also measured with a calibre.

7.3.4 Colour and gloss

To evaluate the change of colour and surface gloss of the archaeological and modern samples, before and after consolidation, a portable spectrophotometer CM-2600d by Konica Minolta® (Figure 106) was used. This type of spectrophotometer is convenient to measure the colour of flat samples, and uses the patented numerical gloss control (NGC), delivering data which includes (SCI) or excludes (SCE) surface conditions. The measuring aperture is 8mm (MAV).

[145] Newton defines the acceleration produced when the force acts on a mass of one kilogram. A newton is defined as the force that when applied to a mass of one kilogram gives it an acceleration of one metre per second per second.
[146] The time you spend applying the force is important because of the stress relaxation effect
[147] Sartorius® MC 1 from IG®

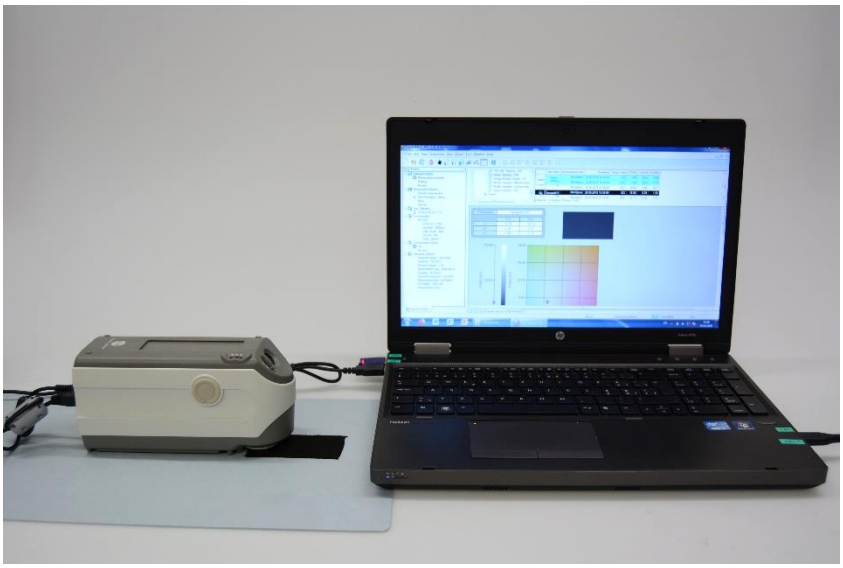

Figure 109 spectrophotometer CM-2600d by Konica Minolta® already connected to the computer and taking measurements ©HE-Arc

Before the measurements, the spectrophotometer was connected to an external computer and calibrated in accordance with the manufacturer's instructions. The device takes three measurements of the same area and gives a mean value, which is recorded through the colour data software SpectraMagic™ NX from Konica Minolta®.

A grey non-acidic cardboard was selected as the support for both modern and archaeological samples during the process. Measurements of the cardboard were also taken with the spectrophotometer to have a record of its colour. Using the same support facilitates the comparison between the samples. In addition, some archaeological samples have an open fabric, which means that the support is visible through the textile, and thus can influence the results of the measurements. If the values of the support are already known, it will be easier to interpret its influence.

Thanks to the sample viewing window, the areas of the sample measured could be easily selected, eluding reprises of the same zone. When possible, a uniform coloured area was selected, avoiding any deformation and surface residues. For the modern samples, five different areas of the same specimen were measured. As the dimensions of the 4 types of sample are almost similar, the same areas were stablished for all. For the archaeological samples, due to the reduced surface area of some of them, one to three measurements were taken per sample, depending on the sample size, and avoiding, when possible, friable areas.

7.4 Results and interpretation

7.4.1 Bending length

The flexibility is the characteristic that, due to the different adhesives applied, changed the most when comparing before and after consolidation. Sadly, it was not possible to measure the flexibility of the archaeological samples, because of the reduced dimensions of some samples, and the brittleness of others (the weight of the sample itself, when bending, could break the threads that are already half broken). To test the flexibility, the samples were manipulated with tweezers and a conservator-restorer carefully evaluated the flexibility of each sample (based on visual observation and the response of the sample when manipulated).

A scale of flexibility was established, using one "x" for the samples less flexible, and up to five "x" for the most flexibles. The symbol "/" indicates that the sample was too small to evaluate its flexibility (See Table 15).

Consolidant	Group A		Group B	
	Samples	Flexibility	Samples	Flexibility
No consolidation	1.16	/	1.5	xxxxx
	3.18	xxxxx	2.03	xxxxx
Klucel® G	1.01	/	2.11	/
	1.29	xxx	1.23	/
	3.1	xxx	2.15	xx
	3.14	xxx	1.6	xx
			1.10	xx
Klucel® E	3.11	xxx	2.1	xx
	1.17	xxx	2.06	xx
	3.4	xxx	2.05	xx
	3.16	xxx	2.08	xx
Aquazol® 500	1.31	/	2.16	xxxx
	3.3	xxxx	2.18	xxxx
	3.8	xxxx	1.30	xxxx
	3.7	xxxx	2.04	xxxx
Paraloid® B72	3.12	x	1.19	x
	3.19	x	2.19	x
	1.02	x	1.18	x
	3.13	/	2.02	x

Table 15 Summary of the flexibility test carried out on the archaeological samples after consolidation

The result of this experiment is that, Aquazol® 500, applied to the archaeological textiles either treated or untreated with PEG 400, let the textiles remain very flexible (almost like the samples not consolidated), while giving a certain strength to the structure and cohesion between the fibres.

All modern samples were tested following the Cantilever test described in the previous chapter. Then, the mean bending length and flexural rigidity was calculated (See Appendix 17). The bending length, which is the average of the overhanging length of the entire sample treated following the same procedure, is expressed in centimetres. As visible in Figure 110 and 111, for the samples freeze-dried without PEG 400, a larger dimension of the sample is needed to bend under its own weight and reach the plate at 41.5 degrees. The flexibility of the samples is inversely proportional to the bending length, so it can be affirmed that the textiles treated with PEG 400 remained flexible after the drying treatment.

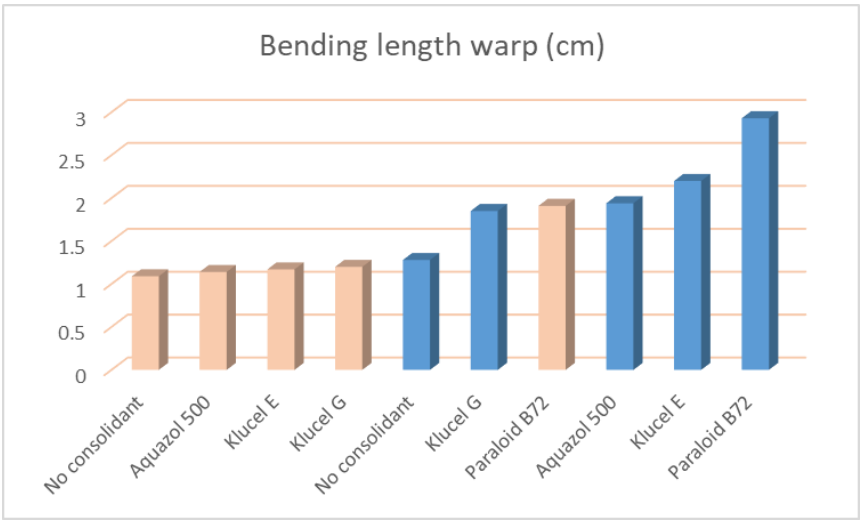

Figure 110 Comparison of the bending length for warp samples. Group A in pink and Group B in blue

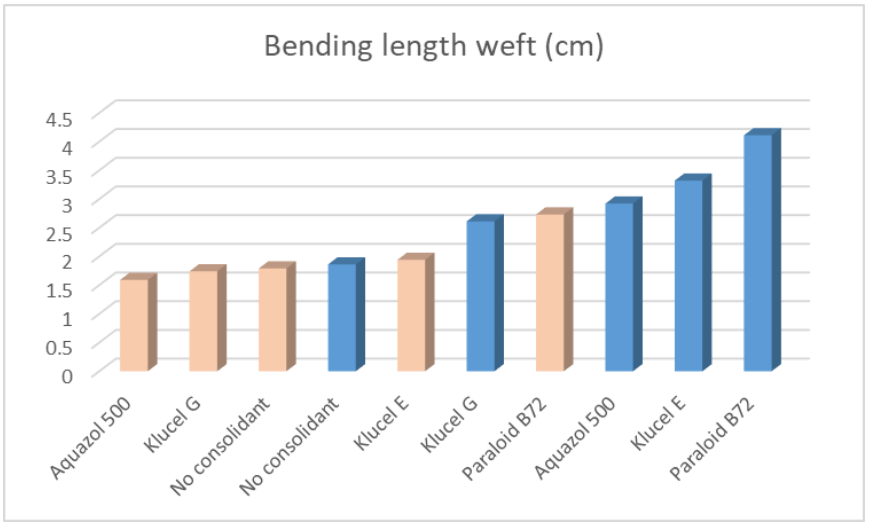

Figure 111 Comparison of the bending length for weft samples. Group A in pink and Group B in blue

Among the consolidants, Aquazol® 500 seemed to perform as the consolidant which allowed the higher flexibility to the textile, followed by Klucel® G, Klucel® E and finally Paraloid® B72. Klucel® E, in theory, should be more flexible than Klucel® G because of its lower molecular weight, but when applied, a higher concentration was used (5% for the Klucel® E and 1% for the Klucel® G).

There are not many differences between the consolidation of warp and weft samples. The bending length of the samples treated with consolidants with a medium flexibility differed slightly.

After calculating the bending length, the flexural rigidity was determined with the formula explained in the previous chapter. The flexural rigidity is directly proportional to the stiffness of the textile, so the higher the flexural rigidity, the more stiff the textile is. Figure 112 and 113 give and idea of the differences between the consolidants and direction of the textile, and a correlation is visible between the results of the bending length and the flexural rigidity. Again, Aquazol® 500 remains as the consolidant allowing the higher flexibility.

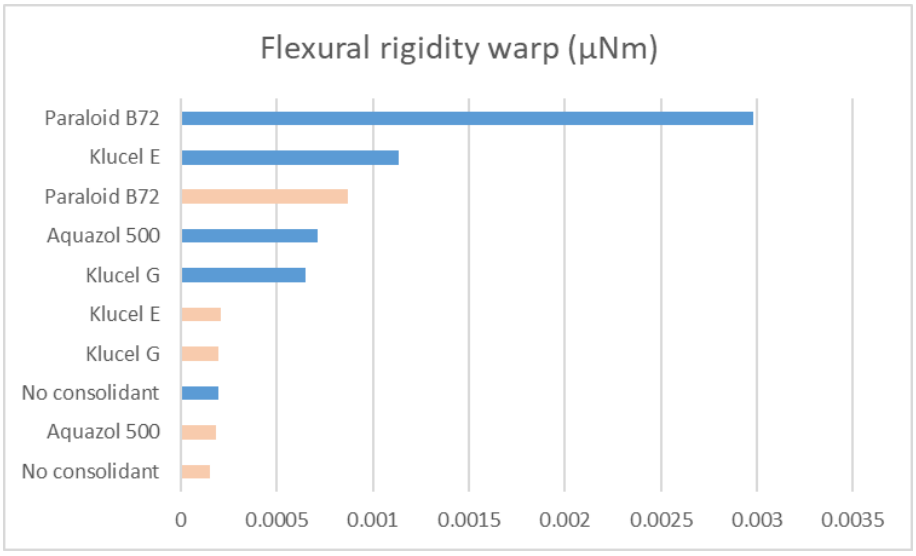

Figure 112 Comparison of the flexural rigidity for warp samples. Group A in pink and Group B in blue

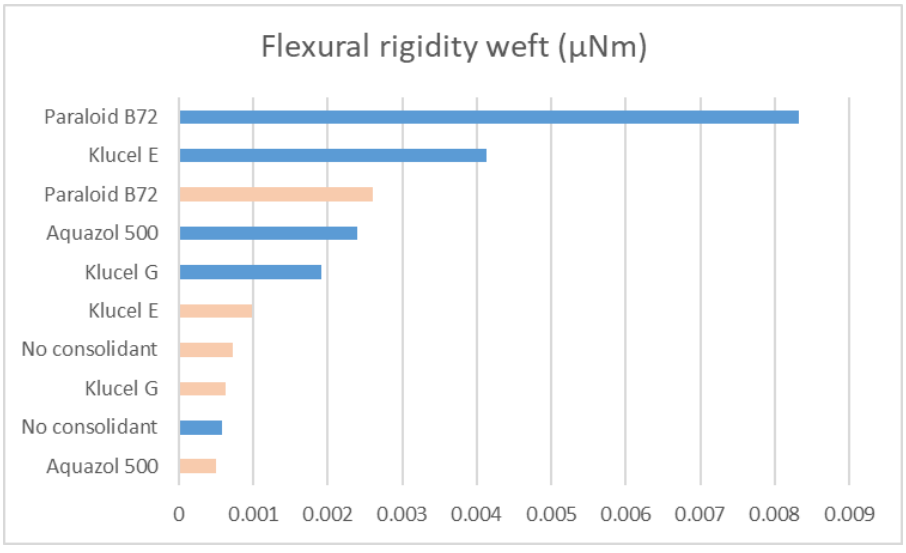

Figure 113 Comparison of the flexural rigidity for warp samples. Group A in pink and Group B in blue

7.4.2 Tensile strength

After testing the samples, a clear difference was visible between warp samples (Figure 114) and weft samples (Figure 115). All measurements per samples are visible in Appendix 18. Stresses applied in each direction do not react the same way, the weft direction being more resistant than the warp direction. The average weight applied to each direction differs almost up to 30g for all measurements. For both warp and weft directions, the samples demonstrated a higher resistance to rupture when pre-treated with PEG 400. The only exception was Aquazol® 500, which presented a higher resistance when the weft samples from Group B were tested.

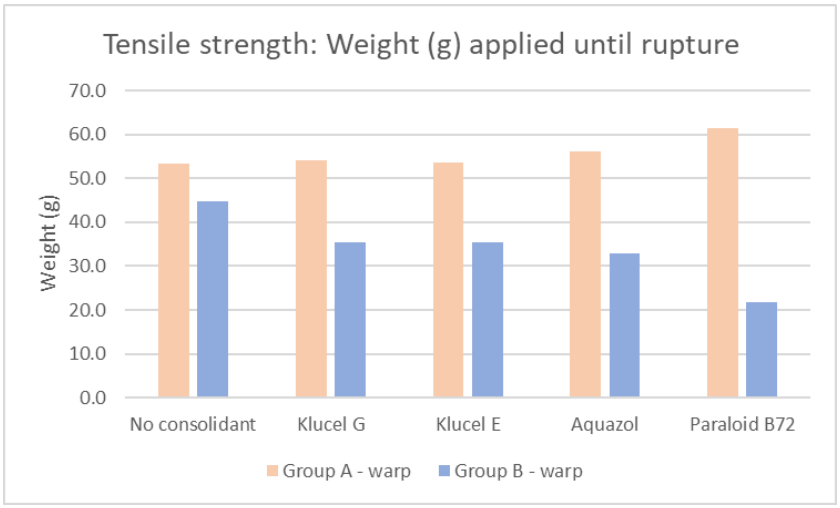

Figure 114 Tensile strength results for the warp samples of Group A and Group B

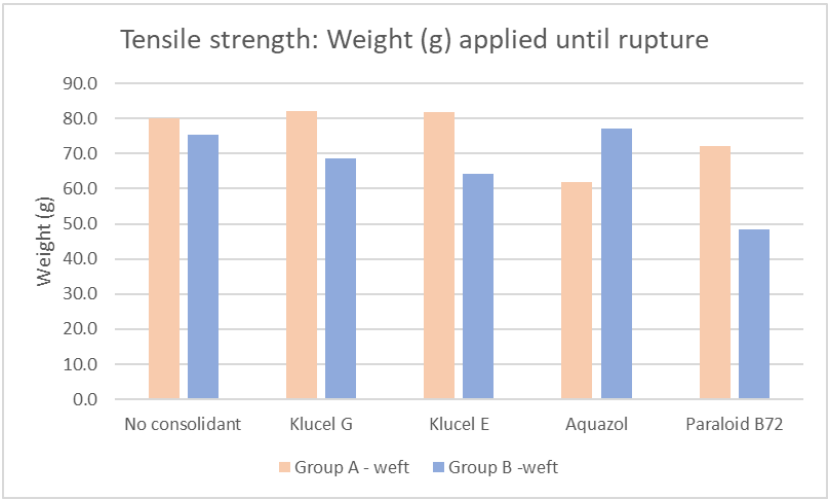

Figure 115 Tensile strength results for the weft samples of Group A and Group

The consolidants showing the most diverse results was Paraloid® B72. Warp samples pre-consolidated with PEG 400 and consolidated with Paraloid® B72 had a high resistance to rupture, while samples consolidated with the same product, but belonging to Group B, were friable.

When comparing all samples (Figure 116), it is visible that highest values belong to Klucel® G and Klucel® E for the samples that were pre-treated with PEG 400. It is thought that PEG 400, as a lubricant and plasticizer, keeps the flexibility of the fibres and increases their elastic properties. The elasticity of the fibres could increase the tensile strength of the fibres, and when it occurs, higher forces must be applied to arrive achieve the rupture. Stronger adhesives like Paraloid® B72, create stronger bonds between the fibres, and therefore, the elastic properties of the material are reduced. Then, lower forces applied to the samples are enough to break them.

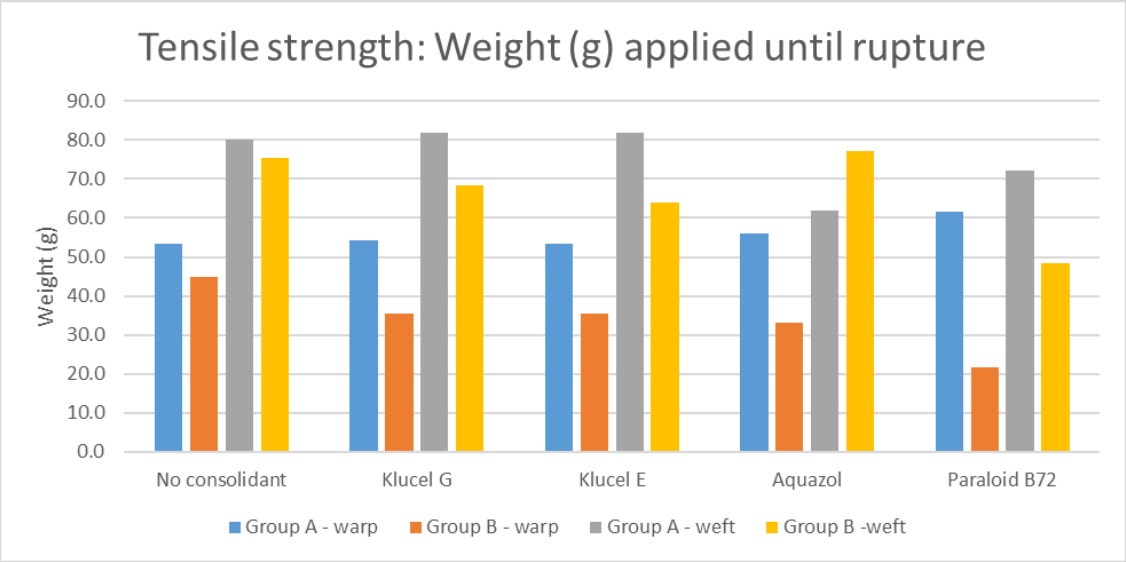

Figure 116 Tensile strength results for all modern samples of Group A and Group B

7.4.3 Colour and gloss

One hundred measurements were taken in total per set of modern textiles (see Digital Appendices). The mean value of the measurements was calculated to have comparable data between the adhesives. Only SCI data was interpreted, because it was desire to add the surface values in case the consolidants penetrated differently. The parameter the most interesting for our study is the L*, which is related to the lightness of the colour, as it gives a value between 0 (black) and 100 (white).

Modern samples, as they present homogenous surfaces which facilitate the comparison of data. Colorimetric plots for Group A (Figure 117) and Group B (Figure 118) demonstrated that samples pre-treated with PEG 400 present a darker surface colour (with the L* value between 17.67 and 15.44) than samples un-pre-treated (ranged between 14.41 and 15.25).

In order to describe the colour variation before and after treatment the parameter ΔE* (colour difference) was calculated for each treatment using the CIE1976 equation[148] and the mean value per treatment. A value is obtained when subtracting the ΔE* value obtained after consolidation to the ΔE* before consolidation. As the a* and b* values are around 0 in most measurements, we can assume that the ΔE* value will be obtained subtracting the L* value after consolidation to the one obtained before:

$$\Delta E^* = \sqrt{[(\Delta L^*)^2 + 0 + 0} \quad \Rightarrow \quad \Delta E^* = \Delta L^*$$

Although, values lower than 3 are considered not perceptible to the human eye, while ΔE* bigger than 5 are considered clearly perceptible. There is no difference perceptible to the human eye for the modern samples, as the colour difference between the darkest measurements from Group A, which correspond to samples treated with Klucel® G (ΔE*=14.46) and the lightest from Group B, which is also Klucel® G (17.35), with a colour difference of 2.89.

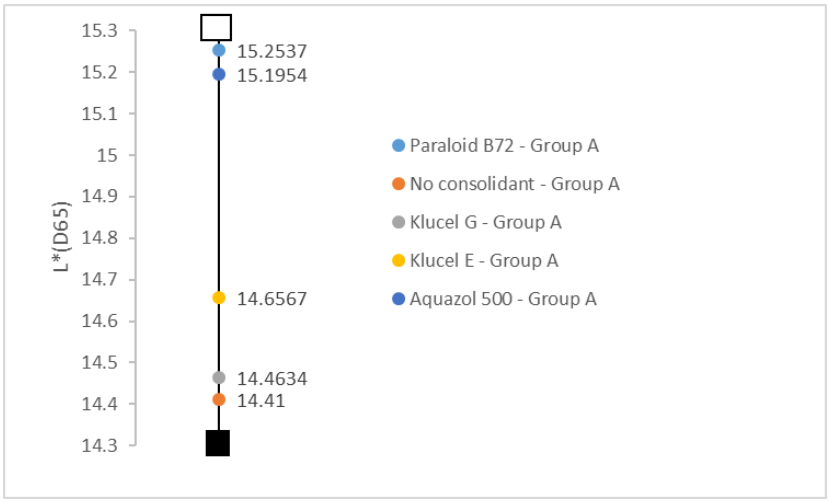

Figure 117 Colorimetric plot representing the colour coordinates for L*. Modern textiles from Group A

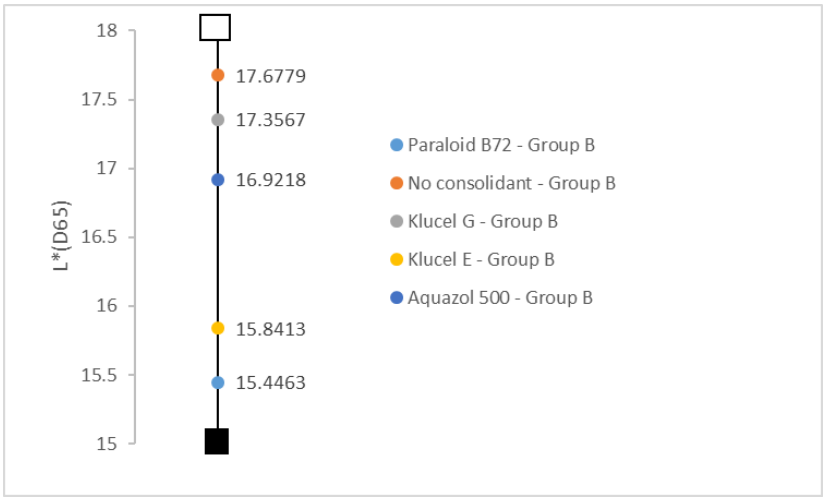

Figure 118 Colorimetric plot representing the colour coordinates for L*. Modern textiles from Group B

[148] $\Delta E^* = \sqrt{[(\Delta L^*)^2 + (\Delta a^*)^2 + (\Delta b^*)^2]}$

The results for the archaeological samples were harder to interpret, as the grey support was sometimes influencing the measurements, depending on the samples with open or closed fabrics. All textiles from Group A (Figure 119) present lighter colours than textiles from Group B (Figure 120). The L* value range goes from 23.50 to 25.62 for consolidated textiles pre-treated with PEG 400, and from 21.07 to 23.21 for Group B textiles.

In theory, a perceptible change should be appreciable as the colour difference (ΔE*) between the darkest consolidants from Group B and the lightest consolidants from Group A differ by more than 3 points. Unfortunately, it is not that visible in practice, which could mean a contamination of the data, influenced probably by the grey support.

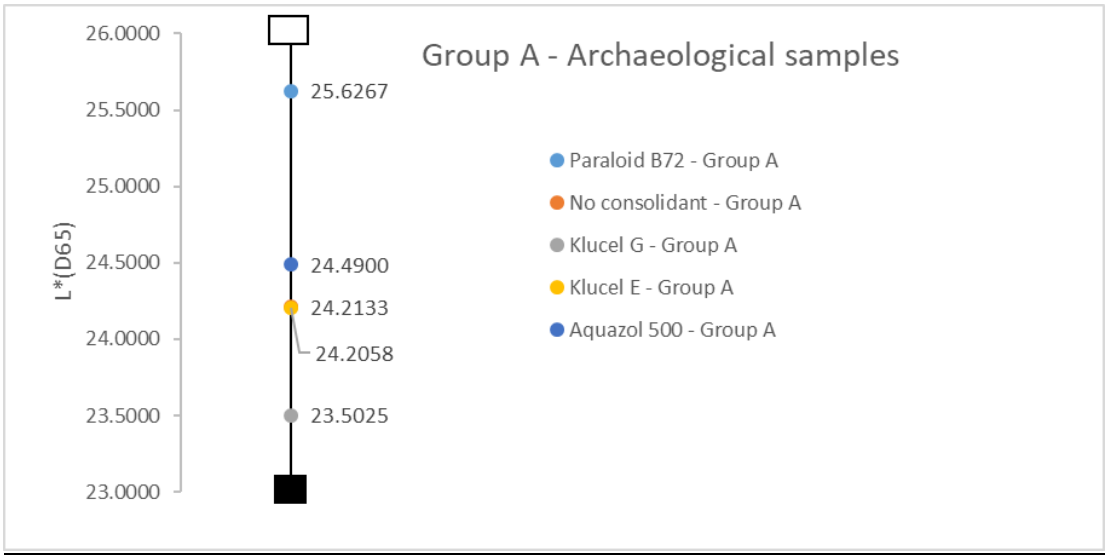

Figure 119 Colorimetric plot representing the colour coordinates for L*. Archaeological textiles from Group A

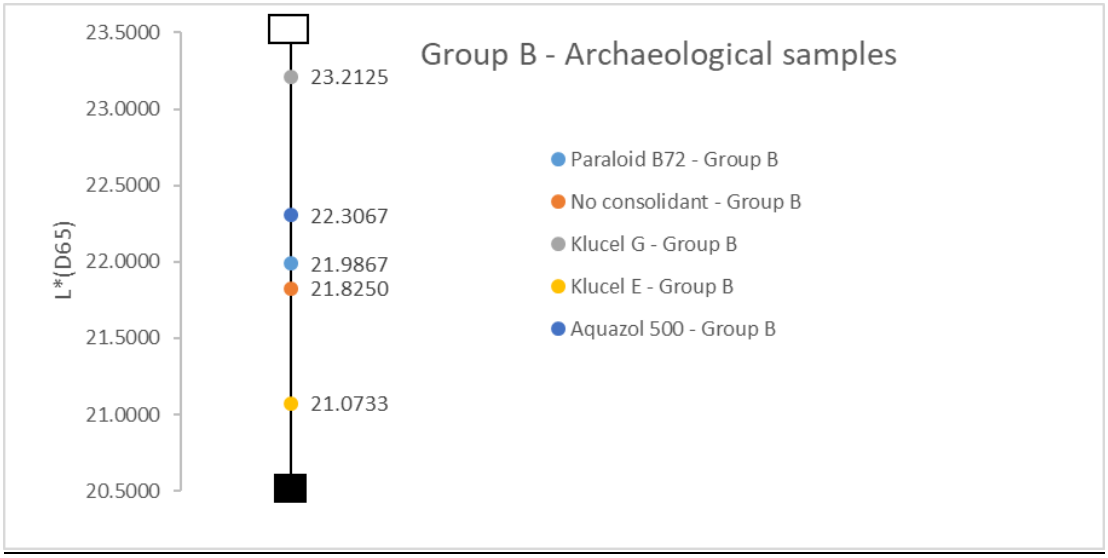

Figure 120 Colorimetric plot representing the colour coordinates for L*. Archaeological textiles from Group B

Discussion

Thanks to the creation of the charred samples, new information was added about the degradation of the textiles when submitted to reducing environments. That information is mainly related to the impressive dimensional change and sudden brittleness of the fibres after carbonisation, which can be extrapolated to the archaeological samples. It is known that charred archaeological textiles after burial don't have an aesthetical appearance similar to their state before carbonisation, but now we have a better understanding of the actual change. Further investigation about the charring process and the carbonisation of textile is extremely recommended, from both the experimental archaeology and conservation points of view.

During the freeze-drying treatment, it was interesting to have a visual observation of the sublimation process using the iced cubes. Most of the time, when organic material is freeze-dried, the only parameter which can give an objective value of the sublimation process is the temperature, as in most cases, it is not possible to see the object. Usually the object is protected with several layers, thus the observation of the surface of the object is impossible.

Although, the test did not provide us with all information wanted. The time spent manipulating the metal samples and the iced cubes was too long, and the pH of the papers changed before starting the treatment. For future tests, better preparation is needed to speed up the manipulation procedure, as time is very short when removing the samples and the cubes from the freezer, before the ice starts melting.

Unfortunately, towards the end of the sublimation procedure, the freeze-drying treatment had to be speeded up, increasing the temperature off the chamber. This fact unable us to keep a stable temperature through the whole process, in order to have a better understanding off the real time needed for the full sublimation process of charred archaeological textiles. It also provoked a sudden increased and decrease of temperature due to a technical problem when setting the temperatures. That are not yet aware of how, such a quick change in temperature, affected the textiles.

The physical tests results have been difficult to interpret due to the scarce number of samples per type of treatment, the different characteristics of the archaeological samples, and the different concentrations depending on the consolidant. For this project, priority was given to the percentages which, as the literature suggest, have already led to successful results. It would be advisable though, for future research, to use the same concentration for all consolidants to reduce variables when comparing the results. It is also highly recommended that, for future projects, a larger quantity of charred textiles is created in order to have a larger number of specimens to test, and thus, more interesting statistical results.

Nevertheless, the results that are presented in this paper are highly interesting. The presence of the PEG 400 in the fibres has an important influence on the flexibility of the samples, even after being consolidated with an adhesive.

The compatibility of the consolidants tested and the polyethylene glycols is still unknown, and as not be studied during this master thesis. However, as all charred samples, archaeological and modern textiles, are going to be stored in the Collection Centre of the Swiss National Museum, it would be interesting to compare, in the future, the actual state of the textiles and their evolution in time. It will allow conservators to evaluate the aging properties of the adhesives when applied to charred textiles, and maybe differences between the PEG 400 and the other consolidants could be highlighted.

Finally, a last comment must be added about the continuous loss of fibre, which has been an issue during the entire research project (Appendix 19 and 20). The archaeological ensemble was losing fibres already from the storage box to their consolidation. Every manipulation has been a risk for the samples, and attention should be paid in future studies about this aspect. During the practical work, solutions were search for the manipulation and cleaning of the textiles (e.g. creating a new support which allow their treatment in a safer way, or using the surface tension of the support to return the samples in their wet state), but It has not been found yet the manipulation procedure which can avoid completely the loss of fibres. In addition, the loss of fibres influenced drastically some tests results, especially when related to the weight of the samples

Conclusion

The late medieval charred archaeological textiles from Elgg, which were very friable when arriving to the Collection Centre of the Swiss National Museum, have been stabilized through freeze-drying under vacuum and consolidation.

During the process, the influence of polyethylene glycol (PEG) 400 on the physical properties of the charred textiles, when applied before a freeze-drying method, was evaluated. The possibility to divide the group of textiles for the freeze-drying treatment has given us the chance to compare their diverse reaction when dried with or without a plasticiser. It is believed that, for charred archaeological samples, applying a polyethylene glycol solution is beneficial to the textile, as the cohesion of the fibres is increased, while remaining flexible.

Modern charred textiles allowed the evaluation of the physical properties modifications when applying one consolidant or another. As a homogeneous support, it was possible to contrast the values obtained when comparing the flexural rigidity, the tensile strength and the variation of lightness.

Aquazol®500 seemed to provide the most performing properties, either for the samples treated or untreated earlier with PEG 400. The textiles remained flexible after consolidation, and the structural stability was strengthened.

However, due to the small number of archaeological sample tested, the results are still not fully significant and further research should be carried out.

Bibliography

Ambers *et al*, 2009: Ambers, J., Higgitt, C., Harrison L., Saunders D. (eds.). *Holding it all together. Ancient and Modern Approaches to Joining, Repair and Consolidation*, Archetype Publications, London, 2009

Bjerregaard, 2016: Bjerregaard, L., Peters, A. (eds.). *Pre Columbian Textile Conference VII*, Centre for Textile Research, University of Copenhagen, [Online]. 2016 [visited on February 2018] https://books.google.ch/books?id=nHdFDwAAQBAJ&pg=PA142&lpg=PA142&dq=charred+textiles+chemistry&source=bl&ots=vQjoQytIIO&sig=jtgjcH52iz1tsajb1QOQ-EWcSOQ&hl=de&sa=X&ved=0ahUKEwiu89TSqI_aAhWR6qQKHS3hD5wQ6AEIUzAG#v=onepage&q=charred%20textiles%20chemistry&f=false

Blackshaw and Ward, 1983: Blackshaw, S.M., Ward, S.E "Simple Tests for Assessing Materials for Use in Conservation" *In Resins in Conservation: Proceedings of the Symposium, Edinburgh 1982*, SSCR Edinburgh, 1983.

Brandenburgh, 2016: Brandenburgh, C.R. *Clothes make the man: early medieval textiles from the Netherlands*, Leiden University Press, Leiden, 2016

Brown and Brown, 2011: Brown, T., Brown, K. *Biomolecular Archaeology: an introduction*, Wiley-Blackwell, Oxford, 2011

Calonder, 2018: Calonder, N., personal communication, March 2018

Carrlee and Senge, 2013: Carrlee, E., Senge, D.K. "Treatment results for waterlogged archaeological basketry at the Alaska State Museum". In *Proceeding s of the 12th ICOM - CC Group on Wet Organic Archaeological Materials Conference* 263-269, 2013

Catling and Gaysonm 1998: Catling, D., Grayson J., *Identification of Vegetable Fibres*, Archetype Publications, Leicester, 1998

Charlet *et al*., 2009: Charlet K., Eve S., Jernot, J.P., Gomina, M., Breard, J. "Tensile deformation of a flax fiber", *Procedia Engineering 1*, Elservier, 2009, pp.233-236.

Cooke, 1988: Cooke, B., "Fibre damage in archaeological textiles", In O'Connor. S.A, Brooks, M.M (eds) "Archaeological Textiles", *Occasional Papers Number 10, The proceedings of the conference Textiles for the archaeological Conservator*, UKIC Archaeology Section, York, 1988

Cooke, 1988: Cooke, B. "Creasing in Ancient Textiles", *Conservation News 35*, UKIC, 1988, p. 27-30.

Dolez *et al*., 2018: Dolez, P., Vermeersch O., Izquierdo V., *Advance characterization and testing of textiles*, The Textile Institute book series, WP Woodhead Publishing, Oxford, 2018

Domac and Trossero, 2008: Domac, J., Trossero M., Industrial Charcoal production, FAO, Zagreb, [Online] 2008 [visited on March 2018] http://www.fao.org/docrep/X5555E/x5555e01.htm#TopOfPage

Down, 2005: Down, J.L. *Adhesive Compendium for Conservation*, Canadian Conservation Institute, Ontario, 2015

Fedorak, 2005: Fedorak, P. M. "Microbial processes in the degradation of fibers". In Blackburn, R. S. (ed.) *Biodegradable and Sustainable Fibres*, Woodhead Publishing Limited, Cambridge, 2005, p.1-35

Florian, 1988: Florian, M.-L. E. "Deterioration of organic materials other than wood" In: Pearson, C. (ed.) *Conservation of Marine Objects*, Butterworths, London, 1988

Florian *et. al.,* 1990: Florian, M.-L. E., Kronkright, D.P., Norton, R.E., *The conservation of Artifacts made from plant materials*, The J. Paul Getty Trust, Los Angeles, 1990

France, 2005: France, F.G. "Scientific analysis in the identification of textile materials", In Janaway, R., Wyeth, P., *Scientific Analysis of Ancient and Historic Textiles: Informing Preservation, Display and Interpretation, First Annual Conference 13-15 July 2004*, AHRC Research Centre for Textile Conservation and Textile Studies, Archetype Publications Ltd, 2005

Geijer, 2011: Geijer, A. "Preservation of Textile Objects", In Brooks, M.M., Eastop, D.D. (ed). *Changing Views of Textile Conservation*, Getty Conservation Institute, Los Angeles, 2011

Gisler and Moser, 2018: Gisler, J., Moser, M. (eds), *Täatigkeitsbericht, Archäaologie und Denkmalpflege 2017*, Kanton Zürich, Dübendorrf, [Online] March 2018 [visited on February 2018],https://are.zh.ch/internet/baudirektion/are/de/archaeologie/denkmalpflege/_jcr_content/contentPar/downloadlist_2/downloaditems/t_tigkeitsbericht_20.spooler.download.1520944558264.p df/Taetigkeitsbericht_2017.pdf

Goffer, 2007: Goffer, Z. *Archaeological chemistry*, Wiley, Hoboken, 2007

Haldane, 2000: Haldane, E-A. « Notes on a New Method of Application for Klucel G: Substrate-free Adhesive Films Developed for Use on a Fragile Appliquéd Embroidered Textile*" Conservation News* 73, IIC, London, 2000

Haldane, 2007: Haldane, E-A., "Encounters with paper conservation: the treatment of a Chinese painted silk dress", Conservation Journal, Issue 49, [Online] 2007, [Visited on April 2018] http://.vam.ac.uk/res_con/conservation/journa/number49/chinesedress/index.html

Hamilton, 2007: Hamilton, D.L. Methods on conserving archaeological material from underwater sites. Reinforcing fragile textiles, Texas A&M University, [Online] 2007, [visited on March 2018] http://nautarch.tamu.edu/class/anth605/file0.htm

Hartmann, 2018: Hartmann, C., personal communication, February 2018.

Hiron, 2003: Hiron, X. Diversité des matériaux organiques fibreux rencontrés sur le site néolithique de Chalain; Problématique de leurs traitements et de leur conservation, et exemples de leur mise en oeuvre à Arc-Nucléeart, Grenoble. In *Incontri di restauro 4. Intrecci vegetali e fibre da ambiente umido Analisi Conservazione e Restauro*, Trento 28-30 maggio, 2003

Horie, 2010: Horie V., *Materials for Conservation. Organic consolidants, adhesives and coatings*, Elservier Ltd, Oxford, 2010

Howell, 1996: Howell, D. "Some mechanical effects of inappropriate humidity on textiles" In *Preprints of the 11th Triennial Meeting of the ICOM Committee for Conservation. Paris: International Council of Museums*, 1996, p. 692-698

Huisman, 2009: Huisman, D. J. (ed.) Degradation of Archaeological Remains, Sdu Uitgevers, Den Haag, 2009

ISO 12751, 1999: *NF EN 12751. Textiles - Sampling of fibres, yarns and fabrics for testing*, International Organization for Standardization, Geneva, 1999

ISO 13934-1, 2013*: NF EN 13934-1. Textiles - Tensile properties of fabrics – Part 1: Determination of maximum force and elongation at maximum force using the strip method,* International Organization for Standardization, Geneva, 2013

ISO 9073-7, 1998*: NF EN ISO 9073-7. Textiles - Test methods for nonwovens – Part 7: Determination of bending length,* International Organization for Standardization, Geneva, 1998

ISO 4602, 2011: *NF EN ISO 4602. Reinforcements – Woven fabrics – Determination of number of yarns per unit length or warp and weft,* International Organization for Standardization, Geneva, 2011

ISO 139, 2005: *NF EN ISO 139. Textiles - Standard atmospheres for conditioning and testing,* International Organization for Standardization, Geneva, 2005

ISO 13934-2, 2014: NF EN ISO 13934-2. Textiles – Tensile properties of fabrics – Part 2: Determination of maximum force using the grab method, International Organization for Standardization, Geneva, 2014

Jakes and Mitchell, 1992: Jakes, K.A., Mitchell J.C. "The recovery and drying of textiles from a deep ocean historic shipwreck", *Journal of the American Institute for Conservation* 31, American Institute for Conservation of Historic and Artistic Works, 1992, p. 343-353

Janaway and Wyeth, 2005: Janaway, R., Wyeth P., "Scientific Analysis of Ancient and Historic Textiles: Informing Preservation, Display and Interpretation*", First Annual Conference 13-15 July 2004*, AHRC Research Centre for Textile Conservation and Textile Studies, Archetype Publications Ltd, 2005

Jones *et al.*, 2007: Jones, J., Unruh, J., Knaller, R., Skals, I., Knudsen, LR., Jordan-Fahrbach, E., Mumford, L., «Guidelines for the Excavation of Archaeological Textiles" In Gillis, C., Nosch, M.-L. B. (eds.) *First Aid for the Excavation of Archaeological Textiles*, The Danish National Research Foundation's Centre for Textile Research, Oxford Books, Oxford, 2007, pp 5-29

Jordan, 2013: Jordan, M. "The conservation of cordage from Newport Medieval Ship" In *Proceedings of the 12th ICOM-CC Group on Wet Organic Archaeological Materials Conference*, 2013, p. 307-311

Karsten, 2003: Karsten, I.F. *Factors affecting the Bond Strength of Textile Artefact/Adhesive/support Fabric Laminates*. PhD Thesis, University of Alberta, Alberta, 2003

Kucerová and Drncová, 2009: Kucerová, I., Drncová, D. "The consolidation of Wood with Paraloid B-72 solutions", In Ambers, J., Higgitt, C., Harrison L., Saunders D. (eds.). *Holding it all*

together. Ancient and Modern Approaches to Joining, Repair and Consolidation, Archetype Publications, London, 2009

Koob, 1981: Koob, SP. "Consolidation with Acrylic Colloidal Dispersion", In *AIC Preprints of Papers Presented at the Ninth Annual Meeting, Philadelphia, PA, 27-31 May 1981*, AIC, Washington, D.C, 1981, p. 86-94

Logan and Young, 1987: Logan J.A., Young G.S., "A message in a bottle: the conservation of waterlogged parchment document", *Journal of the International Institute for conservation – Canadian Group* 12, CCI, Otawa, 1987

Lopez Luján ,2016 : Lopez Luján L., Guilliem Arroyo S., "Mexica Textiles: Archaeological Remains from the Sacred Precincts of Tenochtitlan and Tlatelolco", In Bjerregaard,L., Peters A. (eds.), *Pre Columbian Textile Conference VII*, Centre for Textile Research, University of Copenhagen, 2016

Lundwall, 2003: Lundwall, E. "Silk, Wool and Linen The restoration and conservation of findings made off the Swedish coeast on the ship "Kronan" (1676)", In Incontri di restauro 4. Intrecci vegetali e fibre da ambiente umido Analisi Conservazione e Restauro, Trento 28-30 maggio, 2003

Malmius, 2002: Malmius, A., "Cremation grave textiles. Examples from Vendel upper class in the Vendel and Viking Periods ", *Journal of Nordic Archaeology Science 13*, [Online] 2002 [Visited on May 2018], http://digitalcommons.uri.edu/cgi/viewcontent.cgi?article=1003&context=tmd_major_papers

McClintock, 1986: McClintock, C. "The treatment of waterlogged textile excavated from "La Trinidad Valencera": A Spanish armada transport vessel. Unpublished diploma report" Textile Conservation Centre/Courtauld Institute of Art, Courtauld, 1986

Miksicek, 1987: Miksicek C.H., "Formation Processes of the Archaeobotanical Record" In Schiffer, M.B. (ed.) *Advances in Archaeological Method and Theory*, Academic Press, San Diego, 1987, p. 219-221

Millei, 1999: Millei, I., "Evaluation of conservation methods for banners painted on both sides", in *International Perspectives on Textile Conservation, ICOM-CC Textiles Working Group Meetings*, Archetype Publications Ltd., 1999

Montersinos Ferrandis *et al.*, 2008: Montesinos Ferrandis, E.M., Vicente Palomino, S., Fuster López, L., Yusá Marco, D.J., Doménech Carbó, M.T., Mecklenburg, MF., "Aproximación al studio de adhesivos para la consolidación y refuerzo de tejidos históricos: Materiales y Métodos", *Arché, Num. 3*, Instituto Universitario de Restauración del Patrimonio, UPV, 2008

Moreno, 2007: Moreno de Acevedo Sanchez, C., "Tratamiento de restauracion del conjunto de textiles hallados en el sepulcro de D. Hernando de Aragon (S.XVI) »,[Online] 2007 [Visited on March 2018] http://ge-icc.com/files/1congreso/MorenoCristina.pdf

Morton and Hearle, 2008: Morton W.E, Hearle J.W.S., *Physical Properties of Textile Fibres*, Woodhead Publishing Limited, Woodhead Publishing, 2008

Morton and Bernaciak, 2013: Morton K., Bernaciak, K. "Conservation of a group of Maseolithic fish-trap baskets from Clowanstown, Co. Meath, Ireland." In *Proceeding s of the 12th ICOM - CC Group on Wet Organic Archaeological Materials Conference* , 2013, pp.283-288

Morrison, 1989: Morrison, L., "Treating waterlogged moss rope", *ICOM Committee for Conservation Working Group on Wet Organic Archaeological Materials, Newsletter 17, 1989*

Moulhérat, 2011: Moulhérat, C., "Archéologie des textiles", *Les nouvelles de l'archéologie* [Online] 2011, [visited on May 2018], http://journals.openedition.org/nda/600 ; DOI : 10.4000/nda.600

Neilson and Allard, 2008: Neilson, A. H., and Allard, A. S. *Environmental Degradation and Transformation of Organic Chemicals,* CRC press, Boca Raton, 2008

Newey *et al.*, 1992: Newey, C., R Boff, V. Daniels, M. Pascoe and N. Tennent. "Adhesives and Coatings, Science for Conservators", *Conservation Teaching Series, vol 3*. Editted by J. Ashley-Smith. Routledge, New York, 1992

Peacock, 1990: Peacock, E.E: "freeze-drying archaeological textiles: the need for basic research", *Archaeological Textiles*, London, 1990, p. 22-30

Peacock, 1992: Peacock, E.E., "Drying Archaeological Textiles ", in Bender Jorgensen, L., Munksgaard*, E. (eds.). Archaeological Textiles in Northern Europe*, Report from the 4th NESAT Symposium, Copenhagen, 1-5 May 1990, n° 5, NESAT, Neumünster, 1992, p. 197-207

Peacock, 1993: Peacock, E.E. « The development and drying of simulated water-degraded archaeological textiles » PhD dissertation, UMIST, Manchester, 1993

Peacock, 1999: Peacock, E.E., "A Note on the Effect of Multiple Freeze-Thaw treatment on Natural Fibre Fabrics", *Studies in Conservation*, Vol. 44, Nº1, Taylor & Francis, 1999, pp. 12-18

Peacock, 2003: Peacock, E.E. "The biodeterioration of textile fibres in wet archaeological contexts with implications for conservation choices", In Incontri di restauro 4. Intrecci vegetali e fibre da ambiente umido Analisi Conservazione e Restauro, Trento 28-30 maggio 2003.

Pearson 1987: Pearson, C. (ed.). Conservation of Marine Archaeological Objects, Series in Conservation and Museology, Butterworth, London, 1987

Pertegato, 1993: Pertegato, F., *I tessili, degrade e restauro*, Nardini Editore, Firenze, 1993

Rast-Eicher, 2016: Rast-Eicher, A. *Fibres. Microscopy of Archaeological Textiles and Furs*, Archaeolingua Alapitvany, Budapest, 2016

Rice, 1964: Rice, J. W."Principles of Textile Conservation Science, N°V: The Characteristics of soils and Stains Encountered on Historic Textiles" *Textile Museum Journal I, n°3* (December 1964) p. 8-17

Rice, 1966: Rice, James W. "Principles of Textile Conservation Science, N°VI : The wonders of water in wet cleaning" *Textile Museum Journal 2, n°1* (December 1966) p. 15-38

Rothenhäusler and Travis 2003: Rothenhäusler, U., Travis, K. Conservation of waterlogged archaeological organic material at the Swiss national museum, centre for conservation. In

Incontri di restauro 4. Intrecci vegetali e fibre da ambiente umido Analisi Conservazione e Restauro, Trento 28-30 maggio, 2003

Sease 1987: Sease C., *A Conservation Manual for the Field Archaeologist*, Institute of Archaeology, University of California, Los Angeles, 1987

Serchisu, 2014: Serchisu, F*. Textile fibre preservation and statistical variation in burials: Clothing evidence in Anglo-Saxon and Roman inhumations,* University of York, [Online] December 2014 [Visited on March 2018] http://etheses.whiterose.ac.uk/13759/7/FabioSerchisuThesis.pdf

Shelton, 1994: Shelton, C., "The Use of Aquazol-based Gilding Preparations" *AIC meeting*, WAG Postprints, Norfolk, Virginia, 1994

Wolbers et al., 1994: Wolbers, R., M.McGinn, M., Durbeck, D., "Poly(2-ethyl-2-oxazoline):A New Conservation Consolidant" *Painted Wood, History and Conservation* postprints from symposium in Williamsburg, VA, published by Getty Conservation Institute, Los Angeles, CA, 1994, pp. 514-528.

Solazzo *et al.*, 2013: Solazzo, C., Dyer, J. M., Clerens, S., Plowman, J., Peacock, E., and Collins, M. J. "Proteomic evaluation of the biodegradation of wool fabrics in experimental burials". *International Biodeterioration and Biodegradation*, 80, 2013 48-59.

Stauffer, 2003: Stauffer, A. "Archäologische textillien konsolidiert mit synthethischen produkten : Probleme bei der untersuchung und konservierung". In *Incontri di restauro 4. Intrecci vegetali e fibre da ambiente umido Analisi Conservazione e Restauro*, Trento 28-30 maggio 2003

Stelton, 1975: Stelton, J. "Interfibre forces during wetting and drying", *Science 190* (4209), 1975, p. 15-20

Tarleton and Ordoñez, 1995: Tarleton, K.S., Ordoñez M.T., "Stabilization methods for textiles from wet sites", *Journal of Field Archaeology* 22, 1995, pp. 81-95

Thorvildsen, 1975: Thorvildsen, M., "Problemer med anvendelse af klaebestoffer indenfor textilkon servering" *Textilkonservering och dess problem*, Stockholm, 1975

Tímar-Balázsy, 1999: Tímar-Balázsy, Agnes, "Drying behaviour of fibres", in Bridgland, J. *ICOM Committee for Conservation, 12th Triennial Meeting, Lyon, 20 August-3 September 1999: Preprints*, James and James, London, 1999, p. 661-666

Tímar-Balázsy and Eastop, 1998: Tímar-Balázsy, A., Eastop D., *Chemical Principles of Textile Conservation. Woburn*, Butterworth-Heinemann, MA, 1998

Von Holstein, 2012: Von Holstein, I. «A light stable isotope (C, N, H, O) approach to identifying movement of medieval textiles in North West Europe". PhD thesis, University of York, 2012

Von Holstein *et al.*, 2014: Von Holstein, I., Penkman, K. E. H., Peacock, E. E., and Collins, M. J. "Wet degradation of keratin proteins: linking amino acid, elemental and isotopic composition. Rapid Communications in Mass Spectrometry", 28, 2014, 2121-2133.

Wiener et al., 2003: Wiener,J., Kovačič, V., Dejlová P., "Differences between flax and hemp", *Autex research journal, Vol. 3,* [Online] June 2003 [Visited on May 2018], http://www.autexrj.com/cms/zalaczone_pliki/2-032.pdf

Younger, 2007: Younger, S., "18th century beard work picture", [Online] 2007 [Visited on March 2018] http://www.textile-conservation.com/portfolio/mixed.asp

Illustrations

Appendices

Appendix 1 Summary of the equipment and conservation materials

Analysis	
Light microscopy	Zeiss® (Carl Zeiss, Germany), Axioplan, EL-Einsatz, 451898, 115-230V, 50…60Hz, 200VA - 2,5x, 5x, 10x, 20x, and 50x objectives
Cameras	AxioCam® MRc from Zeiss®
	NIKON D500
Software	AxioVision® Rel.4.6
	SpectraMagic™ NX from Konica Minolta®
FTIR spectroscopy	Excalibur Series FTS 3500GX with UMA-500 Microscope Biorad Co. with a diamond press cell.
Mould test	Lumitester® PD-20 and LuciPac Pen®
Spectrophotometer	Spectrophotometer CM-2600d by Konica Minolta®
Scale	Sartorius® MC 1 from IG® (Instrumenten-Gesellschaft AG)
Calibre	Electronic calibre «toolcraft® M-150»
Conservation Treatments	
Solvents	Hexane
	Ethyl Acetate
	Toluene
	Dimethyl Choride
	Ethanol (2% Butanone)
	Deionized water
Adhesives	Polyethylene glycol 400
	Klucel® G from Kremer® Hydroxypropylcellulose, 300mPas (N° 63706), Bought: Nov. 2014
	Klucel® E from Kremer® Hydroxypropylcellulose, 7mPas, dünnflüssig (N°63700), Bougth: Nov 2014
	Aquazol® 500 from Kremer® Bougth: 27.6.2012
	Paraloid® B72 (Article number: 4120) from Lascaux®
	Meltmount® 2.7.1

Surfactant	Held® by Ecover
Textile	Lining and painting 300(Article number 4452) from Lascaux®
Freeze-dryer	Freeze-drier modified with a cooling system by Lyotec® Christ Alpha 2-4 LD plus Huber unistat 705 Vacuum Pfeiffer - Duo 65 / PK D46 602 A - Duo 20 M / PK D63 712 B
Washing Machine	V-Zug Adora S®
Ironer	PFAFF® steam ironer 580
Kiln	Nabertherm® L3/11/C6 - Mod: L3/12/C6 230 V1 - Nr: 162761 - 50Hz - Jahr 2001 - 5.2A - Max. Cº 1200 - 1,2kW
	Naber® L51/5 R - Mod. L 51/5 R 220V 1~/N - 1,2kW
Supports	Hollytex® (Article number: 3257) from Deffner & Johann®
	Buvar 4551 from Lascaux®
	Polyester mesh (100µm, 65 gsm) from GMW®

Appendix 2 Cross-section observation: Location of the threads sampled

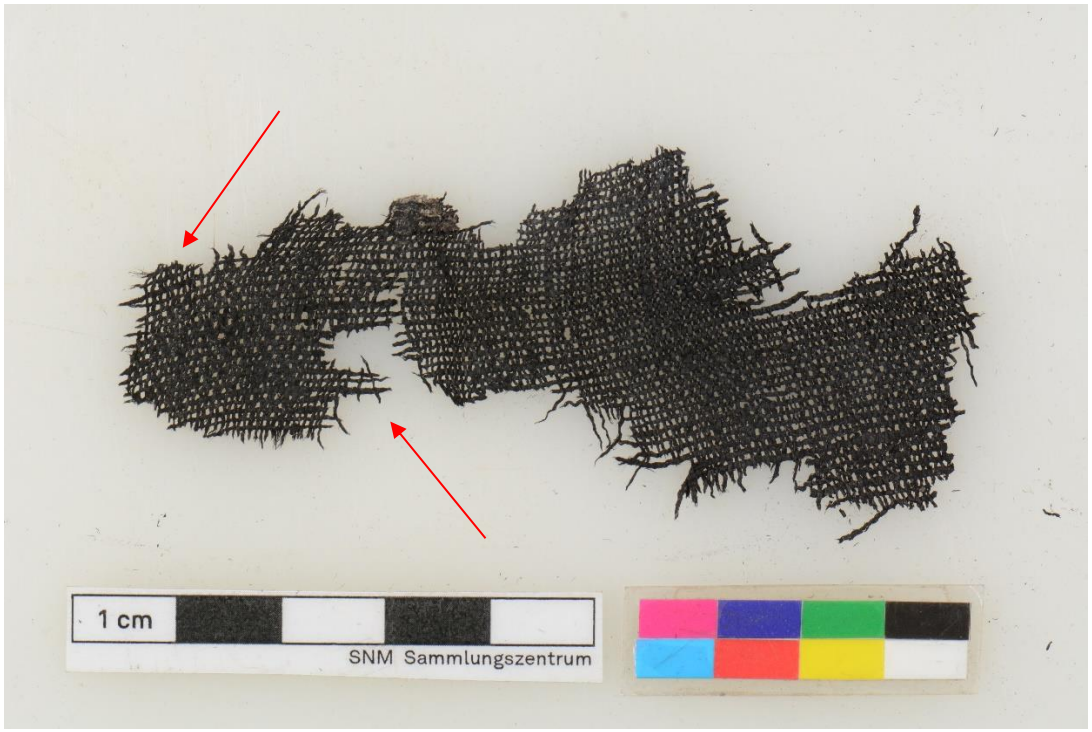

Figure 121 Sample 3.04. Location of the two threads sampled for the cross-section observation ©HE-Arc

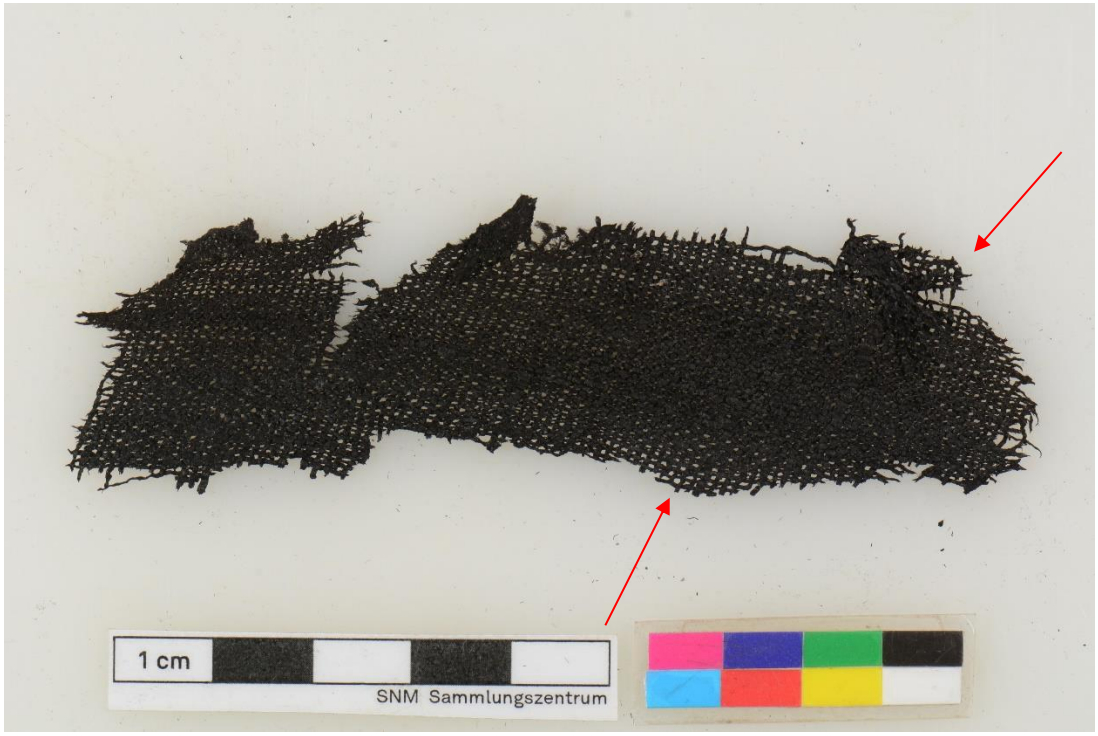

Figure 122 Sample 3.08. Location of the two threads sampled for the cross-section observation ©HE-Arc

Appendix 3 Transversal observation: Location of the threads sampled

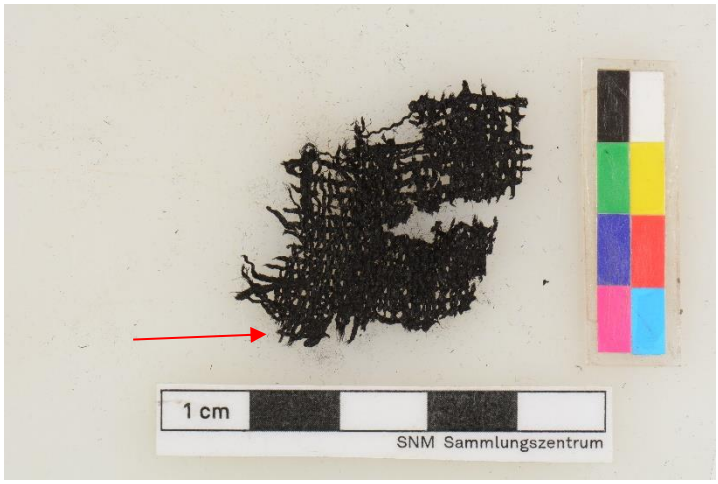

Figure 123 Sample 2.04. Location of the threads sampled for the transversal observation ©HE-Arc

Figure 124 Sample 2.19. Location of the threads sampled for the transversal observation ©HE-Arc

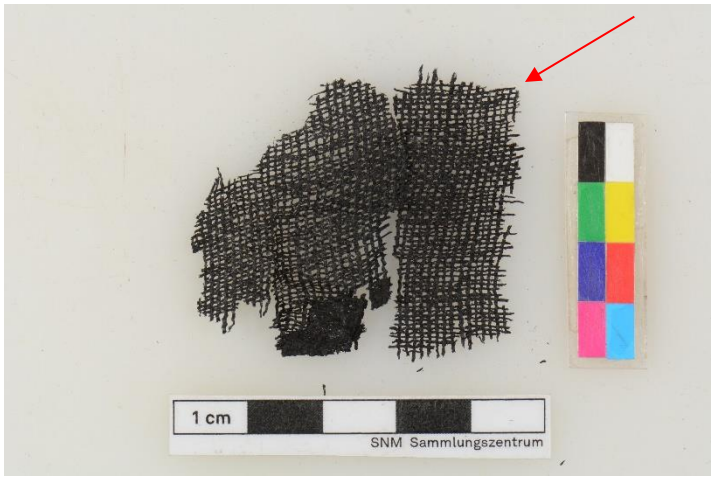

Figure 125 Sample 3.3. Location of the threads sampled for the transversal observation ©HE-Arc

Appendix 4 Photographic documentation of fibres observed with polarised microscopy

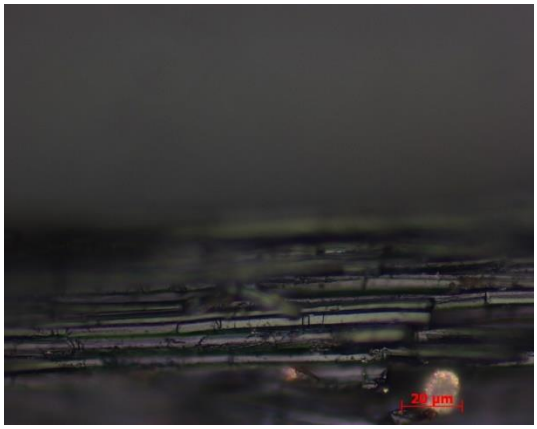

Figure 126 Group of fibres from sample 3.3 under the polarised microscope x50, bright field ©HE-Arc

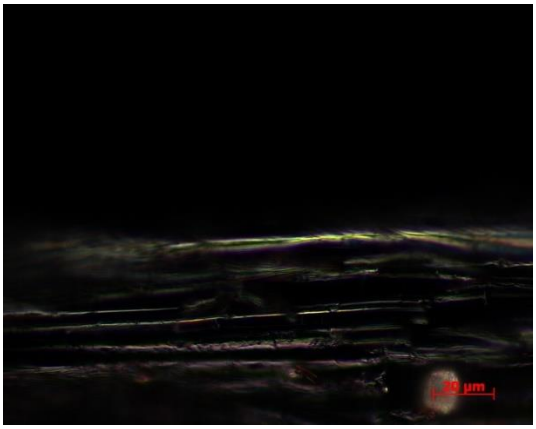

Figure 127 Group of fibres from sample 3.3 under the polarised microscope x50, darkfield ©HE-Arc

Figure 128 Single fibre from sample 2.19 under the polarised microscope x50, bright field ©HE-Arc

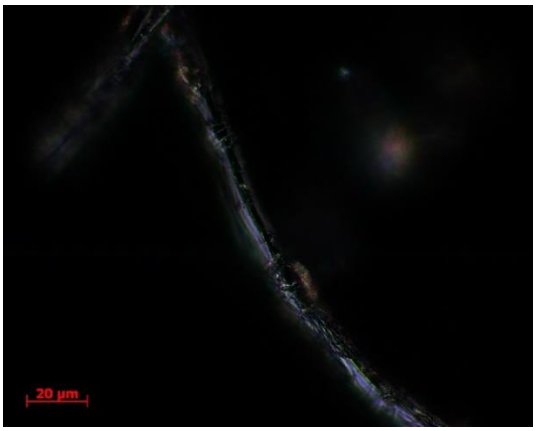

Figure 129 Single fibre from sample 2.19 under the polarised microscope x50, darkfield ©HE-Arc

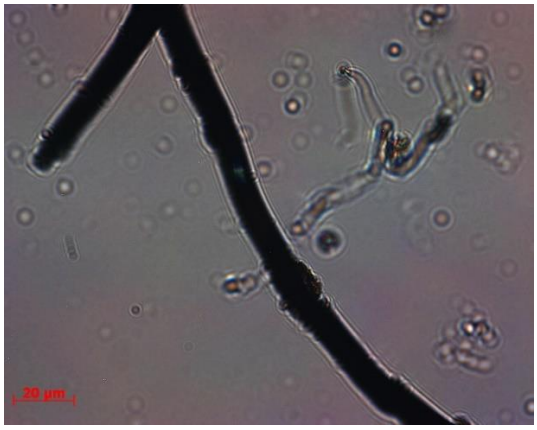

Figure 130 Single fibre from sample 2.19 under the polarised microscope x50, transmitted light ©HE-Arc

Figure 131 Single fibre from sample 2.4 under the polarised microscope x20, transmitted light ©HE-Arc

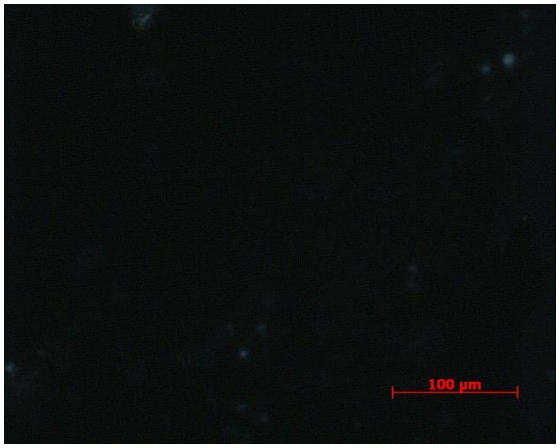

Figure 132 Single fibre from sample 2.4 under the polarised microscope x20, polarized light, and fibre at maximum brightness. No visible colour ©HE-Arc

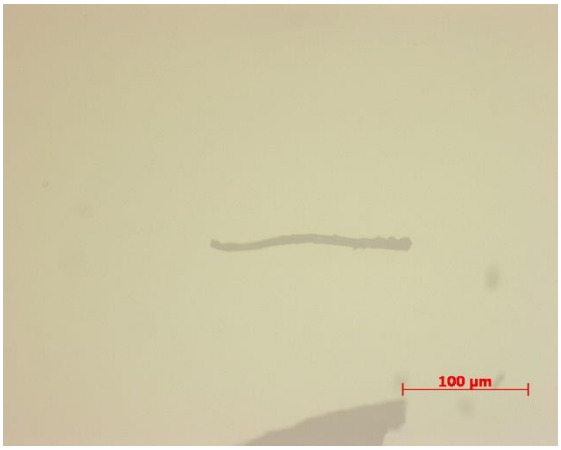

Figure 133 Single fibre from sample 2.4 under the polarised microscope x20, bright field ©HE-Arc

Figure 134 Modern flax fibre under polarised microscope x20, transmitted light ©HE-Arc

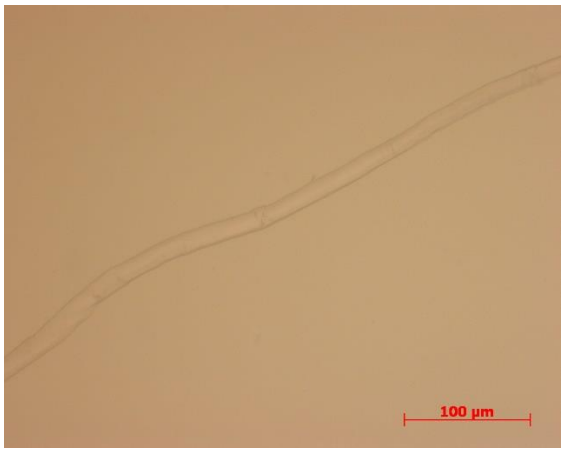

Figure 135 Modern flax fibre under polarised microscope x20, bright field ©HE-Arc

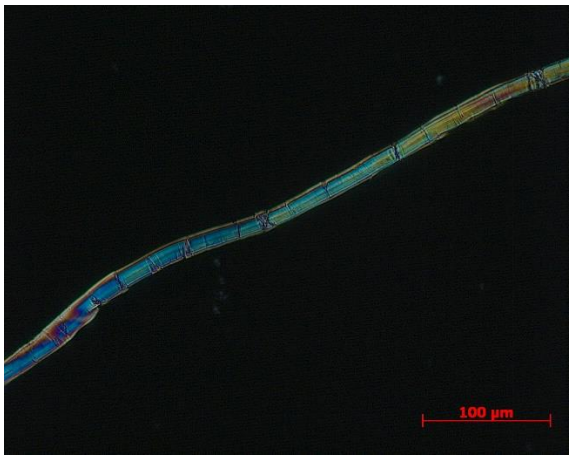

Figure 136 Modern flax fibre under polarised microscope x20, analyser plate, fibre at maximum brightness ©HE-Arc

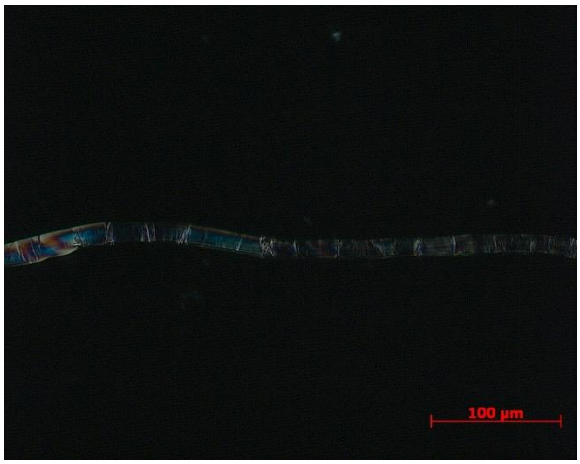

Figure 137 Figure 138 Modern flax fibre under polarised microscope x20, analyser plate, fibre at extinction ©HE-Arc

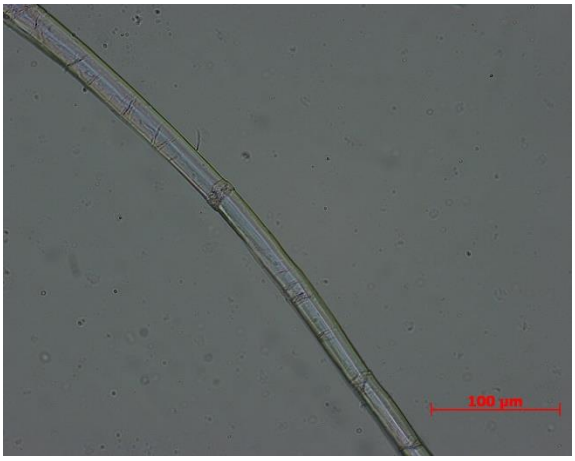

Figure 139 Modern flax fibre under polarised microscope x20, transmitted light ©HE-Arc

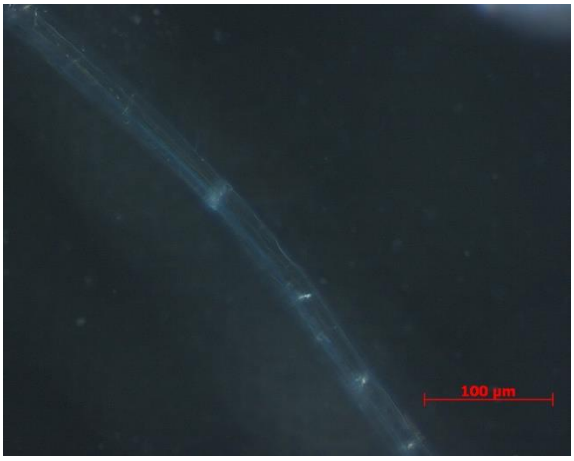

Figure 140 Modern flax fibre under polarised microscope x20, darkfield ©HE-Arc

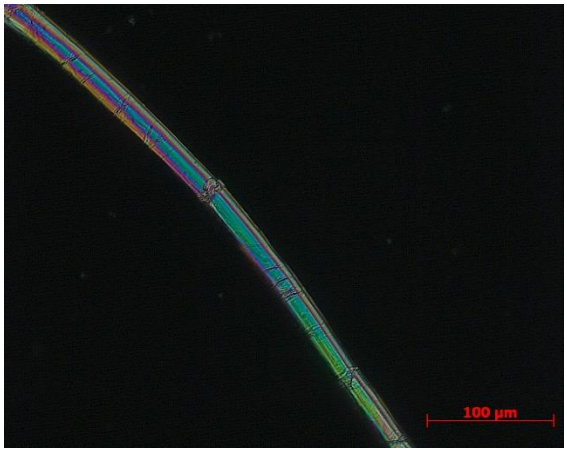

Figure 141 Modern flax fibre under polarised microscope x20, analyser plate, fibre at maximum brightness ©HE-Arc

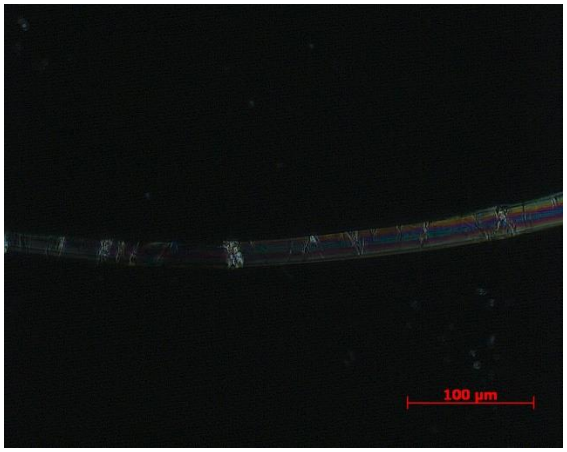

Figure 142 Figure 143 Modern flax fibre under polarised microscope x20, analyser plate, fibre at extinction ©HE-Arc

Figure 144 Modern flax fibre under polarised microscope x20, transmitted light ©HE-Arc

Appendix 5 Charred archaeological textiles: Summary of characteristics and degradation state per sample

SAMP+A1: E17LE	DIMENSIONS (mm)	Number of Threads (1:1cm)	CHARACTERISTICS	DEGRADATION
1,01	23.07x17.95	16x10	1:1, Z both, same diametre in both directions, open fabric, perpendicular	Soil deposits, broken fibres, brittle, partially crushed
1,02	38.32x21.58	16x11	1:1, Z both, same diametre in both directions, open fabric, perpendicular	Soil deposits, broken fibres, brittle, partially crushed, crystal-like material on the surface (something shiny on the surface)
1,05	29.01x23.64	17x10	1:1, Z both, same diametre in both directions, open fabric, perpendicular	Soil deposits, broken fibres, brittle, partially crushed
1,06	26.07x15.89	17x10	1:1, Z both, same diametre in both directions, closed fabric, partially diagonal	Soil deposits, broken fibres, flexible (wet)
1,10	19.82x18.90	17x11	1:1, Z both, same diametre in both directions, open fabric, perpendicular	Soil deposits, broken fibres, very brittle, crystal-like material on the surface (something shiny on the surface), missing threads, folded edge
1,16	32.73x18.82	17x11	1:1, Z both, same diametre in both directions, open fabric, partially diagonal	Soil deposits, broken fibres, still flexible, crystal-like material on the surface (something shiny on the surface), missing threads
1,17	37.65x25.02	17x11	1:1, Z both, same diametre in both directions, semi-open fabric, perpendicular	Two or more layers, Soil deposits, broken fibres, white fibre deposits, still flexible
1,18	53.79x20.28	16x10	1:1, Z both, different diametre (OY thinner), semi-open fabric, perpendicular	Deformed and torned, Soil deposits, broken fibres, still flexible, crushed in the centre, missing threads
1,19	37.21x17.92	17x9	1:1, Z both, same diametre in both directions, open fabric, perpendicular	Soil deposits, broken fibres, still flexible, partially crushed, bended edge, little mess in the edge, white fibre deposits
1,23	28.55x32.62	16x10	1:1, Z both, same diametre in both directions, semi-open fabric, perpendicular	Soil deposit, bended in the edge, mess of fibres
1,29	40.01x17.85	16x11	1:1, Z both, different diameter (OY thinner), semi-open fabric, partially diagonal	Two or more layers, broken, torn, deformed, soil deposits
1,30	45.15x23.40	18x11	1:1, Z both, same diametre in both directions, closed fabric, perpendicular	Soil deposits, crystal-like material on the surface(something shiny on the surface), deformed in the edge, broken fibres
1,31	16.44x31.25	18x11	1:1, Z both, same diametre in both directions, open fabric, partially diagonal	Soil deposit, broken and missing threads, torn, deformed
2,02	132.69x35.59	17x10	1:1, Z both, same diametre in both directions, closed fabric, perpendicular	Soil deposits, broken fibres, still flexible, white fibre deposits
2,03	81.24x41.45	17x11	1:1, Z both, same diametre in both directions, closed fabric, perpendicular	Soil deposits, broken fibres, still flexible, white fibre deposits
2,04	26.17x36.65	17x9	1:1, Z both, same diametre in both directions, open fabric, perpendicular	Soil deposits, broken fibres, torn and deformed, brittle

2,05	79.74x42.47	17x10	1:1, Z both, same diametre in both directions, closed fabric, perpendicular	Soil deposits, broken fibres, still flexible, white fibre deposits
2,06	77.29x45.66	16x10	1:1, Z both, same diametre in both directions, closed fabric, perpendicular	Soil deposits, broken fibres, still flexible, white fibre deposits
2,08	33.18x13.79	16x9	1:1, Z both, same diametre in both directions, closed fabric, perpendicular	Well preserved, broken fibres
2,10	50.65x31.17	16x9	1:1, Z both, same diametre in both directions, closed fabric, perpendicular	Well preserved, Soil deposits, broken fibres, still flexible
2,11	55.18x33.51	18x11	1:1, Z both, same diametre in both directions, semi-open fabric, perpendicular	Soil deposits, broken fibres, deformed, missing threads, partially crushed
2,15	129.54x33.22	17x9	1:1, Z both, same diametre in both directions, semi-open fabric, perpendicular	Soil deposits, crushed fibres, mess in the edges, torn,
2,16	86.62x50.10	17x9	1:1, Z both, same diametre in both directions, closed fabric, perpendicular	Well preserved, Soil deposit, mess in the edges, broken fibres, Creased textil, (simetric with the fold perpendicular en the center)
2,18	41.50x13.30	17x10	1:1, Z both, same diametre in both directions, closed fabric, perpendicular	Well preserved, broken fibres, fibres a little crushed in the edges
2,19	46.01x52.69	16x9	1:1, Z both, same diametre in both directions, closed fabric, perpendicular, Seam	Crushed fibres, deformation and torn textil, broken fibres, soil deposit
3,01	64.77x57.47	18x10	1:1, Z both, same diametre in both directions, semi-open fabric, perpendicular	Soil and charcoal deposits, broken fibres, deformation, mess of fibres in the edges, green deposit, white fibre deposits
3,04	83.62x37.67	17x10	1:1, Z both, same diametre in both directions, open fabric, perpendicular	Soil deposits, deformation, broken fibres, difference in diameter on the same thread, crystal-like material on the surface
3,11	46.95x30.53	18x10	1:1, Z both, different diametre (OY thinner), open fabric, perpendicular	Crystal-like material on the surface (something shiny on the surface), two or more layers of threads in one side, soil deposits
3,12	50.93x49.19	17x11	1:1, Z both, same diametre in both directions, semi-open fabric, perpendicular	Crystal-like material on the surface (something shiny on the surface), whitening, deformation, torned, missing and broken threads, one piece separated
3,14	94.51x61.46	18x10	1:1, Z both, different diametre (OY thinner), closed fabric, partially diagonal	Crystal-like material on the surface (something shiny on the surface) soil deposits, deformation, missing and broken fibres
3,18	29.67x41.23	18x11	1:1, Z both, same diametre in both directions, semi-open fabric, perpendicular	Crystal-like material on the surface (something shiny on the surface), soil deposits, mess of fibres in the edges, missing and broken fibres
3,19	50.11x51.07	18x11	1:1, Z both, same diametre in both directions, open fabric, perpendicular	Heavy deformation, crushed fibres, missing and broken fibres, crystal-like material on the surface (something shiny on the surface)
3,03	50.72x40.40	16x10	1:1, Z both, same diametre in both directions, open fabric, perpendicular	Crushed fibres, deformation, bended edge, mess of fibres in the edges, torn,

3,07	104.27x27.43	17x10	1:1, Z both, different diametre (OY thinner), closed fabric, partially diagonal	Soil deposit, deformation, missing and broken threads, bended in the edge
3,13	88.70x63.45	16x10	1:1, Z both, different diametre (OY thinner), semi-open fabric, perpendicular	Soil deposit, missing part, missing threads, broken threads, deformed, very fragile, mess of threads on one edge, crushed fibres
3,16	110.68x35.51	16x11	1:1, Z both, different diametre (OY thinner), closed fabric, partially diagonal	Soil and charcoal deposits, missing threads, broken fibres, deformation
3,08	102.45x28.19	18x9	1:1, Z both, same diametre in both directions, closed fabric, perpendicular	One bigger threads, white fibre deposits, missing threads, mess of fibres in the edge, broken fibres, bended edge, torn
1,07	53.10x20.73	22x12	1:1, Z both, different diametre (OY thinner), open fabric, perpendicular	Broken and torned textile, bented edge, soil deposits, broken fibres, brittle, partially crushed, mixed threads, warped,
1,08	49.79x26.12	22x12	1:1, Z both, same diametre in both directions, closed fabric, diagonal	Soil deposits, broken fibres, still flexible, partially crushed
1,11	67.85x14.43	19x10	1:1, Z both, different diametre (OY thinner), open fabric, partially diagonal	Soil deposits, broken fibres, still flexible, partially crushed, bent edge, missing threads
1,20	66.35x18.45	21x12	1:1, Z both, same diametre in both directions, closed fabric, perpendicular	Deformed and bended, soil deposits, brittle
1,25	35.07x33.88	20x11	1:1, Z both, different diameter (OY thinner) and thinner threads in comparison with other samples, open fabric, perpendicular	Deformed and torned, Soil deposits, broken fibres, still flexible, partially crushed, bended edge, little mess in the edge, white fibre deposits
1,27	109.17x45.48	20x10	1:1, Z both, different diametre (OY thinner), open fabric, perpendicular	Well preserved, little rigid, little deformation, bended in one edge, soil deposits, broken threads
1,28	37.79x14.11	19x11	1:1, Z both, same diameter in both directions, semi-open fabric, partially diagonal	Soil deposit, broken threads
1,26	37.85x39.06	19x11	1:1, Z both, different diametre (OY thinner), open fabric, perpendicular	Soil deposit, still flexible, broken fibres,missing threads
2,01	141.94x62	20x9	1:1, Z both, same diametre in both directions, semi-open fabric, perpendicular. Edge	Creased textil, (simetric with the fold perpendicular en the center), deformed, broken and missing threads
3,06	104.25x33.45	19x12	1:1, Z both, different diametre (OY thinner), open fabric, partially diagonal	Soil and charcoal deposits, white fibre deposits, missing threads, mess of fibres in the edge, broken fibres
3,10	73.81x35.92	19x12	1:1, Z both, different diametre (OY thinner), closed fabric, partially diagonal	Soil deposits, deformation, broken fibres
3,22	102.91x35.94	19x12	1:1, Z both, different diametre (OY thinner), semi-open fabric, partially diagonal	Soil and charcoal deposits, missing threads, broken fibres, deformation, salts?? (something shiny on the surface), mess of threads
3,21	66.19x52.17	19x10	1:1, Z both, different diametre (OY thinner), closed fabric, partially diagonal	Deformation, broken fibres, mess of fibres in the edge, crystal-like material on the surface (something shiny on the surface), torn

1,12	44.99x36.80	15x10	1:1, Z both, same diametre in both directions, open fabric, perpendicular	Broken textile, missing threads, mess of threads in the edges, still flexible
1,13	44.72x23.51	15x9	1:1, Z both, different diametre (OY thinner), open fabric, perpendicular	Soil deposits, broken fibres, white fibre deposits, missing threads
1,15	84.12x20.39	15x9	1:1, Z both, different diametre (OY thinner), open fabric, perpendicular	Deformed and torned, Soil deposits, broken fibres, still flexible, partially crushed, missing threads, charcoal deposit
2,17	73.90x54.66	15x10	1:1, Z both, same diametre in both directions, closed fabric, perpendicular	Well preserved, Soil deposit, mess in the edges, broken fibres, little deformation, Creased textil, (simetric with the fold perpendicular en the center)
2,07	51.93x55.45	14x9	1:1, Z both, same diametre in both directions, open fabric, perpendicular	Soil deposits, broken fibres, torn and deformed, missing fibres, Creased textil, (simetric with the fold perpendicular en the center),
2,12	53.53x36.87	15x9	1:1, Z both, same diametre in both directions, semi-open fabric, perpendicular	Well preserved, broken fibres, little deformation
2,09	52.20x30.77	16x8	1:1, Z both, same diametre in both directions, semi-open fabric, perpendicular	Soil deposits, broken fibres, still flexible
3,02	59.76x43.80	14x9	1:1, Z both, same diametre in both directions, semi-open fabric, perpendicular	Soil and charcoal deposits, white fibre deposits , torn and deformed
3,05	25.30x31.97	15x9	1:1, Z both, different diameter (OY thinner), open fabric, perpendicular	Missing threads, mess of fibres in the edge, broken fibres
3,09	62.73x34.53	15x9	1:1, Z both, different diameter (OY thinner), open fabric, perpendicular	Brittle ,rigid, broken and missing threads
1,24	39.07x31.66x1.98	18x12	1:1, not visible, same diametre in both directions, closed fabric, perpendicular	Several layers of textile or soil bellow, soil deposits, mess of threads in the edge
B	63.89x52.25x15.45	17x13	1:1, Z both, same diameter in both directions, close fabric, perpendicular	Textile with soil or charcoal underneath, soil deposits, red fibre deposit, mess of fibres, broken fibres
1,22	46.40x42.07	16x12	1:1, Z both, same diameter in both directions, close fabric, perpendicular	Two or more layers, broken, torn, fragile, Soil deposits, , broken fibres,missing threads, still flexible, white and red fibre deposits
2,14	78.66x54.89	16x12	1:1, Z both, same diametre in both directions, closed fabric, perpendicular	Soil deposits, broken fibres, still flexible, white and red fibre deposits
3,15	55.65x35.33	17x12	1:1, Z both, same diametre in both directions, closed fabric, perpendicular	Crystal-like material on the surface (something shiny on the surface), Soil and deposits, white fibre deposits, crushed and broken fibres
3,20	32.64x68.21	16x12	1:1, Z both, same diameter in both directionss, closed fabric, partially diagonal	Crushed fibres, deformation, mess of fibres in the edges, torn, missing parts
1,04	50.37x32.86	21x15	1:1, Z both, same diametre in both directions, semi-open fabric, perpendicular	Soil deposits, broken fibres (mixed threads), white fibre deposits, missing threads, charcoal deposit

3.02	59.76x43.80	14x9	1:1, Z both, same diametre in both directions, semi-open fabric, perpendicular	Soil and charcoal deposits, white fibre deposits , torn and deformed
3.05	25.30x31.97	15x9	1:1, Z both, different diameter (OY thinner), open fabric, perpendicular	Missing threads, mess of fibres in the edge, broken fibres
3.09	62.73x34.53	15x9	1:1, Z both, different diameter (OY thinner), open fabric, perpendicular	Brittle ,rigid, broken and missing threads
3.15	55.65x35.33	17x12	1:1, Z both, same diametre in both directions, closed fabric, perpendicular	Crystal-like material on the surface (something shiny on the surface), Soil and deposits, white fibre deposits, crushed and broken fibres
3.20	32.64x68.21	16x12	1:1, Z both, same diameter in both directionss, closed fabric, partially diagonal	Crushed fibres, deformation, mess of fibres in the edges, torn, missing parts
3.17	89.68x23.19	21x13	1:1, Z both, different diametre (OY thinner), closed fabric, partially diagonal	Soil and charcoal deposits, missing threads, broken fibres, deformation, crystal-like material on the surface (something shiny on the surface)
2,13	2891x33.66	21x14	1:1, Z both, same diametre in both directions, closed fabric, perpendicular	Well preserved, broken fibres, fibres a little crushed
3,17	89.68x23.19	21x13	1:1, Z both, different diametre (OY thinner), closed fabric, partially diagonal	Soil and charcoal deposits, missing threads, broken fibres, deformation, crystal-like material on the surface (something shiny on the surface)
1,03	43.10x26.43	19x17	1:1, Z both, same diametre in both directions, semi-open fabric, perpendicular	Threads really broken (impossible to differentiate some thrads), warped, threads in wrong position
1,09	109.61x55.59	18x15	1:1, Z both, same diametre in both directions, closed fabric, perpendicular	Broken and torned textile, bented edge, partially deformed, mess of threads, still flexible
1,14	25.07x26.41x2	not possible	not visible	Several layers of textile or soil bellow, soil deposits, mess of threads (impossible to see the details), heavy abrassion
1,21	65.20x29.57	25x18	1:1, Z both, same diametre in both directions, closed fabric, diagonal	Bended or edge?, soil and charcoal deposits, mess of threads
A	60.16x47.33x17	15x13	1:1, Z both, not visible, closed fabric, not clear	Textile with soil or charcoal underneath, soil deposits, red fibre deposit, mess of fibres, broken fibres
B.1	7.62x8.98	not possible	Same than B	Same than B

Appendix 6 Identification of the crystal-like material: FTIR spectroscopy

FTIR analysis were carried on by Erwin Hildbrand, laboratory assistant of the Conservation Research Team, on the Swiss National Museum.

Results:

The crystal-like material is a long-chained organic compound with a C=O-group (ester) and a hydroxide group (OH group) (Figure 212).

Long-chained organic compound: 2956 /1 394 cm^{-1} (CH_3 groups) / 2918 / 2851 / 1470 / 720 cm^{-1} (CH_2 groups)

Hydroxide group (OH group): 3248 cm^{-1}

Ester compound (C=O group): 1739 / 1731 cm^{-1}

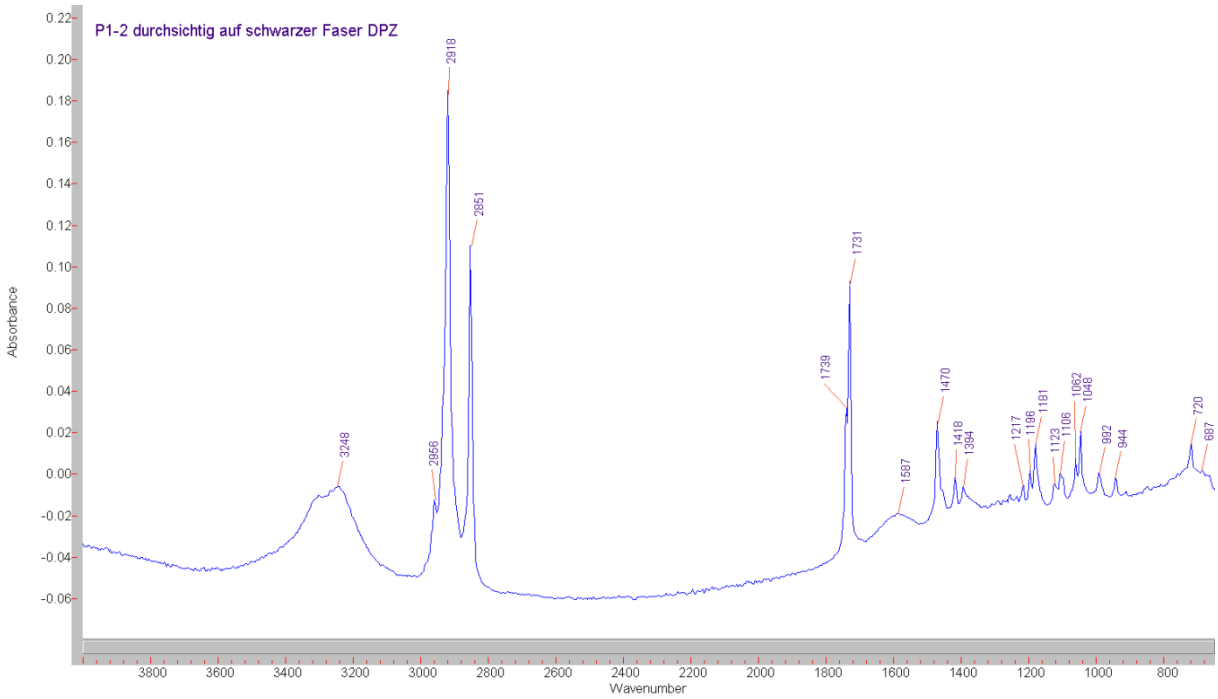

Figure 145 FTIR-spectrum substance on the historical textile

Appendix 7 Identification of the crystal-like material: Mold test with the Lumitester® PD-20 & LuciPac Pen®

Four samples were tested with the Lumitester® PD-20 and LuciPac Pen®. A surface is not considered to be contaminated if the RLU value is under 1000.

Figure 146 Recorded values during the mould test for samples 3.17 (up, left), 3.04 (up, right), 1.10 (down, left) and 1.16 (down, right)

Appendix 8 Photographic documentation of the samples selected

Pictures have been taken from both sides, but for extremely fragile samples

Figure 147 Sample 1.01 recto ©HE-Arc

Figure 148 Sample 1.01 verso ©HE-Arc

Figure 149 Sample 1.02 recto ©HE-Arc

Figure 150 Sample 1.02 verso ©HE-Arc

Figure 151 Sample 1.6 recto ©HE-Arc

Figure 152 Sample 1.02 verso ©HE-Arc

Figure 153 Sample 2.03 recto ©HE-Arc

Figure 154 Sample 2.03 verso ©HE-Arc

Figure 155 Sample 2.04 recto ©HE-Arc

Figure 156 Sample 2.04 verso ©HE-Arc

Figure 157 Sample 2.05 recto ©HE-Arc

Figure 158 Sample 2.05 verso ©HE-Arc

Figure 159 Sample 2.06 recto ©HE-Arc

Figure 160 Sample 2.06 verso ©HE-Arc

Figure 161 Sample 2.08 recto ©HE-Arc

Figure 162 Sample 2.08 verso ©HE-Arc

Figure 163 Sample 2.10 recto ©HE-Arc

Figure 164 Sample 2.10 verso ©HE-Arc

Figure 165 Sample 2.11 recto ©HE-Arc

Figure 166 Sample 2.11 verso ©HE-Arc

Figure 167 Sample 2.15 recto ©HE-Arc

Figure 168 Sample 2.15 verso ©HE-Arc

Figure 169 Sample 2.16 recto ©HE-Arc

Figure 170 Sample 2.16 verso ©HE-Arc

Figure 171 Sample 2.18 recto ©HE-Arc

Figure 172 Sample 2.18 verso ©HE-Arc

Figure 173 Sample 2.19 recto ©HE-Arc

Figure 174 Sample 2.19 verso ©HE-Arc

Figure 175 Sample 1.5 recto ©HE-Arc

Figure 176 Sample 1.5 verso ©HE-Arc

Figure 177 Sample 3.1 recto ©HE-Arc

Figure 178 Sample 3.1 verso ©HE-Arc

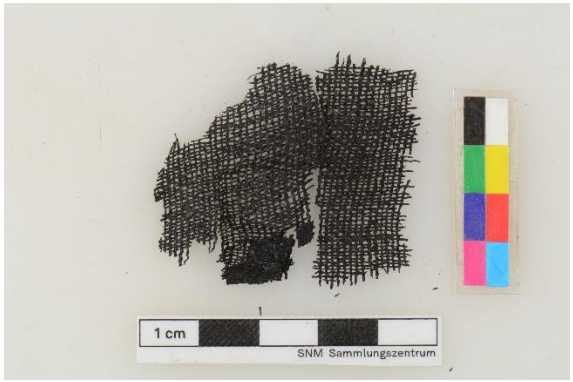

Figure 179 Sample 3.3 recto ©HE-Arc

Figure 180 Sample 3.3 verso ©HE-Arc

Figure 181 Sample 3.4 recto ©HE-Arc

Figure 182 Sample 3.4 verso ©HE-Arc

Figure 183 Sample 3.7 recto ©HE-Arc

Figure 184 Sample 3.7 verso ©HE-Arc

Figure 185 Sample 3.8 recto ©HE-Arc

Figure 186 Sample 3.8 verso ©HE-Arc

Figure 187 Sample 3.11 recto ©HE-Arc

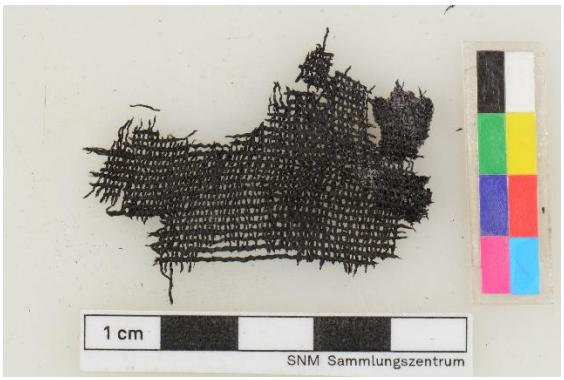

Figure 188 Sample 3.11 verso ©HE-Arc

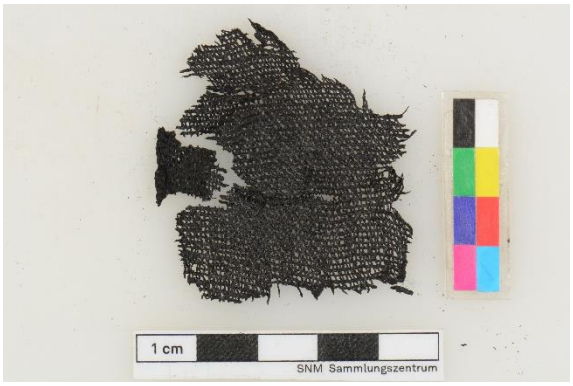

Figure 189 Sample 3.12 recto ©HE-Arc

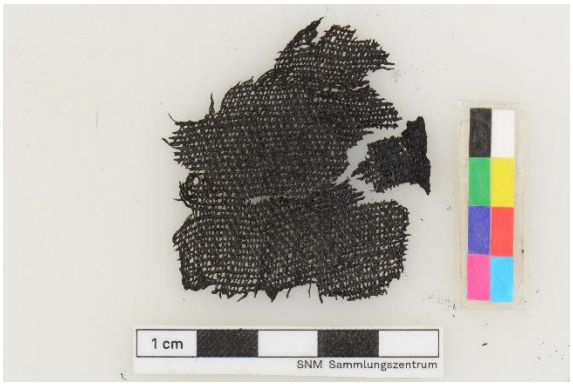

Figure 190 Figure 191 Sample 3.12 verso ©HE-Arc

Figure 192 Sample 3.13 recto ©HE-Arc

Figure 193 Figure 194 Sample 3.13 verso ©HE-Arc

Figure 195 Sample 3.11 recto ©HE-Arc

Figure 196 Sample 3.8 verso ©HE-Arc

Figure 197 Sample 3.11 recto ©HE-Arc

Figure 198 Sample 3.8 verso ©HE-Arc

Figure 199 Sample 3.11 recto ©HE-Arc

Figure 200 Sample 3.8 verso ©HE-Arc

Figure 201 Sample 3.11 recto ©HE-Arc

Figure 202 Sample 3.8 verso ©HE-Arc

Figure 203 Sample 1.10 recto ©HE-Arc

Figure 204 Sample 1.16 recto ©HE-Arc

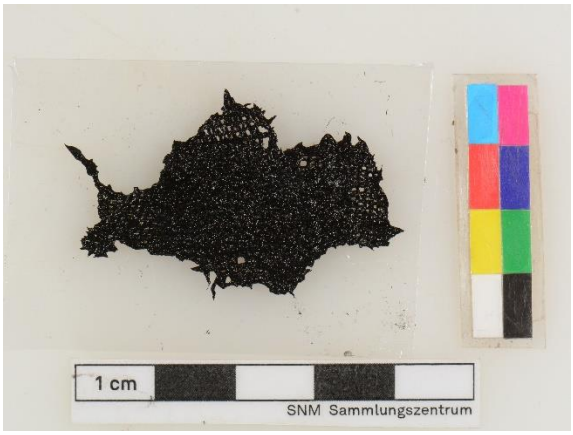

Figure 205 Sample 1.17 recto ©HE-Arc

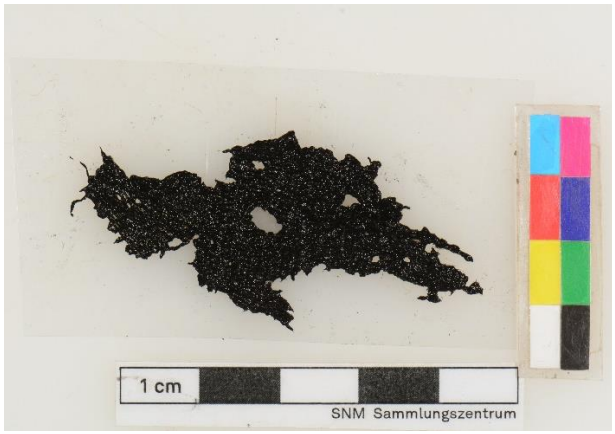

Figure 206 Sample 1.18 recto ©HE-Arc

Figure 207 Sample 1.19 recto ©HE-Arc

Figure 208 Sample 1.23 recto ©HE-Arc

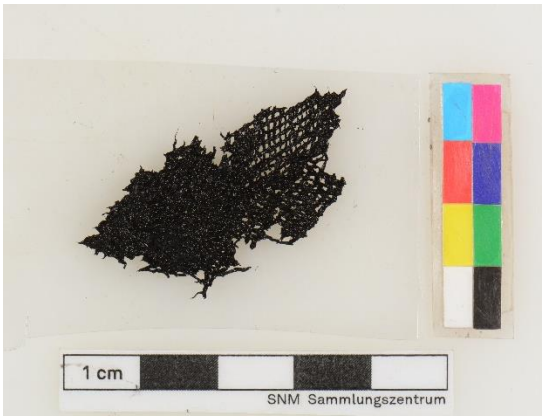

Figure 209 Sample 1.29 recto ©HE-Arc

Figure 210 Sample 1.31 recto ©HE-Arc

Figure 211 Sample 2.2 verso ©HE-Arc

Figure 212 Sample 2.2 recto ©HE-Arc

Figure 213 Sample 1.30 recto ©HE-Arc

Appendix 9. FTIR spectroscopy: Analysis of carbonisation degree of modern samples

FTIR analysis were carried on by Erwin Hildbrand, laboratory assistant of the Conservation Research Team, on the Swiss National Museum.

Unheated linen sample

This is a typical cellulose spectrum with the peak for organic materials at 2899 cm^{-1} (Figure 213)

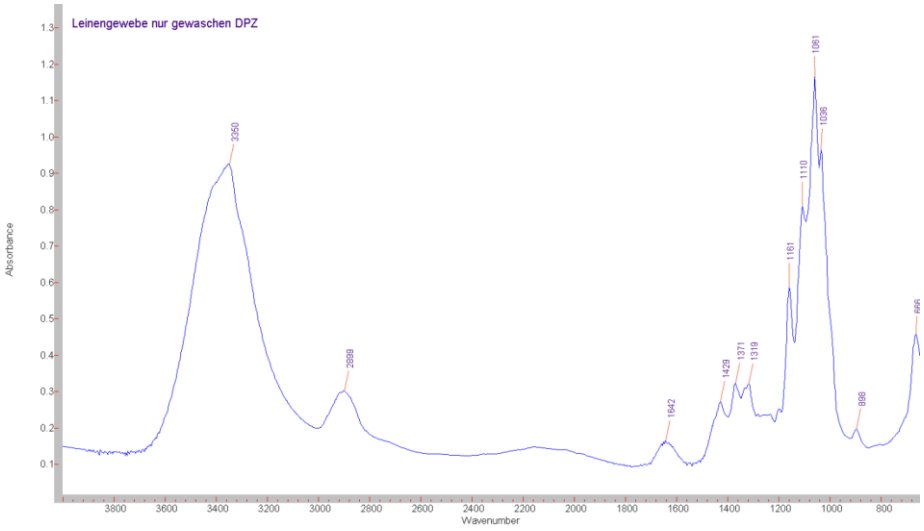

Figure 214 FTIR spectrum. Unheated linen textile

Linen sample treated 30 minutes at 300°C

This sample is very similar to the unheated textile (Fig. 1). There is still evidence of organic substances at 2897 cm^{-1}. The small peak at 1723 cm^{-1} shows oxidation (C=O-peaks) (Figure 214).

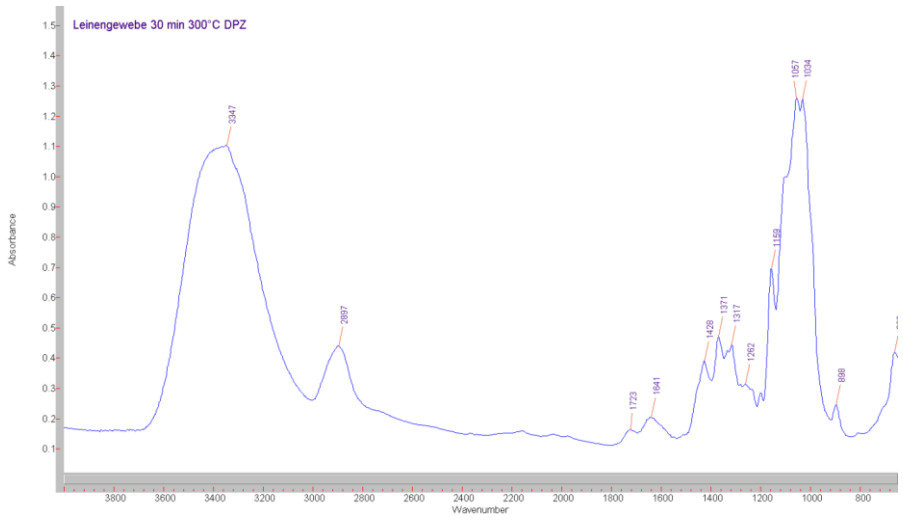

Figure 215 FTIR spectrum linen textile treated 30 minutes at 300°C

Linen sample treated 30 minutes at 400°C

Still evidence of organic substances (Peaks at 2960 / 2929 / 2877 cm^{-1}). The peak at 1704 cm^{-1} show oxidation (C=O-Peak) (Figure 215).

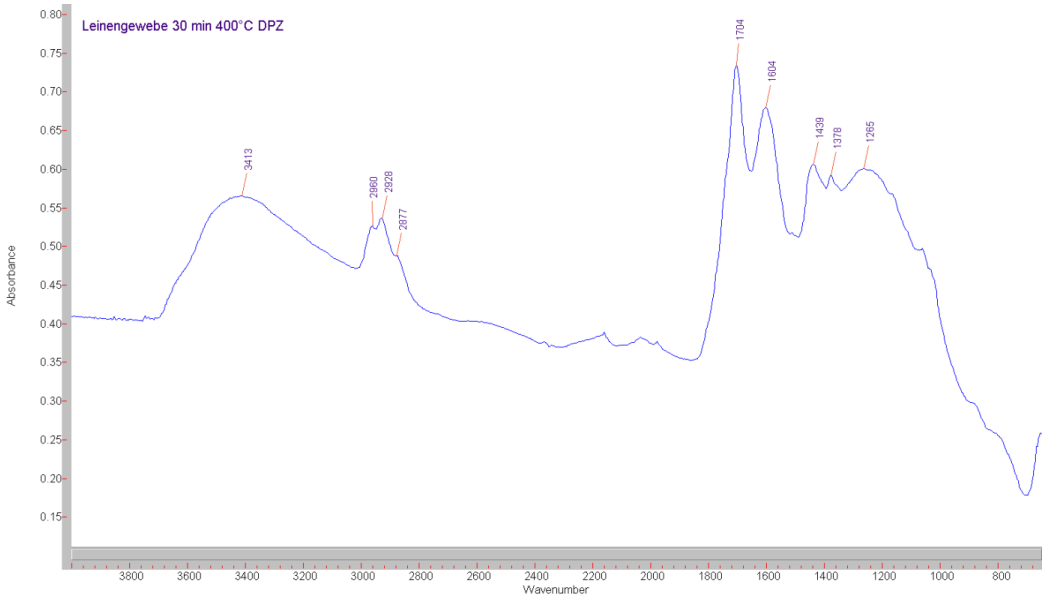

Figure 216 FTIR spectrum linen textile treated 30 minutes at 400°C

Linen samples treated 30 minutes at 500°C

Still small peaks of organic substances (2964 and 2925 cm^{-1}) and oxidation (1701 cm^{-1}) (Figure 216).

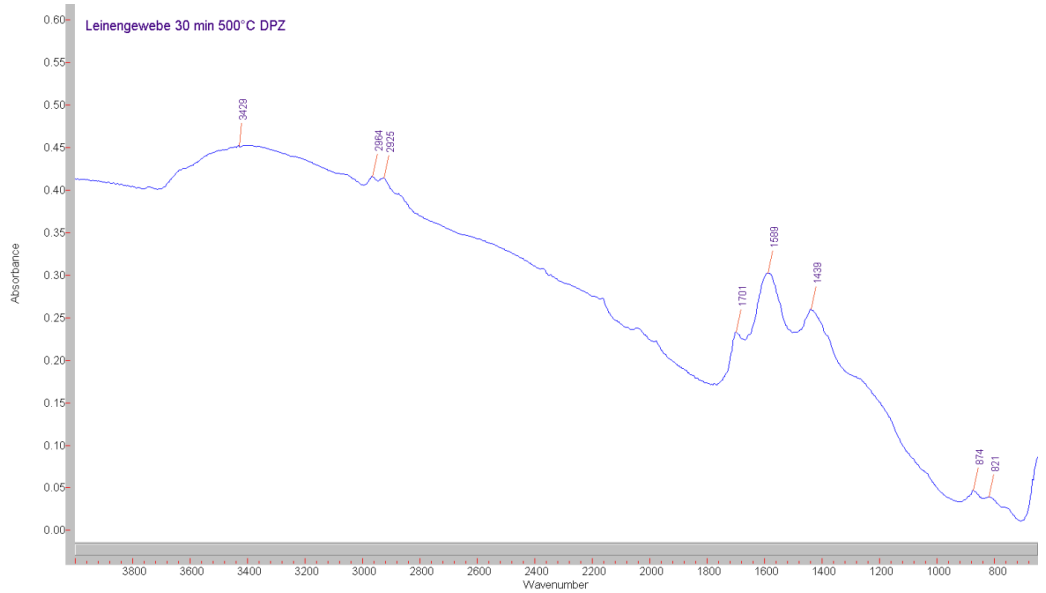

Figure 217 FTIR spectrum linen textile treated 30 minutes at 500°C

Linen textile treated 30 minutes at 600°C

No hint for organic substances. The linen textile seems to be totally carbonised (Figure 217).

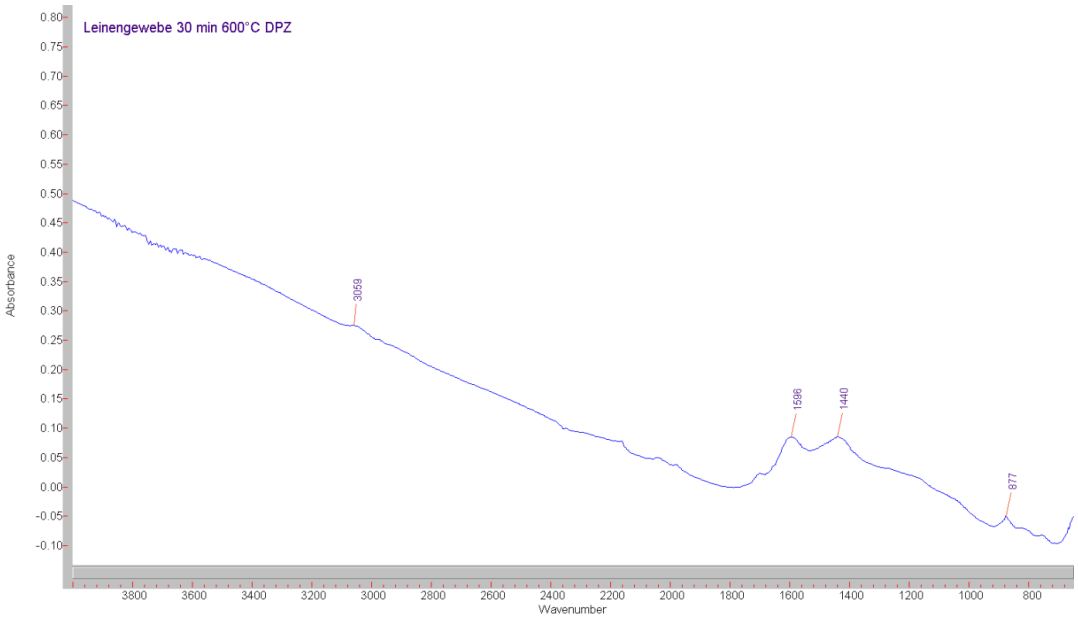

Figure 218 FTIR spectrum linen textile treated 30 minutes at 600°C

Archaeological sample 2.3

No hint for organic substances or oxidation. The peaks at 3391, 1410 and 1007 cm^{-1} are signs for –OH groups, the peak at 1586 cm^{-1} might be -C-C- of carbon (Figure 218).

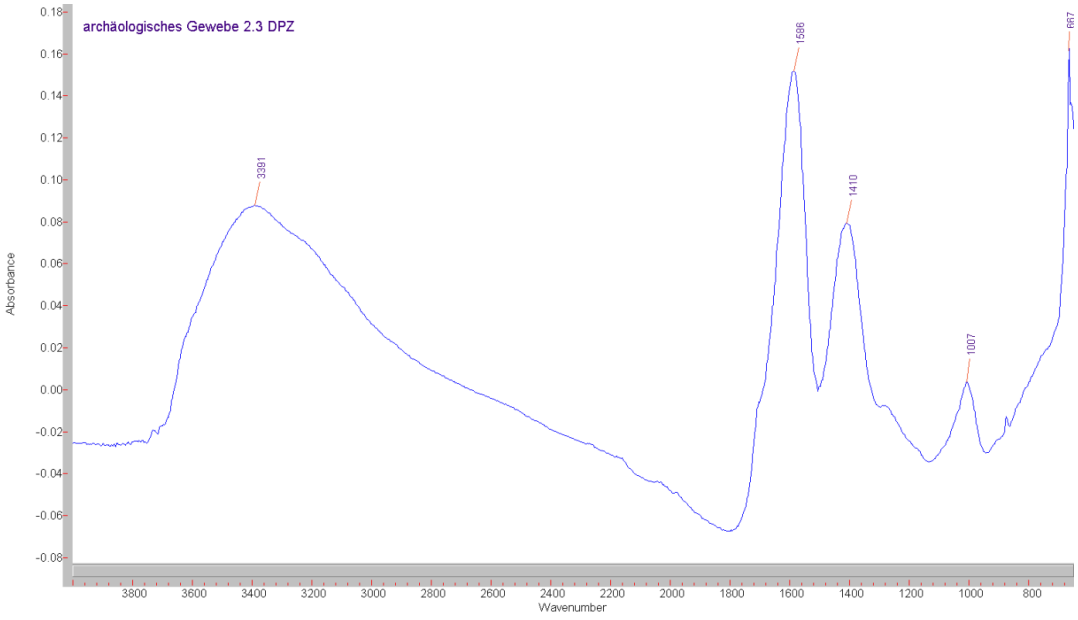

Figure 219 FTIR spectrum historical textile 2.3

Archaeological sample 2.6

No hint for organic substances or oxidation. The peaks at 3391 and 1397 cm^{-1} are signs for –OH groups, the peak at 1586 cm^{-1} might be -C-C- of carbon (Figure 219).

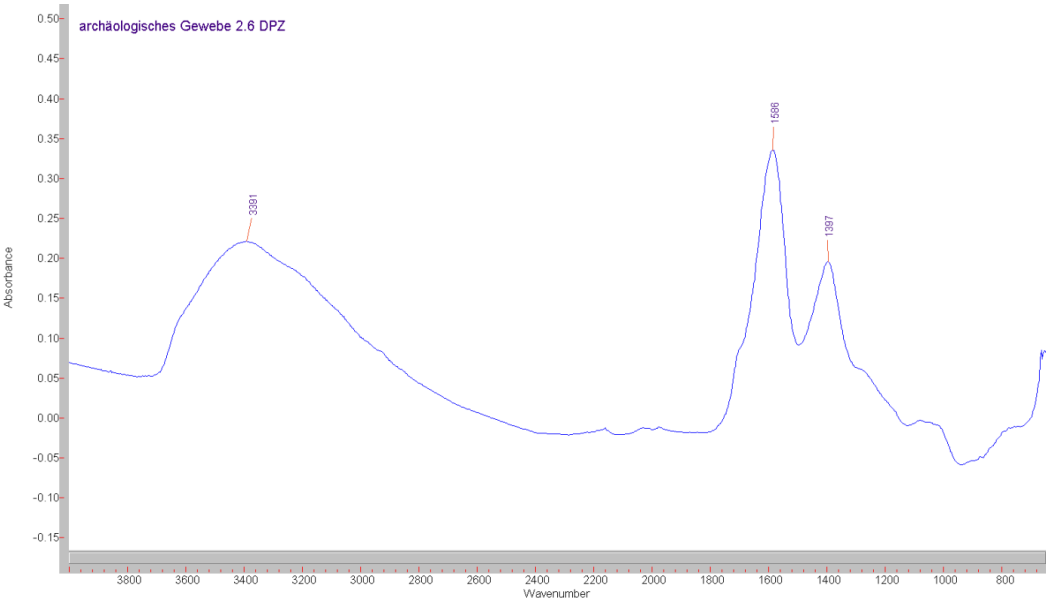

Figure 220 FTIR spectrum historical textile 2.6

Comparison of treatment :2hours at 500°C and 30 minutes at 600°C

The two spectra look similar but the spectra 2 hours at 500°C still shows the peaks at around 2965 and 2922 cm^{-1} (organic) and 1697 cm^{-1} (oxidation) (Figure 221).

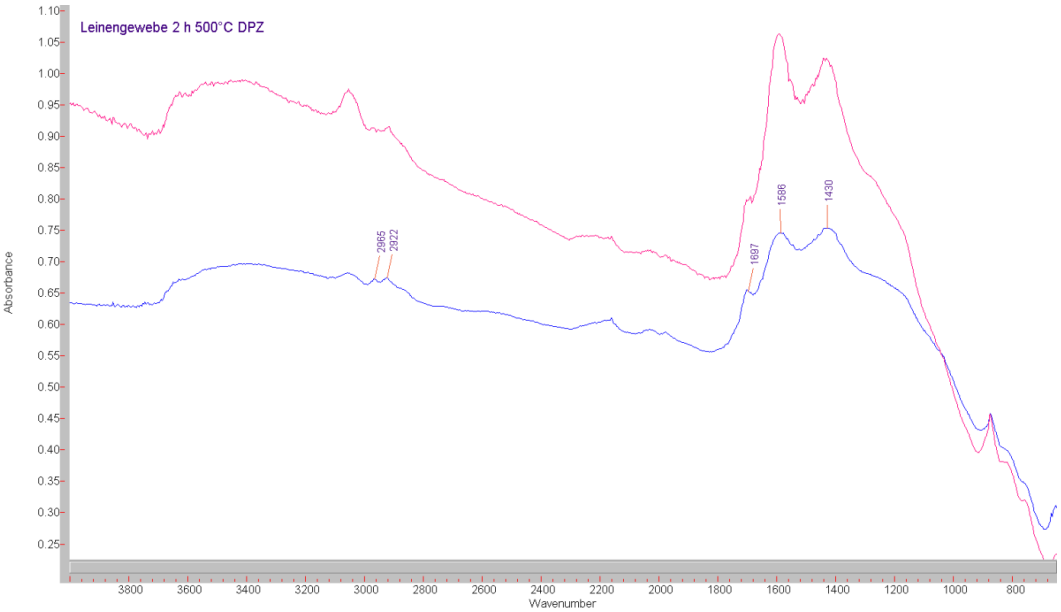

Figure 221 FTIR-spectra linen treated 2 hours at 500°C (blue) and 30 minutes at 600°C (magenta)

Appendix 10: Colorimetric measurements: Modern samples with different degree of carbonisation

Technical information:

- Software: SpectraMagic
- Instrument: Spectrophotometer
- Instrument settings :
    - Instrument name : CM-2600d
    - Serial Nº : 1012615
    - Firmware Version : 1.42
    - Measurement Type : Reflectance
    - Geometry : di : 8, de : 8
    - Specular Component : SCI + SCE
    - Measurement Area : MAV (8mm)
    - UV Settings : 100% Full
    - Measurement Cond : -

Colonne1	Data Name	Measurement Area	Timestamp	Group Traits	L*(D65)	a*(D65)	b*(D65)	Mean value of L*	Mean value of a*	Mean value of b*
Target	Modern samples - different temperature	MAV(8mm)	28.06.2018 17:04	SCI	63.16	1.41	11.22			
1	100°C	MAV(8mm)	28.06.2018 17:04	SCI	63.15	1.41	11.22	61.88	1.478	11.392
2	100°C	MAV(8mm)	28.06.2018 17:05	SCI	61.11	1.5	11.34			
3	100°C	MAV(8mm)	28.06.2018 17:05	SCI	62.76	1.42	11.37			
4	100°C	MAV(8mm)	28.06.2018 17:05	SCI	61.18	1.47	11.23			
5	100°C	MAV(8mm)	28.06.2018 17:06	SCI	61.2	1.59	11.8			
6	200°C	MAV(8mm)	28.06.2018 17:06	SCI	63.26	1.11	10.59	62.496	1.066	10.334
7	200°C	MAV(8mm)	28.06.2018 17:07	SCI	62.47	1.03	10.05			
8	200°C	MAV(8mm)	28.06.2018 17:07	SCI	63.01	1.04	10.45			
9	200°C	MAV(8mm)	28.06.2018 17:07	SCI	61.93	1.11	10.57			
10	200°C	MAV(8mm)	28.06.2018 17:07	SCI	61.81	1.04	10.01			
11	300°C	MAV(8mm)	28.06.2018 17:08	SCI	52.1	6.82	22.74	49.248	7.628	23.484
12	300°C	MAV(8mm)	28.06.2018 17:08	SCI	49.82	7.06	22.64			
13	300°C	MAV(8mm)	28.06.2018 17:08	SCI	46.47	8.58	24.26			
14	300°C	MAV(8mm)	28.06.2018 17:09	SCI	50.25	7.41	23.67			
15	300°C	MAV(8mm)	28.06.2018 17:09	SCI	47.6	8.27	24.11			
16	400°C	MAV(8mm)	28.06.2018 17:10	SCI	16.74	0.22	0.64	15.322	0.162	0.41
17	400°C	MAV(8mm)	28.06.2018 17:10	SCI	15.27	0.12	0.28			
18	400°C	MAV(8mm)	28.06.2018 17:10	SCI	14.92	0.09	0.27			
19	400°C	MAV(8mm)	28.06.2018 17:11	SCI	15.35	0.21	0.47			
20	400°C	MAV(8mm)	28.06.2018 17:11	SCI	14.33	0.17	0.39			
21	500°C	MAV(8mm)	28.06.2018 17:12	SCI	15.87	0.09	0.28	17.4	0.088	0.428
22	500°C	MAV(8mm)	28.06.2018 17:12	SCI	17.99	0.09	0.49			
23	500°C	MAV(8mm)	28.06.2018 17:12	SCI	17.88	0.07	0.45			
24	500°C	MAV(8mm)	28.06.2018 17:13	SCI	17.47	0.1	0.52			
25	500°C	MAV(8mm)	28.06.2018 17:13	SCI	17.79	0.09	0.4			
26	600°C	MAV(8mm)	28.06.2018 17:14	SCI	15.86	0.24	1.01	15.552	0.25	1.07
27	600°C	MAV(8mm)	28.06.2018 17:14	SCI	18	0.27	1.12			
28	600°C	MAV(8mm)	28.06.2018 17:15	SCI	14.3	0.26	1.11			
29	600°C	MAV(8mm)	28.06.2018 17:15	SCI	12.17	0.23	0.95			
30	600°C	MAV(8mm)	28.06.2018 17:16	SCI	17.43	0.25	1.16			

Colonne1	Data Name	Measurement Area	Timestamp	Group Traits	L*(D65)	a*(D65)	b*(D65)	Mean value of L*	Mean value of a*	Mean value of b*
Target	Modern samples - different temperature	MAV(8mm)	28.06.2018 17:04	SCE	63.25	1.44	11.27			
1	100°C	MAV(8mm)	28.06.2018 17:04	SCE	63.25	1.43	11.26			
2	100°C	MAV(8mm)	28.06.2018 17:05	SCE	61.19	1.52	11.39			
3	100°C	MAV(8mm)	28.06.2018 17:05	SCE	62.83	1.44	11.41			
4	100°C	MAV(8mm)	28.06.2018 17:05	SCE	61.29	1.49	11.28			
5	100°C	MAV(8mm)	28.06.2018 17:06	SCE	61.31	1.61	11.85			
6	200°C	MAV(8mm)	28.06.2018 17:06	SCE	63.3	1.14	10.64			
7	200°C	MAV(8mm)	28.06.2018 17:07	SCE	62.53	1.06	10.1			
8	200°C	MAV(8mm)	28.06.2018 17:07	SCE	63.12	1.07	10.5			
9	200°C	MAV(8mm)	28.06.2018 17:07	SCE	62.03	1.13	10.63			
10	200°C	MAV(8mm)	28.06.2018 17:07	SCE	61.91	1.05	10.07			
11	300°C	MAV(8mm)	28.06.2018 17:08	SCE	52.22	6.84	22.81			
12	300°C	MAV(8mm)	28.06.2018 17:08	SCE	49.92	7.07	22.7			
13	300°C	MAV(8mm)	28.06.2018 17:08	SCE	46.6	8.6	24.33			
14	300°C	MAV(8mm)	28.06.2018 17:09	SCE	50.37	7.42	23.73			
15	300°C	MAV(8mm)	28.06.2018 17:09	SCE	47.72	8.29	24.19			
16	400°C	MAV(8mm)	28.06.2018 17:10	SCE	16.76	0.26	0.67			
17	400°C	MAV(8mm)	28.06.2018 17:10	SCE	15.28	0.19	0.32			
18	400°C	MAV(8mm)	28.06.2018 17:10	SCE	14.96	0.1	0.31			
19	400°C	MAV(8mm)	28.06.2018 17:11	SCE	15.38	0.24	0.51			
20	400°C	MAV(8mm)	28.06.2018 17:11	SCE	14.36	0.21	0.42			
21	500°C	MAV(8mm)	28.06.2018 17:12	SCE	15.91	0.09	0.3			
22	500°C	MAV(8mm)	28.06.2018 17:12	SCE	18.03	0.11	0.53			
23	500°C	MAV(8mm)	28.06.2018 17:12	SCE	17.93	0.11	0.5			
24	500°C	MAV(8mm)	28.06.2018 17:13	SCE	17.53	0.12	0.57			
25	500°C	MAV(8mm)	28.06.2018 17:13	SCE	17.85	0.1	0.43			
26	600°C	MAV(8mm)	28.06.2018 17:14	SCE	15.9	0.28	1.03			
27	600°C	MAV(8mm)	28.06.2018 17:14	SCE	18.03	0.31	1.18			
28	600°C	MAV(8mm)	28.06.2018 17:15	SCE	14.32	0.3	1.14			
29	600°C	MAV(8mm)	28.06.2018 17:15	SCE	12.19	0.27	1			
30	600°C	MAV(8mm)	28.06.2018 17:16	SCE	17.45	0.26	1.19			

Appendix 11: Three wrapping methods tested for the carbonisation of modern samples

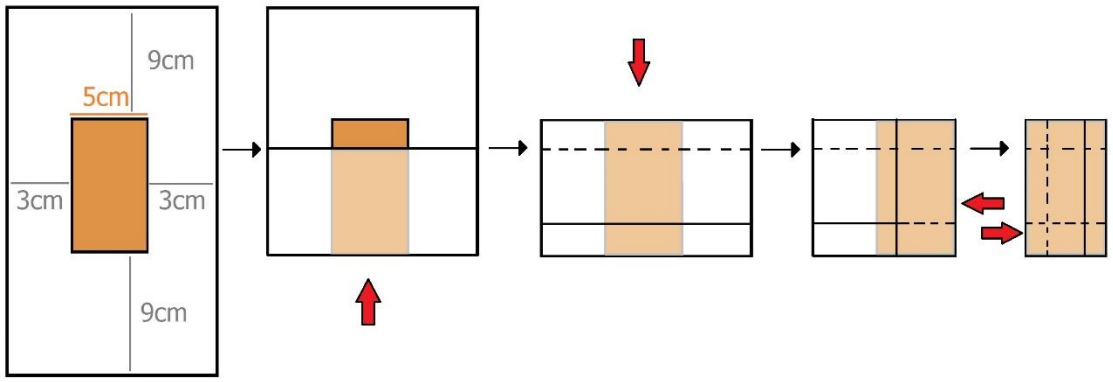

Figure 222 Wrapping method number 1

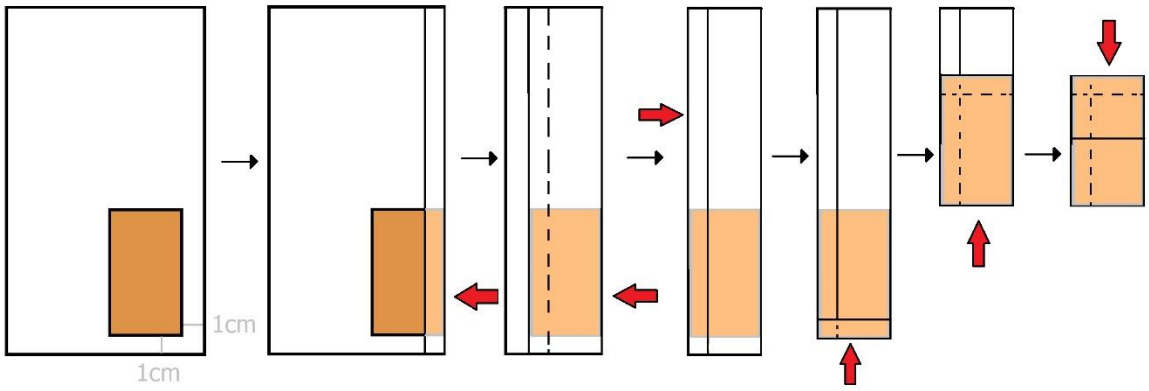

Figure 223 Wrapping method number 2

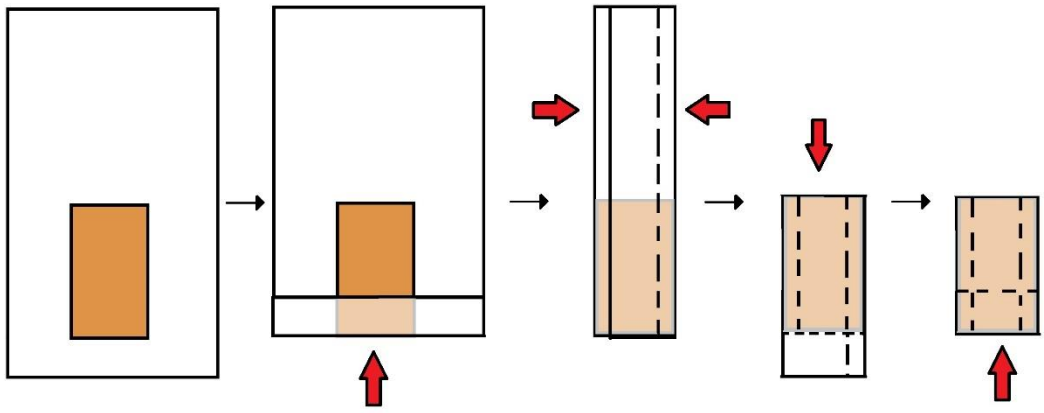

Figure 224 Wrapping method number 3

Appendix 12: Temperatures recorded during the carbonisation process.

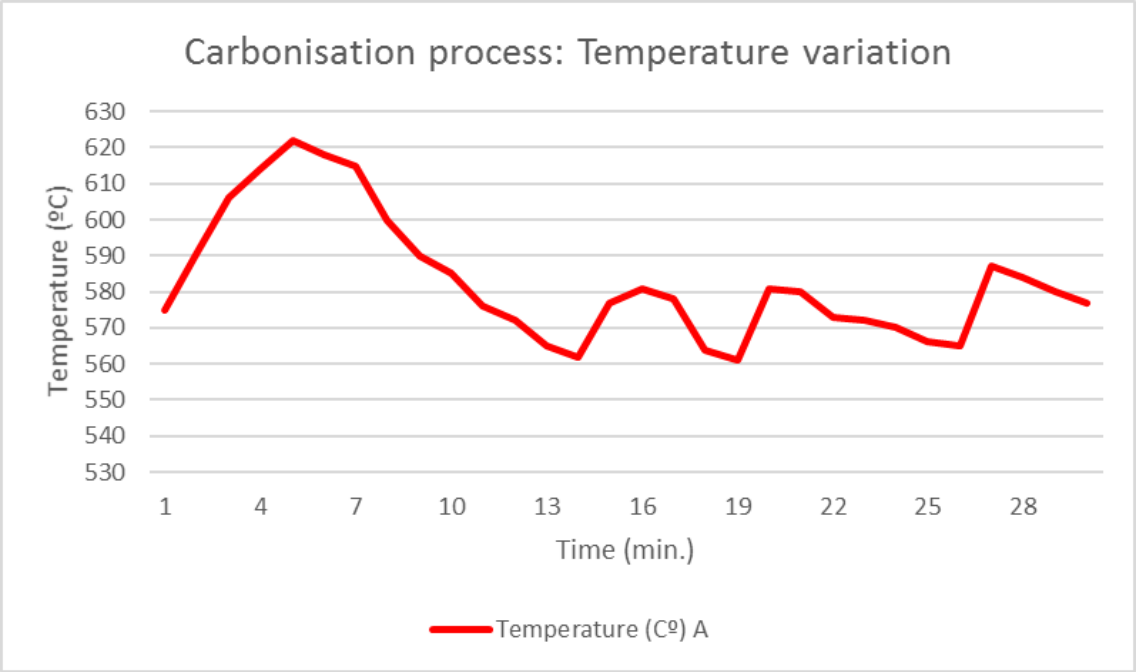

Figure 225 Temperatures recorded while carbonising warp samples

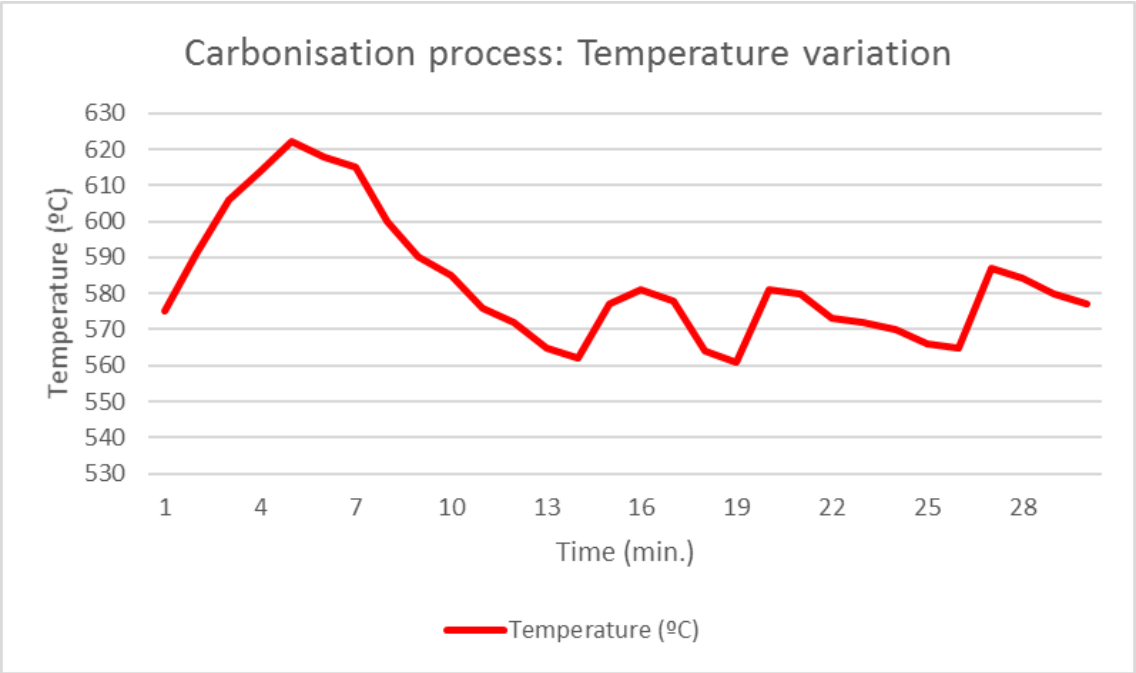

Figure 226 Temperatures recorded while carbonising weft samples

Appendix 13 Photographic documentation of the modern samples after carbonisation

Figure 227 Original big warp sample (brown) and two carbonised big warp samples (black) with the aluminium foil used for their carbonisation

Figure 228 Original big warp sample (brown) and carbonised big warp samples (black) with the aluminium foil used for their carbonisation

Figure 229 Samples carbonised with the wrapping system 1 (up), 2 (middle) and 3 (down)

Figure 230 Warp big samples carbonised without using a weight. They are all deformed

Figure 231 Carbonised big weft samples with an un-carbonised reference.

Figure 232 Carbonised big warp samples with an un-carbonised reference.

Figure 233 Carbonised small warp samples with an un-carbonised reference.

Figure 234 Carbonised small weft samples with a un-carbonised reference.

Appendix 14: New support to clean archaeological samples

A new support was created to clean an return the archaeological samples whithout manipulating them. It is composed by a two frames A and B, two pieces of flexible mesh, and four screws with their corresponding nuts. Each mesh was glued to the internal part of both frames.

When cleaning, the internal part of the frame A (where the mesh as being glued) is used as the support for the textiles. To return the samples, frame B, with the mesh facing down, is placed on frame A and fixed with the screws. Then, the samples is safely secure between the two mesh pieces. The sandwich created with the two frames with the textile in between can be then returned. When removing frame A, the other side of the sample can be cleaned.

Dimensions of the frame:

- External: 30x21cm
- Internal 25x16cm
-

Figure 235 Frame A an B. View from the exterior (left) and the interior (right)

Figure 236 Support view without (left) and with (right) nuts.

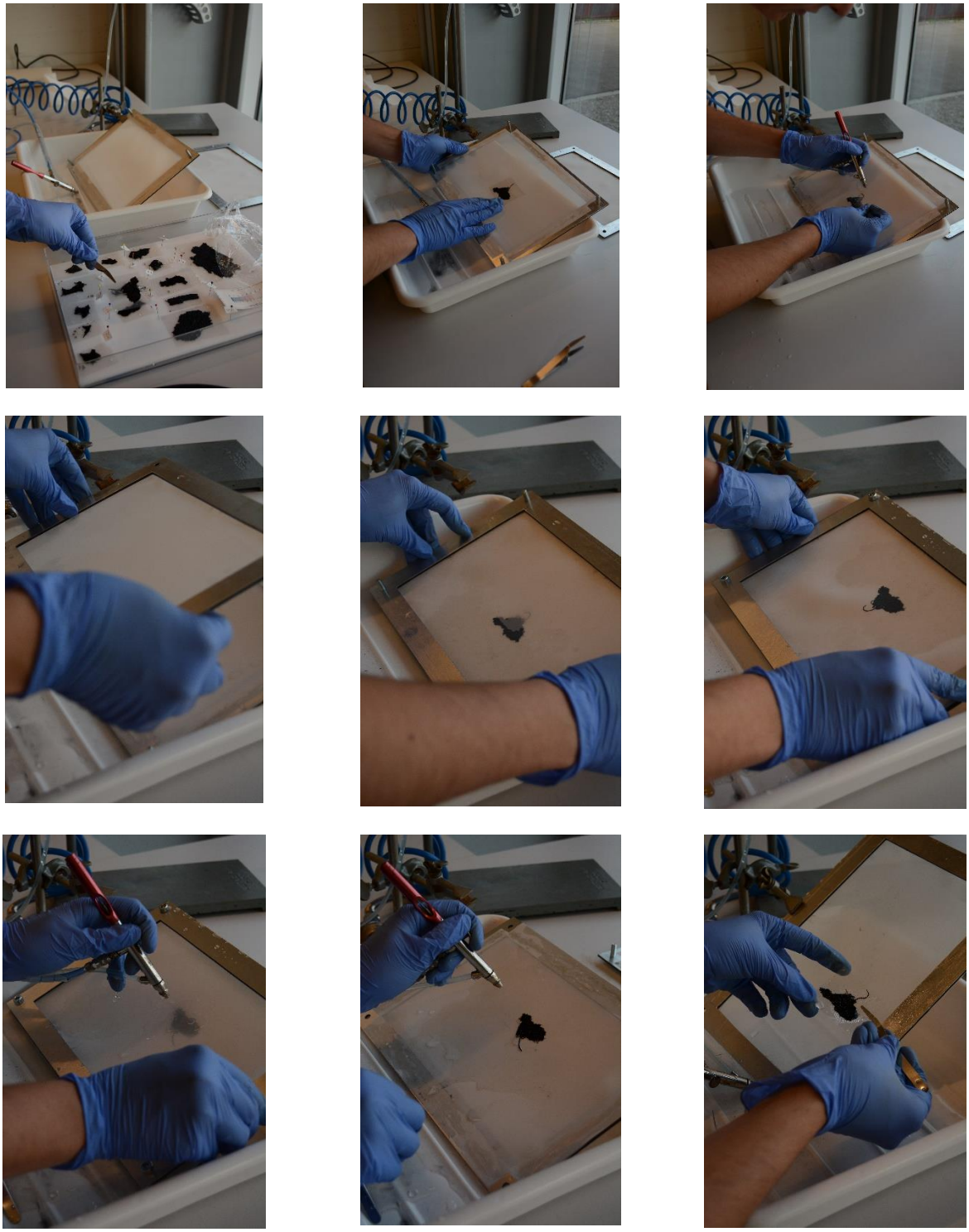

Figure 237 Cleaning procedure starting from the top left: 1) Manipulation de sample using soft tweezers and the plastic support. 2) Positioning the sample. 3) Removing the plastic support and cleaning with air-brush. 4) Placing frame B. 5) Fixing frame A and B together with the sample inside. 6) Returning both frames together 7) Removing frame A. The sample remain in frame B when applying water with the airbrush. 8)Cleaning the other side of the sample.9) Using the plastic support to remove the sample from the frame

Appendix 15: Freeze-drying under vacuum: Summary of the dimensions and weight per sample before and after treatment

Consolidant	Sample	Initial (cm)			After freeze-drying (cm)			Difference of the surface area (cm²)	Difference of the surface area (%)	Mean difference of the surface area (cm²)	Estandard Deviation (cm2)	Coefficient of variation of the surface area (cm²)	Mean difference of surface area (%)
		Length	Width	Surface area (cm²)	Length	Width	Surface area (cm²)						
Group A													
	1,16	3,273	1,882	6,160	2,290	1,420	3,252	2,908	47,209	3,966	2,835	0,715	21,397
	3,18	4,830	3,530	17,050	4,123	2,967	12,233	4,817	28,252				
	1,01	1,795	2,307	4,141	1,700	2,070	3,519	0,622	15,022				
	1,29	4,001	2,500	10,003	3,580	1,785	6,390	3,612	36,113				
	3,01	6,477	5,747	37,223	5,410	5,050	27,321	9,903	26,604				
	3,14	9,451	6,146	58,086	8,180	6,190	50,634	7,452	12,829				
	3,11	4,995	3,053	15,250	4,590	3,110	14,275	0,975	6,392				
	1,17	3,765	2,502	9,420	3,620	1,920	6,950	2,470	26,217				
	3,04	8,362	3,767	31,500	8,380	3,570	29,917	1,583	5,026				
	3,16	11,068	3,551	39,302	10,650	3,150	33,548	5,755	14,643				
	1,31	3,125	1,644	5,138	2,190	1,600	3,504	1,634	31,796				
	3,03	5,072	4,040	20,491	4,300	4,050	17,415	3,076	15,011				
	3,80	10,245	2,819	28,881	9,640	2,940	28,342	0,539	1,866				
	3,07	10,427	2,743	28,601	10,030	2,710	27,181	1,420	4,965				
	3,12	5,093	4,919	25,052	4,940	3,810	18,821	6,231	24,872				
	3,19	5,011	5,107	25,591	4,704	4,358	20,500	5,091	19,894				
	1,02	3,822	2,158	8,248	2,866	1,367	3,918	4,330	52,499				
	3,13	8,870	6,345	56,280	7,999	5,915	47,314	8,966	15,931				

Consolidant	Sample	Initial (cm)			After freeze-drying (cm)			Difference of the surface area (cm²)	Difference of the surface area (%)	Mean difference of the surface area (cm²)	Estandard Deviation (cm2)	Coefficient of variation of the surface area (cm²)	Mean difference of surface area (%)
		Length	Width	Surface area (cm²)	Length	Width	Surface area (cm²)						
Group B													
	1,05	3,162	2,364	7,475	2,901	1,891	5,486	1,989	26,611	2,339	2,372	1,014	17,036
	2,03	8,124	4,145	33,674	7,867	4,121	32,420	1,254	3,724				
	2,11	5,555	3,351	18,615	5,518	3,353	18,502	0,113	0,607				
	1,23	2,855	3,901	11,137	2,444	3,262	7,972	3,165	28,418				
	2,15	12,954	3,853	49,912	12,415	3,322	41,243	8,669	17,369				
	1,06	2,607	1,589	4,143	1,310	0,920	1,205	2,937	70,907				
	1,10	1,982	2,050	4,063	1,910	1,890	3,610	0,453	11,154				
	2,10	5,065	3,117	15,788	5,138	3,039	15,614	0,173	1,097				
	2,06	7,729	4,566	35,291	6,858	4,719	32,363	2,928	8,296				
	2,05	7,974	4,247	33,866	7,849	3,917	30,745	3,121	9,216				
	2,08	3,318	1,379	4,576	2,975	1,356	4,034	0,541	11,833				
	2,16	8,662	5,010	43,397	8,170	5,280	43,138	0,259	0,597				
	2,18	4,230	1,330	5,626	4,150	1,330	5,520	0,106	1,891				
	1,30	4,515	2,340	10,565	3,770	1,910	7,201	3,364	31,844				
	2,04	2,617	3,635	9,513	2,200	3,465	7,623	1,890	19,866				
	1,19	3,721	1,792	6,668	3,660	1,280	4,685	1,983	29,742				
	2,02	13,269	3,559	47,224	12,341	3,225	39,800	7,425	15,722				
	2,19	4,601	5,269	24,243	4,770	4,980	23,755	0,488	2,013				
	1,18	5,379	2,028	10,909	3,630	2,020	7,333	3,576	32,782				

Consolidants	Sample	Initial Weight (g)	After freeze-dryng (g	Weight loss (g)	Mean weight loss (g)	Standard deviation(	Coefficient of variation (g)	weight loss (%)	Mean weight loss(%)	Standard deviation	Coefficient of variation (%)
Group B											
Nothing	1,05	0,030	0,019	0,011	0,181	0,274	1,511	36,667	40,792	28,792	0,706
	2,03	0,319	0,238	0,081				25,392			
Klucel G	2,11	0,188	0,145	0,043				22,872			
	1,23	0,600	0,056	0,544				90,667			
	2,15	1,259	0,245	1,014				80,540			
	1,06	0,200	0,060	0,140				70,000			
	1,10	0,030	0,019	0,011				36,667			
Klucel E	2,1	0,146	0,113	0,033				22,603			
	2,06	0,350	0,280	0,070				20,000			
	2,05	0,892	0,222	0,670				75,112			
	2,08	0,054	0,046	0,008				14,815			
Aquazol 500	2,16	0,497	0,416	0,081				16,298			
	2,18	0,064	0,060	0,004				6,250			
	1,30	0,312	0,051	0,261				83,654			
	2,04	0,311	0,053	0,258				82,958			
Paraloid B72	1,19	0,040	0,031	0,009				22,500			
	2,02	0,492	0,350	0,142				28,862			
	2,19	0,274	0,226	0,048				17,518			
	1,18	0,060	0,047	0,013				21,667			
Group A											
Nothing	1,16	0,030	0,017	0,013	0,088	0,175	1,975	43,333	30,030	31,209	1,039
	3,18	0,073	0,064	0,009				12,329			
Klucel G	1,01	0,030	0,022	0,008				26,667			
	1,29	0,620	0,050	0,570				91,935			
	3,01	0,230	0,173	0,057				24,783			
	3,14	0,237	0,213	0,024				10,127			
Klucel E	3,11	0,108	0,053	0,055				50,926			
	1,17	0,600	0,059	0,541				90,167			
	3,04	0,144	0,135	0,009				6,250			
	3,16	0,273	0,253	0,020				7,326			
Aquazol 500	1,31	0,200	0,025	0,175				87,500			
	3,03	0,103	0,095	0,008				7,767			
	3,8	0,262	0,224	0,038				14,504			
	3,07	0,222	0,197	0,025				11,261			
Paraloid B72	3,12	0,144	0,132	0,012				8,333			
	3,19	0,122	0,120	0,002				1,639			
	1,02	0,050	0,028	0,022				44,000			
	3,13	0,177	0,174	0,003				1,695			

Consolidants	Sample	Initial Weight (g)	After freeze-dryng (g	After consolidation (	Weight gain (g)2	Weight gain (g)3	Weight gain %	Mean weight gain %	Estandard Deviation
Group B									
Nothing	1,05	0,030	0,019	0,018	-0,001	0,000	-5,556	0,000	
	2,03	0,319	0,238	0,224	-0,014		-6,250		
Klucel G	2,11	0,188	0,145	0,147	0,002	0,002	1,361	4,999	0,002
	1,23	0,600	0,056	0,055	-0,001		-1,818		
	2,15	1,259	0,245	0,243	-0,002		-0,823		
	1,06	0,200	0,060	0,060	0,000		0,000		
	1,10	0,030	0,019	0,022	0,003		13,636		
Klucel E	2,1	0,146	0,113	0,125	0,012	0,014	9,600	8,641	0,007
	2,06	0,350	0,280	0,304	0,024		7,895		
	2,05	0,892	0,222	0,235	0,013		5,532		
	2,08	0,054	0,046	0,052	0,006		11,538		
Aquazol 500	2,16	0,497	0,416	0,418	0,002	0,001	0,478	0,159	0,001
	2,18	0,064	0,060	0,060	0,000		0,000		
	1,30	0,312	0,051	0,051	0,000		0,000		
	2,04	0,311	0,053	0,052	-0,001		-1,923		
Paraloid B72	1,19	0,040	0,031	0,037	0,006	0,012	16,216	9,019	0,008
	2,02	0,492	0,350	0,370	0,020		5,405		
	2,19	0,274	0,226	0,242	0,016		6,612		
	1,18	0,060	0,047	0,051	0,004		7,843		
Group A									
Nothing	1,16	0,030	0,017	0,018	0,001	0,003	5,556	5,719	0,002
	3,18	0,073	0,064	0,068	0,004		5,882		
Klucel G	1,01	0,030	0,022	0,025	0,003	0,008	12,000	9,870	0,004
	1,29	0,620	0,050	0,062	0,012		19,355		
	3,01	0,230	0,173	0,182	0,009		4,945		
	3,14	0,237	0,213	0,22	0,007		3,182		
Klucel E	3,11	0,108	0,053	0,056	0,003	0,013	5,357	8,333	0,014
	1,17	0,600	0,059	0,065	0,006		9,231		
	3,04	0,144	0,135	0,145	0,010		6,897		
	3,16	0,273	0,253	0,287	0,034		11,847		
Aquazol 500	1,31	0,200	0,025	0,029	0,004	0,005	13,793	5,033	0,004
	3,03	0,103	0,095	0,095	0,000		0,000		
	3,8	0,262	0,224	0,233	0,009		3,863		
	3,07	0,222	0,197	0,202	0,005		2,475		
Paraloid B72	3,12	0,144	0,132	0,151	0,019	0,014	12,583	8,701	0,009
	3,19	0,122	0,120	0,14	0,020		14,286		
	1,02	0,050	0,028	0,028	0,000		0,000		
	3,13	0,177	0,174	0,189	0,015		7,937		

Appendix 16 Consolidants: Summary of the characteristics and references

Product	Solubility	Tg (°C)	pH	Molecular weight	Characteristics	Concentration	References
Klucel® G (Hydroxypropyl cellulose)	Water (below 38°C) and polar solvents	100-105	5.0-8.8 (1%)	370.000	Excellent photochemical stability Low peroxide formation Good combination with PEG, glycerol and mannitol Medium viscosity Loss of viscosity and weight upon aging Weak bonding strength	1-2%w/w in ethanol	Peacock 1990, Landi 1997, Eastop y Timar-Balazsy 1998, Haldane 2000/2007, Moreno 2007, Younder 2007, Montesinos Ferrandis *et al* 2000, Down 2015, Horie 2010
Klucel® E (Hydroxypropyl cellulose)	Water, ethanol, acetone, and other organic solvents	100-150	5.0-8.8 (1%)	80.000	Excellent photochemical stability Low peroxide formation Good combination with PEG, glycerol and mannitol Low viscosity Loss of viscosity and weight upon aging Can yellowed with time Weak bonding strength	5%w/w in ethanol	Peacock 1990, Montesinos Ferrandis *et al* 2000, Down 2015, Horie 2010
Paraloid® B-72 (copolymer resin with 70% ethyl methacrylate and 30% methyl acrylate)	Isopropanol, acetone, toluene and xylene	40	7-9 for liquid dispersions	105.000	Semi-glassy and semi-flexible at 22°C Remains soluble in non-polar solvents after aging Good colour stability, reversibility and retained flexibility upon aging	5%w/w. in ethanol	Pertegato 1993, Landi 1997, Millei 1999, Hamilton 2007, Blackshaw and Ward 1983, Montesinos Ferrandis et al 2008, Down 2015, Horie 2010
Aquazol® 500 Poly(2-ethyl-2-oxazoline)	Water and organic solvents	69-71	6.4	500.000	Thermally stable up to 220°C Non-toxic Allows re-treatment with other adhesives Do not shrink or become brittle Do not support mould growth When aging, it does not discolour, shrank, change pH or change its solubility. Also recommended as a plasticizer for other adhesives like Paraloid® B72 Mechanical properties can be affected when exposed to high RH	1%w/w in ethanol	Wolbers 2008, Wolbers et al. 1998, Kroschwitz et al. 1985, Shelton, 1994, Arslanoglu and Tallent 2003, Down 2015, Horie 2010

Table 16 Properties and bibliographic references for the consolidants selected

Appendix 17 Bending length and flexural rigidity: Charred modern textiles

Sample	Length (cm)	Width (cm)	Weight (g)	Mass per unit area g/m²	Mean mass per unit area g/m²	Overhanging lenght (cm)	Bending lenght (cm)	Sample mean bending lenght (cm)	*C:* Overal mean bending lenght (cm)	*G:* Flexural rigidity (µNm)	Standard deviation for *C*	Coefficient of variation for *C*	*G: Average*	Standard deviation for *G*	Coefficient of variation for *G*
NO CONSOLIDATION															
Group A							0								
WARP SMALL							0								
S1	8,9	2,3	0,250	0,012212995	0,011768604	2,1	1,05	1,15	1,0925	0,000153458	0,06823672	0,062459241	0,000443634	0,00041037	0,92502121
						2,2	1,1								
						2,4	1,2								
						2,5	1,25								
S2	8,1	2,4	0,239	0,012294239		2	1	1,075							
						2,2	1,1								
						2,2	1,1								
						2,2	1,1								
S3	8,6	2,4	0,245	0,011870155		2,2	1,1	1,05							
						2	1								
						2,1	1,05								
						2,1	1,05								
S4	8,5	2,4	0,216	0,010588235		2,1	1,05	1,175							
						2,1	1,05								
						2,6	1,3								
						2,6	1,3								
S5	8,7	2,4	0,248	0,011877395		2	1	1,0125							
						2	1								
						2,1	1,05								
						2	1								
WEFT SMALL							0								
S1	10,7	1,9	0,257	0,012641417	0,01279453	3,3	1,65	1,7	1,79	0,00073381	0,132110276	0,073804623			
						3,5	1,75								
						3,3	1,65								
						3,5	1,75								
S2	10,6	1,8	0,246	0,012893082		3,4	1,7	1,675							
						3	1,5								
						3,5	1,75								
						3,5	1,75								
S3	10,5	1,9	0,251	0,012581454		3,7	1,85	1,725							
						3,7	1,85								
						3,3	1,65								
						3,1	1,55								
S4	10,7	1,8	0,247	0,012824507		3,8	1,9	1,9875							
						4	2								
						4,1	2,05								
						4	2								
S5	10,7	1,8	0,251	0,013032191		3,6	1,8	1,8625							
						3,7	1,85								
						3,8	1,9								
						3,8	1,9								

Sample	Length (cm)	Width (cm)	Weight (g)	Mass per unit area g/m²	Mean mass per unit area g/m²	Overhanging lenght (cm)	Bending lenght (cm)	Sample mean bending lenght (cm)	*C:* Overal mean bending lenght (cm)	*G:* Flexural rigidity (µNm)	Standard deviation for *C*	Coefficient of variation for *C*	*G: Average*	Standard deviation for *G*	Coefficient of variation for *G*
NO CONSOLIDATION															
Group B															
WARP SMALL															
S1	8,6	2,4	0,187	0,009060078	0,009118796	2,3	1,15	1,125	1,2875	0,000194616	0,12593401	0,097812824	0,000388359	0,00027399	0,70551595
						2,3	1,15								
						2,2	1,1								
						2,2	1,1								
S2	8,9	2,3	0,205	0,010014656		3	1,5	1,4375							
						2,7	1,35								
						2,8	1,4								
						3	1,5								
S3	7,9	2,3	0,178	0,009796368		2,4	1,2	1,225							
						2,4	1,2								
						2,4	1,2								
						2,6	1,3								
S4	9,2	2,6	0,185	0,007734114		2,5	1,25	1,2625							
						2,6	1,3								
						2,5	1,25								
						2,5	1,25								
S5	8,9	2,3	0,184	0,008988764		2,8	1,4	1,3875							
						2,8	1,4								
						2,7	1,35								
						2,8	1,4								
WEFT SMALL							0								
S1	11	2,3	0,202	0,00798419	0,008973506	3	1,5	1,6625	1,865	0,000582101	0,228000822	0,122252452			
						3,3	1,65								
						3,8	1,9								
						3,2	1,6								
S2	10,4	2	0,185	0,008894231		3,6	1,8	1,75							
						3,2	1,6								
						3,6	1,8								
						3,6	1,8								
S3	10,7	1,8	0,206	0,010695742		3,6	1,8	2							
						3,7	1,85								
						4,5	2,25								
						4,2	2,1								
S4	10,3	1,8	0,198	0,010679612		3,3	1,65	1,7125							
						3,3	1,65								
						3,6	1,8								
						3,5	1,75								
S5	11,2	2,7	0,200	0,006613757		4	2	2,2							
						4,2	2,1								
						4,7	2,35								
						4,7	2,35								

Sample	Length (cm)	Width (cm)	Weight (g)	Mass per unit area g/m²	Mean mass per unit area g/m²	Overhanging lenght (cm)	Bending lenght (cm)	Sample mean bending lenght (cm)	*C:* Overal mean bending lenght (cm)	*G:* Flexural rigidity (µNm)	Standard deviation for *C*	Coefficient of variation for *C*	*G: Average*	Standard deviation for *G*	Coefficient of variation for *G*
Klucel E®															
Group A							0								
WARP SMALL							0								
S1	9,1	2,4	0,249	0,011401099	0,013073871	2,1	1,05	1,1875	1,1725	0,000210738	0,062123868	0,05298411	0,00021074	0,00054524	2,58726581
						2,3	1,15								
						2,6	1,3								
						2,5	1,25								
S2	8,1	2,3	0,262	0,014063339		2	1	1,0875							
						2	1								
						2,3	1,15								
						2,4	1,2								
S3	8,1	2,3	0,255	0,013687601		2,3	1,15	1,1375							
						2,4	1,2								
						2,2	1,1								
						2,2	1,1								
S4	8,4	2,3	0,240	0,01242236		2,2	1,1	1,25							
						2,4	1,2								
						2,7	1,35								
						2,7	1,35								
S5	8,1	2,3	0,257	0,013794954		2,2	1,1	1,2							
						2,3	1,15								
						2,6	1,3								
						2,5	1,25								
WEFT SMALL							0								
S1	10	1,9	0,271	0,014263158	0,013395143	3,3	1,65	1,7625	1,9425	0,000981817	0,125809876	0,06476699			
						3,5	1,75								
						3,7	1,85								
						3,6	1,8								
S2	10,6	1,9	0,263	0,01305859		4	2	1,9125							
						4	2								
						3,7	1,85								
						3,6	1,8								
S3	10,6	1,9	0,255	0,01266137		3,8	1,9	1,975							
						3,8	1,9								
						4,2	2,1								
						4	2								
S4	10,3	1,8	0,265	0,01429342		4	2	1,95							
						3,8	1,9								
						4	2								
						3,8	1,9								
S5	10,9	1,9	0,263	0,012699179		4	2	2,1125							
						4	2								
						4,4	2,2								
						4,5	2,25								

Sample	Length (cm)	Width (cm)	Weight (g)	Mass per unit area g/m²	Mean mass per unit area g/m²	Overhanging lenght (cm)	Bending lenght (cm)	Sample mean bending lenght (cm)	*C:* Overal mean bending lenght (cm)	*G:* Flexural rigidity (µNm)	Standard deviation for *C*	Coefficient of variation for *C*	*G: Average*	Standard deviation for *G*	Coefficient of variation for *G*
Klucel E®															
Group B															
WARP SMALL															
S1	8,1	2,3	0,217	0,01164788	0,010638745	3,6	1,8	2,2125	2,2	0,001132814	0,101165088	0,04598413	0,00262799	0,00211449	0,80460569
						4,8	2,4								
						4,3	2,15								
						5	2,5								
S2	8	2,4	0,227	0,011822917		3,8	1,9	2,225							
						4,9	2,45								
						4,5	2,25								
						4,6	2,3								
S3	8,7	2,4	0,221	0,010584291		3,7	1,85	2,1							
						4,5	2,25								
						4	2								
						4,6	2,3								
S4	8,6	2,4	0,211	0,010222868		3,7	1,85	2,1125							
						4,6	2,3								
						4	2								
						4,6	2,3								
S5	9,3	2,4	0,199	0,008915771		4	2	2,35							
						5	2,5								
						4,6	2,3								
						5,2	2,6								
WEFT SMALL							0								
S1	9,9	1,7	0,233	0,013844326	0,011191173	5,9	2,95	2,85	3,3275	0,004123156	0,420509364	0,12637396			
						5,6	2,8								
						5,8	2,9								
						5,5	2,75								
S2	10,8	2	0,240	0,011111111		8	4	3,8625							
						7,6	3,8								
						8	4								
						7,3	3,65								
S3	10,9	1,9	0,220	0,010622887		6,1	3,05	3,0875							
						6	3								
						6,5	3,25								
						6,1	3,05								
S4	10,1	1,8	0,226	0,012431243		6,2	3,1	3,175							
						6,6	3,3								
						6,4	3,2								
						6,2	3,1								
S5	10,6	2,6	0,219	0,007946299		7,6	3,8	3,6625							
						7,6	3,8								
						7,1	3,55								
						7	3,5								

Sample	Length (cm)	Width (cm)	Weight (g)	Mass per unit area g/m²	Mean mass per unit area g/m²	Overhanging lenght (cm)	Bending lenght (cm)	Sample mean bending lenght (cm)	*C:* Overal mean bending lenght (cm)	*G:* Flexural rigidity (µNm)	Standard deviation for *C*	Coefficient of variation for *C*	*G: Average*	Standard deviation for *G*	Coefficient of variation for *G*
Aquazol 500®															
Group A							0								
WARP SMALL							0								
S1	9	2,5	0,280	0,012444444	0,012116172	2,3	1,15	1,125	1,1425	0,00018069	0,319965818	0,28005761	0,000338	0,00022247	0,65819584
						2,1	1,05								
						2,3	1,15								
						2,3	1,15								
S2	8,2	2,3	0,226	0,011983033		2,3	1,15	1,1375							
						2,3	1,15								
						2,2	1,1								
						2,3	1,15								
S3	8,6	2,4	0,243	0,011773256		2,5	1,25	1,25							
						2,6	1,3								
						2,4	1,2								
						2,5	1,25								
S4	8,3	2,4	0,230	0,011546185		2,2	1,1	1,1125							
						2,3	1,15								
						2,2	1,1								
						2,2	1,1								
S5	8,3	2,3	0,245	0,012833944		2	1	1,0875							
						2,1	1,05								
						2,3	1,15								
						2,3	1,15								
WEFT SMALL							0								
S1	10,5	1,9	0,233	0,011679198	0,012206625	3	1,5	1,625	1,595	0,000495311					
						3,2	1,6								
						3,4	1,7								
						3,4	1,7								
S2	10,5	1,9	0,228	0,011428571		3,1	1,55	1,5125							
						3,2	1,6								
						3	1,5								
						2,8	1,4								
S3	10	1,9	0,244	0,012842105		3,1	1,55	1,575							
						3,3	1,65								
						3	1,5								
						3,2	1,6								
S4	10,1	1,8	0,241	0,013256326		3,3	1,65	1,6875							
						3,6	1,8								
						3,2	1,6								
						3,4	1,7								
S5	10,4	2	0,246	0,011826923		3	1,5	1,575							
						2,9	1,45								
						3,4	1,7								
						3,3	1,65								

Sample	Length (cm)	Width (cm)	Weight (g)	Mass per unit area g/m²	Mean mass per unit area g/m²	Overhanging lenght (cm)	Bending lenght (cm)	Sample mean bending lenght (cm)	*C:* Overal mean bending lenght (cm)	*G:* Flexural rigidity (µNm)	Standard deviation for *C*	Coefficient of variation for *C*	*G: Average*	Standard deviation for *G*	Coefficient of variation for *G*
Aquazol 500®															
Group B															
WARP SMALL															
S1	8,7	2,4	0,191	0,00914751	0,0096906	3,6	1,8	1,9375	1,9425	0,000710287	0,069372185	0,03571284	0,0015571	0,00119757	0,76910401
						4	2								
						4	2								
						3,9	1,95								
S2	7,7	2,4	0,199	0,010768398		3,8	1,9	1,975							
						4	2								
						4,1	2,05								
						3,9	1,95								
S3	8,2	2,4	0,194	0,009857724		3,6	1,8	1,825							
						3,6	1,8								
						3,8	1,9								
						3,6	1,8								
S4	8,6	2,4	0,198	0,009593023		3,7	1,85	1,975							
						4	2								
						4,1	2,05								
						4	2								
S5	8,3	2,4	0,181	0,009086345		4	2	2							
						4,1	2,05								
						4	2								
						3,9	1,95								
WEFT SMALL							0								
S1	11,1	2,3	0,194	0,007598903	0,009581345	5,6	2,8	2,775	2,9275	0,002403904					
						5,6	2,8								
						5,4	2,7								
						5,6	2,8								
S2	10,6	1,9	0,198	0,009831182		5,3	2,65	2,9375							
						5,7	2,85								
						6,2	3,1								
						6,3	3,15								
S3	10,5	1,8	0,201	0,010634921		5,8	2,9	3,125							
						6,4	3,2								
						6,5	3,25								
						6,3	3,15								
S4	10,4	1,9	0,202	0,010222672		5,4	2,7	2,775							
						5,3	2,65								
						5,8	2,9								
						5,7	2,85								
S5	10,5	2	0,202	0,009619048		6	3	3,025							
						5,9	2,95								
						6,2	3,1								
						6,1	3,05								

Sample	Length (cm)	Width (cm)	Weight (g)	Mass per unit area g/m²	Mean mass per unit area g/m²	Overhanging lenght (cm)	Bending lenght (cm)	Sample mean bending lenght (cm)	*C:* Overal mean bending lenght (cm)	*G:* Flexural rigidity (µNm)	Standard deviation for *C*	Coefficient of variation for *C*	*G: Average*	Standard deviation for *G*	Coefficient of variation for *G*
Klucel G®															
Group A							0								
WARP SMALL							0								
S1	9,2	2,4	0,227	0,010280797	0,011195469	2,1	1,05	1,05	1,2025	0,000194669	0,098583721	0,0819823	0,00040841	0,00030227	0,74012072
						2,1	1,05								
						2	1								
						2,2	1,1								
S2	8,4	2,4	0,232	0,011507937		2,5	1,25	1,2							
						2,5	1,25								
						2,3	1,15								
						2,3	1,15								
S3	8,3	2,3	0,225	0,011786276		2,3	1,15	1,2125							
						2,7	1,35								
						2,2	1,1								
						2,5	1,25								
S4	8,3	2,4	0,238	0,011947791		2,4	1,2	1,325							
						2,7	1,35								
						2,7	1,35								
						2,8	1,4								
S5	8,8	2,5	0,230	0,010454545		2,4	1,2	1,225							
						2,6	1,3								
						2,3	1,15								
						2,5	1,25								
WEFT SMALL							0								
S1	10,5	1,9	0,242	0,012130326	0,011809818	3,4	1,7	1,75	1,74	0,000622144	0,13270032	0,07626455			
						3,6	1,8								
						3,5	1,75								
						3,5	1,75								
S2	10,8	2,1	0,242	0,010670194		3,8	1,9	1,8375							
						3,7	1,85								
						3,5	1,75								
						3,7	1,85								
S3	10,4	1,9	0,226	0,011437247		3	1,5	1,5375							
						3	1,5								
						3,2	1,6								
						3,1	1,55								
S4	10	1,9	0,245	0,012894737		3,3	1,65	1,7							
						3,3	1,65								
						3,5	1,75								
						3,5	1,75								
S5	10,6	1,9	0,240	0,011916584		4	2	1,875							
						4	2								
						3,5	1,75								
						3,5	1,75								

Sample	Length (cm)	Width (cm)	Weight (g)	Mass per unit area g/m²	Mean mass per unit area g/m²	Overhanging lenght (cm)	Bending lenght (cm)	Sample mean bending lenght (cm)	*C:* Overal mean bending lenght (cm)	*G:* Flexural rigidity (µNm)	Standard deviation for *C*	Coefficient of variation for *C*	*G: Average*	Standard deviation for *G*	Coefficient of variation for *G*
Klucel G®															
Group B															
WARP SMALL															
S1	8,5	2,3	0,188	0,009616368	0,010158355	3,9	1,95	2	1,86	0,000651043	0,099843628	0,05375162	0,00128074	0,00089053	0,69532182
						4,3	2,15								
						3,8	1,9								
						4	2								
S2	7,8	2,3	0,186	0,010367893		3,2	1,6	1,75							
						3,8	1,9								
						3,5	1,75								
						3,5	1,75								
S3	8,4	2,3	0,194	0,010041408		3,7	1,85	1,8875							
						4	2								
						3,6	1,8								
						3,8	1,9								
S4	8	2,3	0,198	0,01076087		3,4	1,7	1,78							
						3,7	1,85								
						3,5	1,75								
						3,6	1,8								
S5	8,3	2,3	0,191	0,010005238		3,6	1,8	1,875							
						3,8	1,9								
						3,6	1,8								
						4	2								
WEFT SMALL							0								
S1	10,9	2,2	0,201	0,008381985	0,010653029	6	3	2,9625	2,6175	0,001910439	0,198549427	0,0758546			
						5,6	2,8								
						6,1	3,05								
						6	3								
S2	10,1	1,7	0,209	0,012172394		5	2,5	2,4625							
						4,7	2,35								
						5	2,5								
						5	2,5								
S3	10,6	1,7	0,196	0,010876804		5	2,5	2,5125							
						5	2,5								
						5,1	2,55								
						5	2,5								
S4	10,8	1,9	0,203	0,009892788		5,3	2,65	2,575							
						5,2	2,6								
						5,2	2,6								
						4,9	2,45								
S5	10	1,7	0,203	0,011941176		5,3	2,65	2,575							
						5	2,5								
						5,3	2,65								
						5	2,5								

Sample	Length (cm)	Width (cm)	Weight (g)	Mass per unit area g/m²	Mean mass per unit area g/m²	Overhanging lenght (cm)	Bending lenght (cm)	Sample mean bending lenght (cm)	*C:* Overal mean bending lenght (cm)	*G:* Flexural rigidity (µNm)	Standard deviation for *C*	Coefficient of variation for *C*	*G: Average*	Standard deviation for *G*	Coefficient of variation for *G*
Paraloid® B72															
Group A										0					
WARP SMALL										0					
S1	8,5	2,4	0,253	0,0124	0,0124	3,8	1,9	1,7875	1,913	0,000867	0,138	0,072	0,002	0,00123	0,70961905
						3,7	1,85			0					
						3,2	1,6			0					
						3,6	1,8			0					
S2	8,5	2,4	0,252	0,0124		3,7	1,85	1,925		0					
						3,6	1,8			0					
						4	2			0					
						4,1	2,05			0					
S3	8,6	2,4	0,250	0,0121		3,7	1,85	2		0					
						4,1	2,05			0					
						4	2			0					
						4,2	2,1			0					
S4	8,3	2,4	0,238	0,0119		4	2	2,0875		0					
						4,2	2,1			0					
						4,2	2,1			0					
						4,3	2,15			0					
S5	8,5	2,3	0,257	0,0131		3,7	1,85	1,7625		0					
						3,7	1,85			0					
						3	1,5			0					
						3,7	1,85			0					
WEFT SMALL										0					
S1	10,6	2	0,257	0,0121	0,0128	4,6	2,3	2,5	2,733	0,002613	0,187	0,068			
						4,8	2,4			0					
						5,3	2,65			0					
						5,3	2,65			0					
S2	10,6	2	0,238	0,0112		5,6	2,8	2,825		0					
						5,6	2,8			0					
						5,9	2,95			0					
						5,5	2,75			0					
S3	10,6	1,8	0,253	0,0133		5,9	2,95	2,7875		0					
						5,7	2,85			0					
						5,3	2,65			0					
						5,4	2,7			0					
S4	10,3	1,8	0,265	0,0143		5,4	2,7	2,5875		0					
						5,2	2,6			0					
						5	2,5			0					
						5,1	2,55			0					
S5	10,7	1,9	0,267	0,0131		6	3	2,9625		0					
						6	3			0					
						5,8	2,9			0					
						5,9	2,95			0					

Sample	Length (cm)	Width (cm)	Weight (g)	Mass per unit area g/m²	Mean mass per unit area g/m²	Overhanging lenght (cm)	Bending lenght (cm)	Sample mean bending lenght (cm)	*C:* Overal mean bending lenght (cm)	*G:* Flexural rigidity (µNm)	Standard deviation for *C*	Coefficient of variation for *C*	*G: Average*	Standard deviation for *G*	Coefficient of variation for *G*
Paraloid® B72															
Group B															
WARP SMALL															
S1	8,9	2,4	0,214	0,0100	0,0118	5,2	2,6	2,65	2,933	0,003	0,169	0,058	0,006	0,004	0,668
						5,4	2,7			0					
						5,4	2,7			0					
						5,2	2,6			0					
S2	8	2,4	0,244	0,0127		5,8	2,9	3,0375		0					
						6,5	3,25			0					
						6	3			0					
						6	3			0					
S3	7,8	2,3	0,221	0,0123		5,9	2,95	3,0375		0					
						6,3	3,15			0					
						5,8	2,9			0					
						6,3	3,15			0					
S4	8,1	2,3	0,233	0,0125		5,9	2,95	3,0375		0					
						6,3	3,15			0					
						6	3			0					
						6,1	3,05			0					
S5	8,9	2,3	0,237	0,0116		5,5	2,75	2,9		0					
						5,8	2,9			0					
						6,2	3,1			0					
						5,7	2,85			0					
WEFT SMALL										0					
S1	10,9	2	0,233	0,0107	0,0120	8,5	4,25	4,2625	4,110	0,008327	0,267	0,065			
						8,6	4,3			0					
						8,7	4,35			0					
						8,3	4,15			0					
S2	10,6	1,9	0,240	0,0119		8,3	4,15	4,1		0					
						7,4	3,7			0					
						9	4,5			0					
						8,1	4,05			0					
S3	10,8	1,8	0,236	0,0121		8,7	4,35	4,025		0					
						7,8	3,9			0					
						8,2	4,1			0					
						7,5	3,75			0					
S4	10,5	1,9	0,237	0,0119		8	4	3,725		0					
						7	3,5			0					
						7,7	3,85			0					
						7,1	3,55			0					
S5	10,4	1,7	0,236	0,0133		9,1	4,55	4,4375		0					
						8,8	4,4			0					
						9	4,5			0					
						8,6	4,3			0					

Appendix 18: Tensile strength: Weight applied until rupture and dimensions of the broken fragment

	Total weight (g)	Mean Value (g)	Standard deviation	Coeficient of variation	Dimension of the broken fragment (cm)	Mean value of the broken fragment	Standard deviation of the broken fragment
Group A							
Small warp							
No consolidant	38,838	53,458	14,91	0,278843887	3,000	2,920	0,178885438
	50,858				3,000		
	73,408				2,600		
	40,548				3,000		
	63,638				3,000		
Klucel G	63,375	54,267	13,33	0,245685843	2,500	2,600	0,141
	32,655				2,500		
	62,695				2,700		
	62,695				2,500		
	49,915				2,800		
Klucel E	60,345	53,515	6,42	0,119937036	3,000	2,940	0,054772256
	60,335				3,000		
	51,315				2,900		
	48,575				2,900		
	47,005				2,900		
Aquazol	84,385	56,099	16,56	0,295259336	2,900	2,960	0,054772256
	41,115				3,000		
	54,695				3,000		
	50,325				2,900		
	49,975				3,000		
Paraloid B72	81,025	61,487	18,12	0,294733919	2,900	2,900	0,070710678
	62,105				2,900		
	76,945				2,900		
	49,085				2,800		
	38,275				3,000		

	Total weight (g)	Dimension of the broken fragment (cm)	Mean Value (g)	Standard deviation	Coeficient of variation	Dimension of the broken fragment (cm)	Mean value of the broken fragment	Standard deviation of the broken fragment
Group B								
Small warp								
No consolidant								
	58,018	2,8	223,62	44,724	12,0643703	3,26	0,88204308	0,88204308
	43,248	4,6						
	26,138	3,6						
	52,288	2,3						
	43,928	3						
Klucel G	43,005	2,8	176,985	35,397	12,3579679	2,58	0,44384682	0,44384682
	27,755	2,9						
	42,505	1,8						
	17,385	2,7						
	46,335	2,7						
Klucel E	29,595	2,8	142,1	35,525	4,96849407	2,9	0,06324555	0,07071068
	35,095	3						
	41,745	2,9						
	64,535	2,9						
	35,665	2,9						
Aquazol	41,105	2,9	165,055	33,011	10,7970172	2,92	0,04472136	0,04472136
	14,485	2,9						
	40,235	3						
	34,965	2,9						
	34,265	2,9						
Paraloid B72	45,895	3	87,243	21,81075	5,93086662	3	0	0
	19,518	3						
	14,485	3						
	27,035	3						
	26,205	3						

	Weight of method	Weight	Total weight (g)	Dimension of the broken fragment (cm)	Mean Value (g)	Standard deviation	Coeficient of variation	Dimension of the broken fragment (cm)	Mean value of the broken fragment	Standard deviation of the broken fragment
Group B										
small weft										
No consolidant	14,485	32,39	46,875	2,8	376,825	75,365	33,1663331	2,82	0,10954451	0,10954451
	14,485	27,16	41,645	3						
	14,485	98,84	113,325	2,8						
	14,485	91,93	106,415	2,7						
	14,485	54,08	68,565	2,8						
Klucel G	14,485	92,99	107,475	3	342,435	68,487	36,0145189	3	0,07071068	0,07071068
	14,485	15,46	29,945	2,9						
	14,485	84,69	99,175	3,1						
	14,485	57,88	72,365	3						
	14,485	18,99	33,475	3						
Klucel E	14,485	65,25	79,735	3	320,435	64,087	33,9932621	2,98	0,04472136	0,04472136
	14,485	99,37	113,855	3						
	14,485	45,56	60,045	3						
	14,485	18,31	32,795	2,9						
	14,485	19,52	34,005	3						
Aquazol	14,485	78,67	93,155	3	385,185	77,037	14,5273404	2,94	0,11401754	0,11401754
	14,485	72,55	87,035	3,1						
	14,485	61,2	75,685	2,9						
	14,485	40,79	55,275	2,8						
	14,485	59,55	74,035	2,9						
Paraloid B72	14,485	52,43	66,915	3	242,075	48,415	22,1812274	2,98	0,04472136	0,04472136
	14,485	41,45	55,935	2,9						
	14,485	23,98	38,465	3						
	14,485	0	14,485	3						
	14,485	51,79	66,275	3						

	Weight of method	Weight	Total weight (g)	Dimension of the broken fragment (cm)	Mean Value (g)	Standard deviation	Coeficient of variation	Dimension of the broken fragment (cm)	Mean value of the broken fragment	Standard deviation of the broken fragment
Group A										
Small weft										
No consolidant	14,485	64,69	79,175	2,8	400,905	80,181	10,2375256	2,7	0,316227766	0,31622777
	14,485	72,46	86,945	3						
	14,485	57,66	72,145	2,6						
	14,485	79,19	93,675	2,2						
	14,485	54,48	68,965	2,9						
Klucel G	14,485	64,45	78,935	2,8	410,075	82,015	21,1304626	2,92	0,083666003	0,083666
	14,485	80,02	94,505	2,9						
	14,485	59,43	73,915	2,9						
	14,485	39	53,485	3						
	14,485	94,75	109,235	3						
Klucel E	14,485	23,77	38,255	2,9	409,405	81,881	29,6154703	2,88	0,109544512	0,10954451
	14,485	75,95	90,435	3						
	14,485	54,87	69,355	2,9						
	14,485	80,19	94,675	2,9						
	14,485	102,2	116,685	2,7						
Aquazol	14,485	67,64	82,125	2,7	309,145	61,829	21,4526952	2,62	0,192353841	0,19235384
	14,485	66,1	80,585	2,6						
	14,485	29,31	43,795	2,7						
	14,485	20,54	35,025	2,3						
	14,485	53,13	67,615	2,8						
Paraloid B72	14,485	20,94	35,425	3	360,925	72,185	26,0275037	2,94	0,054772256	0,05477226
	14,485	84,14	98,625	2,9						
	14,485	70,16	84,645	2,9						
	14,485	40,79	55,275	3						
	14,485	72,47	86,955	2,9						

Appendix 19 Photographic documentation of the archaeological samples from Group B after consolidation

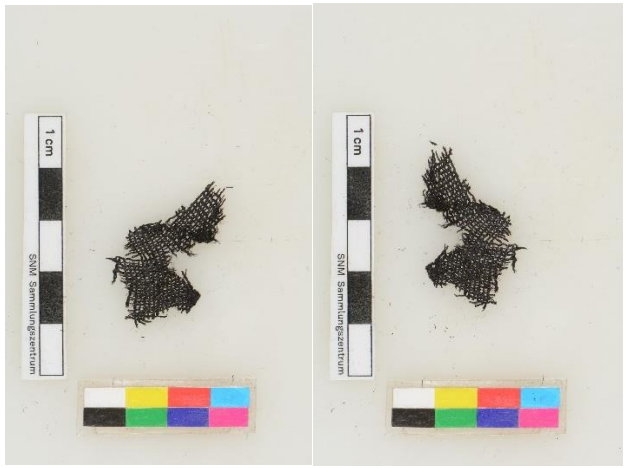

Figure 238 Sample 1.5

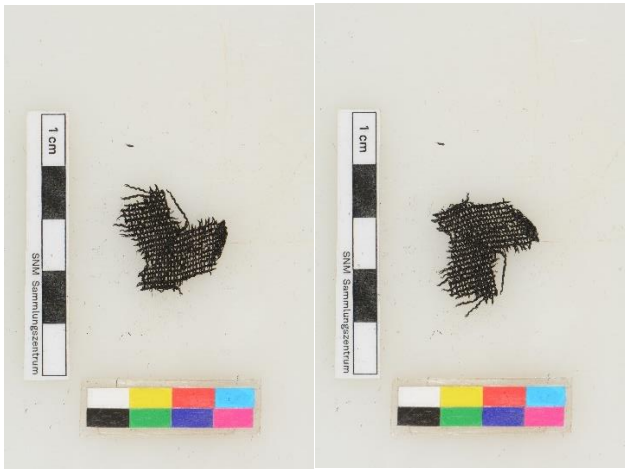

Figure 239 Sample 1.10

Figure 240 Sample 1.18

Figure 241 Sample 1.19

Figure 242 Sample 1.23

Figure 243 Sample 1.30

Figure 244 Sample 2.02

Figure 245 Sample 2.03

Figure 246 Sampel 2.04

Figure 247Sample 2.05

Figure 248 Sample 2.06

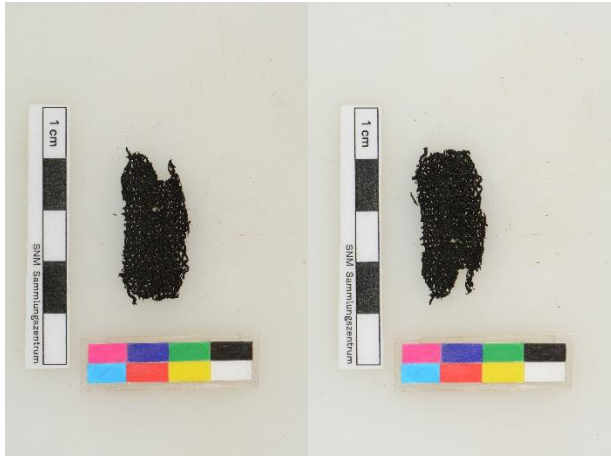

Figure 249 Sample 2.08

Figure 250 Sample 2.10

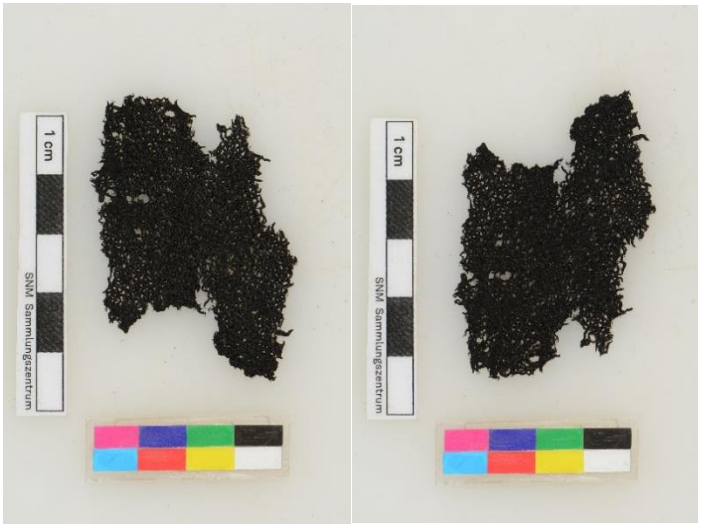

Figure 251 Sample 2.11

Figure 252 Sample 2.15

Figure 253 Sample 2.16

Figure 254 Sample 2.18

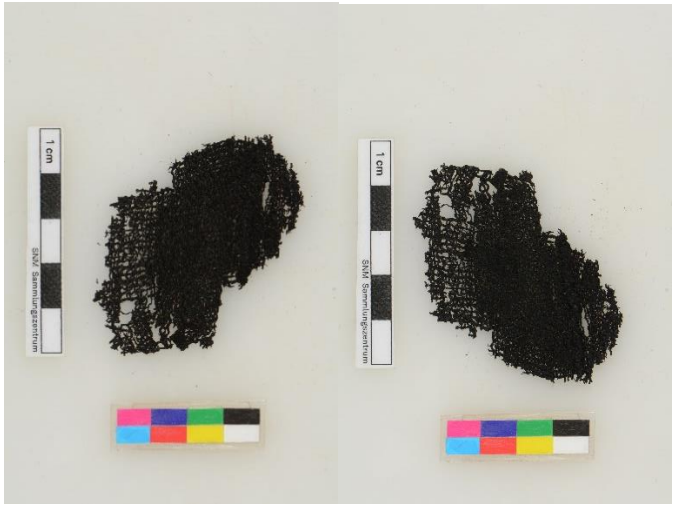

Figure 255 Sample 2.19

Figure 256 Sample 1.06

Appendix 20 Photographic documentation of the archaeological samples from Group A after consolidation

Figure 257 Sample 1.01

Figure 258 Sample 1.02

Figure 259 Sample 1.16

Figure 260 Sample 1.17

Figure 261 Sample 1.29

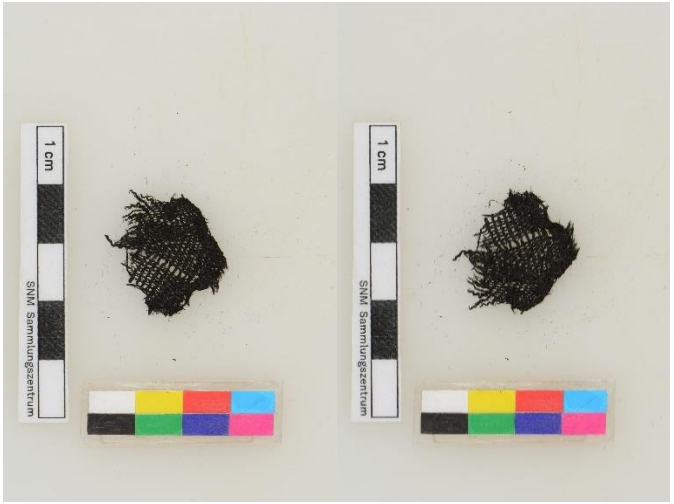

Figure 262 Sample 1.31

Figure 263 Sample3.01

Figure 264 Sample 3.03

Figure 265 Sample 3.04

Figure 266 Sample 3.07

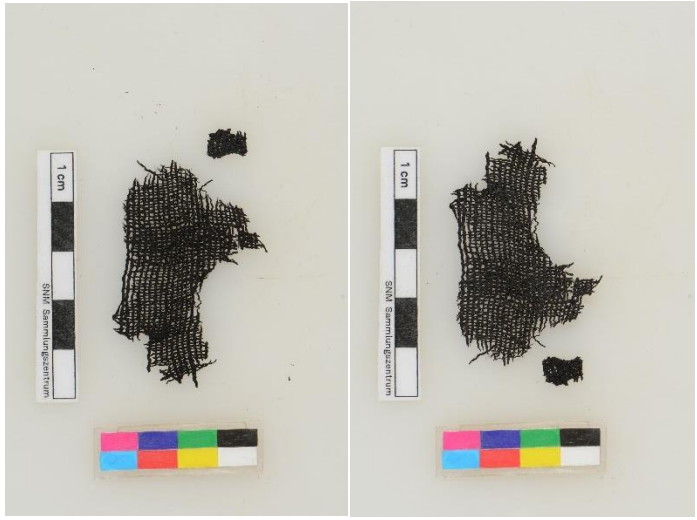

Figure 267 Sample 3.11

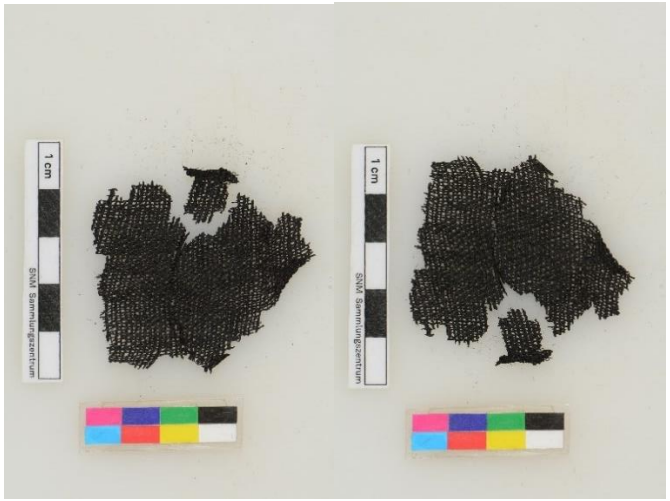

Figure 268 Sample 3.12

Figure 269 Sample 3.13

Figure 270 Sample 3.14

Figure 271 Sample 3.16

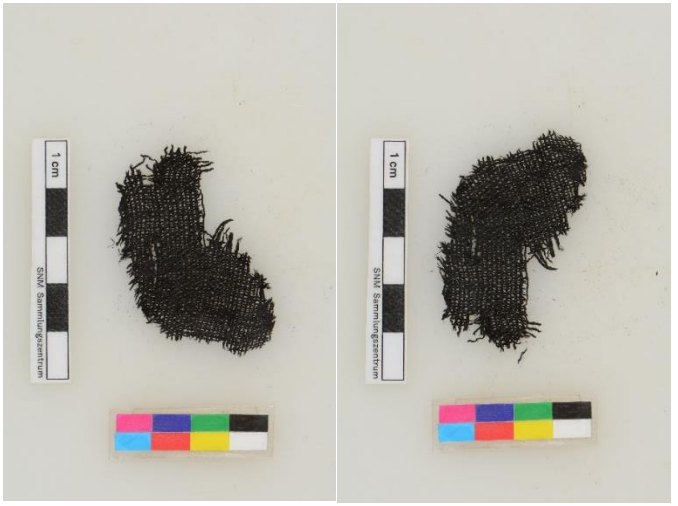

Figure 272 Sample 3.18

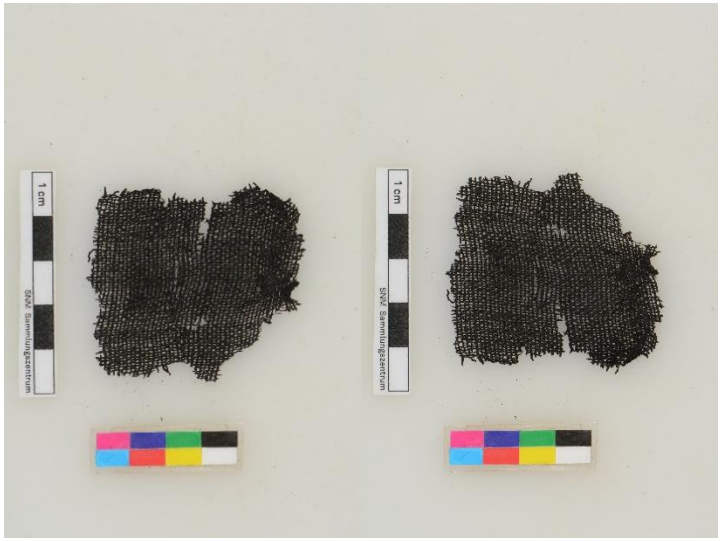

Figure 273 Sample 3.19

Figure 274 Sample 3.08

Appendix 21: Content of the Digital Appendices

A.1 Technical Data for conservation Materials

A.2 Thermocouples: Temperature Measurements during the freeze-drying treatment

A.3 Spectrophotometer: Colorimetric values of the samples